REACTOR MATERIALS

A Quarterly Technical Progress Review

Prepared for DIVISION OF TECHNICAL INFORMATION, USAEC, by
R. W. DAYTON, E. M. SIMONS, and ASSOCIATES, BATTELLE MEMORIAL INSTITUTE

Summer 1964

● VOLUME 7

● NUMBER 2

TECHNICAL PROGRESS REVIEWS

To meet the needs of industry for concise summaries of current atomic developments, the Atomic Energy Commission is publishing this series, Technical Progress Reviews. Issued quarterly, each of the reviews digests and evaluates the latest findings in a specific area of nuclear technology and science.

The five journals published in this series are:

Isotopes and Radiation Technology, P. S. Baker, A. F. Rupp, and associates, Oak Ridge National Laboratory

Nuclear Safety, Wm. B. Cottrell, W. H. Jordan, and associates, Oak Ridge National Laboratory

Power Reactor Technology, W. H. Zinn and J. R. Dietrich, General Nuclear Engineering Corporation

Reactor Fuel Processing, Stephen Lawroski and associates, Chemical Engineering Division, Argonne National Laboratory

Reactor Materials, R. W. Dayton, E. M. Simons, and associates, Battelle Memorial Institute

Each journal may be purchased from the Superintendent of Documents, U. S. Government Printing Office, Washington, D. C., 20402. *Isotopes and Radiation Technology* at $2.00 per year for subscription or $0.55 for individual issues; the other four journals at $2.50 per year and $0.70 per issue. See back cover for remittance instructions and foreign postage requirements.

The views expressed in this publication do not necessarily represent those of the United States Atomic Energy Commission, its divisions or offices, or of any Commission advisory committee or contractor.

Availability of Reports Cited in This Review

Unclassified AEC reports are available for inspection at AEC depository libraries and are sold by the Office of Technical Services, Department of Commerce, Washington, D. C., 20230. Some of the reports cited are not available owing to their preliminary nature; however, the information contained in them will eventually be made available in formal progress or topical reports.

Unclassified reports issued by other Government agencies or private organizations should be requested from the originator.

Unclassified British and Canadian reports may be inspected at AEC depository libraries. British reports are sold by the British Information Service, 45 Rockefeller Plaza, New York, N. Y.; Canadian reports (AECL series) are sold by the Scientific Document Distribution Office, Atomic Energy of Canada, Ltd., Chalk River, Ontario, Canada.

Classified U. S. and foreign reports identified in this journal as Classified may be purchased by properly cleared Access Permit Holders from the Division of Technical Information Extension, U. S. Atomic Energy Commission, P. O. Box 1001, Oak Ridge, Tenn., 37831. Such reports may be inspected at classified AEC depository libraries.

REACTOR MATERIALS

A REVIEW OF RECENT DEVELOPMENTS

Prepared for DIVISION OF TECHNICAL INFORMATION, USAEC,
by R. W. DAYTON, E. M. SIMONS, and ASSOCIATES,
BATTELLE MEMORIAL INSTITUTE

SUMMER 1964

VOLUME 7

NUMBER 2

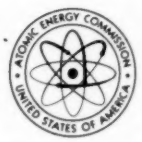

Foreword

Reactor Materials is one of a series of quarterly technical progress reviews broadly covering the field of nuclear science and technology. Under the auspices of the AEC Division of Technical Information, *Reactor Materials* is prepared by Battelle personnel from worldwide literature. It covers properties, behavior, and fabrication processes of materials applicable to nuclear reactor components and associated equipment.

The reader will recognize that the scope of this Review is too broad to permit detailed coverage of every topic. Rather, the authors and editors attempt to combine the highlights of significant new developments into an informative summary of current research for both management and the technical specialist. As a rule, enough of the results are presented to define the research and summarize the findings. For readers desiring more information on any particular topic, a complete set of references is provided at the end of each section.

Each quarter a number of bibliographies, monographs, and books appear on subjects within the scope of *Reactor Materials*. Although the main purpose of this Review is to call attention to findings that are new and significant, such publications are noted in the text because they often represent excellent compilations of available information on important materials topics.

R. W. DAYTON
E. M. SIMONS
R. W. ENDEBROCK
Battelle Memorial Institute

DEPOSITED BY THE
UNITED STATES OF AMERICA

Contents

Foreword

I FUEL AND FERTILE MATERIALS . . 81
Uranium Metal and Alloys 81
Plutonium 83
Thorium 88
Metal-Ceramic Fuels 89
Coated-Particle Fuel Materials 90
Uranium Oxide Fuel Materials 95
Uranium Carbides and Nitrides 98
Mechanism of Corrosion of Fuel Alloys . 100
Basic Studies of Irradiation Effects in Fuel Materials 100
References 102

II MODERATOR MATERIALS 106
Graphite 106
Beryllium Metal and Alloys 106
Beryllium Oxide 113
Beryllium Compounds 115
Solid Hydrides 115
References 116

III NUCLEAR POISONS 118
Metallic Poisons 118
Dispersion Poison Materials 118
References 118

IV CLADDING AND STRUCTURAL MATERIALS 119
Corrosion 119
Selected Mechanical Properties of Cladding and Structural Materials . . 125
Selected Metallurgical Aspects of Cladding and Structural Materials . . 126
Diffusion Studies 126
Ceramic Technology 128
Radiation Effects in Nonfuel Materials 128
References 134

V SPECIAL FABRICATION TECHNIQUES 139
Melting, Casting, and Working 139
Cladding 140
Explosive Forming 144
Welding and Brazing 144
Nondestructive Testing 145
References 146

(Note: The pagination of this journal will henceforth be consecutive throughout the four issues of each volume.)

Issued quarterly by the U. S. Atomic Energy Commission. Use of funds for printing this publication approved by the Director of the Bureau of the Budget on October 14, 1963.

DEPOSITED BY THE
UNITED STATES OF AMERICA

Section

I

Reactor Fuel Processing

Fuel and Fertile Materials

Uranium Metal and Alloys

Unalloyed Uranium and Intermetallics

The results of a four-year study by Nuclear Metals on the beta heat-treatment of uranium have been published. Readers interested in the textures developed as a result of varying many heat-treating parameters will find the summary report[1] most helpful.

Argonne[2] data on the diffusion of copper, chromium, cobalt, iron, magnanese, nickel, and niobium in gamma uranium are presented in Table I-1 and Fig. I-1.

In studies of the uranium-cadmium system performed at Iowa State College,[3] the compound UCd_{11} was found to be the only compound formed in the system.

Bufferd et al.[4] report that the dispersion strengthening of uranium and alumina is feasible. Creep-rupture tests indicate significant improvement in the high-temperature properties of dispersion-strengthened uranium as compared to unalloyed uranium.

The National Lead Co. of Ohio[5] has determined the tensile properties of slightly enriched uranium metal with high phosphorus content and the properties of normal uranium metal having a lower phosphorus content. At the three test temperatures utilized, the two types of materials tested had similar tensile properties. The only significant difference observed was in the ductility of the materials at room temperature. The high-phosphorus material exhibited a much lower percentage reduction in area at this temperature; however, it is felt that this

Table I-1 PARAMETERS FOR DIFFUSION IN GAMMA URANIUM[2]

Diffusing element	Activation energy, kcal/mole	D_0, cm²/sec
U	26.500	1.12×10^{-3}
Cr	23.000 ± 0.450	$4.0 \times 10^{-3} \pm 20\%$
Mn	14.700 ± 1.300	$2.6 \times 10^{-4} \pm 78\%$
Fe	11.900 ± 0.310	$2.7 \times 10^{-4} \pm 14\%$
Co	12.500 ± 0.590	$3.5 \times 10^{-4} \pm 28\%$
Ni	15.500 ± 0.330	$5.2 \times 10^{-4} \pm 15\%$
Cu	23.900 ± 0.410	$1.9 \times 10^{-3} \pm 20\%$
Nb	39.400 ± 0.520	$4.6 \times 10^{-2} \pm 30\%$

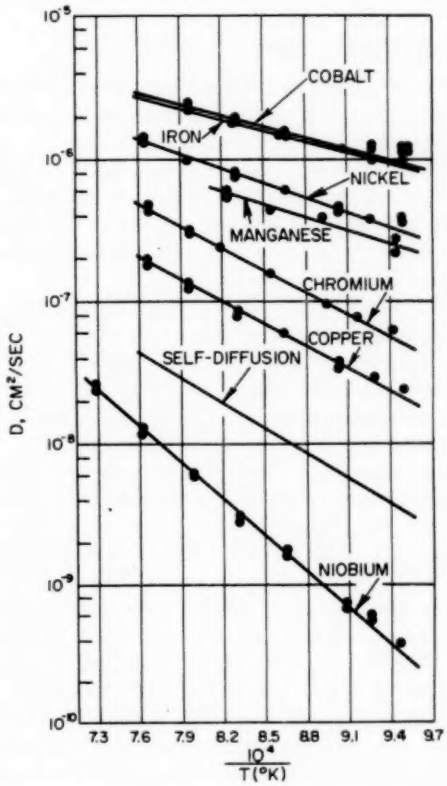

Fig. I-1 Arrhenius plots for the diffusion of transition metals in gamma uranium.[2]

Table I-2 TENSILE PROPERTIES FOR URANIUM CONTAINING INTENTIONAL PHOSPHORUS IMPURITIES[5]

Test temp., °C	Ultimate tensile strength, psi	Yield strength (0.2% offset), psi	Elongation in 2-in. gauge length, %	Reduction in area, %
Low-Phosphorus Uranium: P = 13 ppm, H_2 = 0.9 ppm				
21	94,500	~53,700	9	14
350	47,100	~29,600	22	42
450	34,600	~23,700	22	51
High-Phosphorus Uranium: P = 204 ppm, H_2 = 2.6 ppm				
21	89,600	~52,200	7	7
350	49,200	~30,600	19	42
450	32,800	~24,000	18	49

was due, at least in part, to the difference in hydrogen content of the two types of materials. The test data are presented in Table I-2.

(M. S. Farkas)

Alpha-Phase Uranium Alloys

Investigators at Argonne[6] have determined the heat capacity of high-purity uranium and uranium-fissium alloys containing 3, 5, and 8 wt.% fissium. The total heat content from 0 to 1200°C was found to be 16.1 ± 0.3, 16.3 ± 0.6, 16.3 ± 0.6, and 16.4 ± 0.4 kcal per equivalent gram atom, for the 0, 3, 5, and 8 wt.% fissium alloys, respectively.

Nuclear Metals[7] is developing a method of producing uranium alloys containing fine dispersions of metallic particles. The alloying elements are those which are highly insoluble in the solid state and, thus, have little tendency to agglomerate (overage) at elevated temperatures. Uranium-copper alloys were prepared by dissolving copper in liquid uranium and then quenching rapidly. Examination of an as-quenched uranium–1.2 wt.% copper alloy at magnifications up to 20,000× failed to reveal any precipitate. After compaction at 600°C, particles having an average diameter of 0.08 μ and a concentration of $7 \times 10^{13}/cm^3$ were observed. Aging for up to 500 hr at 800°C produced only a moderate increase in particle size. The results of the program demonstrate that it is possible to produce fine dispersions of particles that are insoluble in gamma uranium.

A review report on the effects of irradiation on metallic fuels has been issued by Battelle.[8] The data presented are intended to summarize the literature published since *Materials*, Vol. 1 of the second edition of *Reactor Handbook*, was published. Information on the effects of nuclear radiation on uranium, alpha-uranium alloys, and dilute uranium alloys is given. (M. S. Farkas)

Gamma-Phase Uranium Alloys

In a study of fuel-rod fabrication problems at Atomics International,[9] fuel rods of uranium–10 wt.% molybdenum clad with aluminum or APM have been fabricated using thin-wall niobium or titanium tubing as diffusion barriers between fuel and cladding. Isostatic bonding at 8000 psi and 1000°F for times up to 28.5 hr resulted in bonding between the niobium tubing and the cladding but not between the niobium and the fuel.

A study of deformation characteristics of metastable gamma-phase structures in uranium-molybdenum alloys has been performed at Harwell[10] using X-ray and metallographic techniques. Slip was observed in alloys containing 15 and 20 at.% molybdenum but not in alloys containing 11, 12.5, or 30 at.% molybdenum. Twinning was observed at all compositions, but the habit plane varied with composition. In the 30 at.% alloy, the habit plane was determined to be {1 1 2}, and in the remaining alloy the habit plane was {1 2 2}. In the lower molybdenum compositions, {1 1 2} twinning of the twins themselves apparently also is observed.

A report has been issued by the Radiation Effects Information Center[8] in which the effects of irradiation on gamma-phase uranium-molybdenum and uranium-niobium alloys are summarized. The summary includes effects on volume stability during irradiation and during postirradiation annealing. It also includes changes in physical and mechanical properties and corrosion behavior as a result of irradiation.

(A. A. Bauer)

Epsilon-Phase Uranium Alloys

The irradiation behavior of zirconium-uranium and the U_3Si epsilon-phase alloys is summarized in a report issued by the Radiation Effects Information Center.[8] Available information concerning the effects of irradiation on physical, mechanical, and corrosion properties is included. (A. A. Bauer)

Dilute Uranium Alloys

Alloys of aluminum containing 17.3 wt.% uranium were irradiated by Argonne.[11] Annealing at

550°C produced severe localized blistering on specimens having burnups of 5.9×10^{20} fissions/cm^3, whereas similar conditions produced only a small uniform volume increase when the burnup was 1.4×10^{20} fissions/cm^3. The observed stability is attributed to a defect structure in the compound UAl_4 in which unoccupied uranium sites trap fission products and, in particular, fission-product gases. Table I-3 shows the results of the irradiation and the annealing experiments. (M. S. Farkas)

Plutonium

Plutonium Metal and Alloys

Lawrence Radiation Laboratory[12] has measured the effects of pressure up to 35 kbars on the phase transitions of plutonium. Three triple points were detected, the gamma-delta-epsilon at 398 ± 10°C and 0.9 ± 0.2 kbar, the gamma-epsilon-liquid at 518 ± 10°C and 19.5 ± 1 kbars, and the beta-gamma-liquid at 500 ± 10°C and 27.0 ± 1 kbars. Measuring techniques were not sufficiently sensitive to detect delta-delta prime transition and thus no gamma-delta-delta prime triple point was determined. Initial slopes of transition lines are shown below:

Transition	Initial slope of transition lines, °C/kbar
Alpha-beta	11.2
Beta-gamma	27.3
Gamma-delta	88
Delta-epsilon	−87
Epsilon-liquid	−4.4

Recent investigations at Hanford[13] indicate that unalloyed alpha plutonium can be deformed up to 90% reductions by flat rolling in the temperature range of 25 to 70°C. X-ray diffraction data revealed no indication of line broadening, and no significant changes in hardness were noted after deformation, suggesting that both recovery and recrystallization temperatures are low.

Curves of time-temperature-transformation (T-T-T) for the gamma ⇌ beta ⇌ alpha transformations of moderately high-quality plutonium (less than 250 ppm impurities) are shown in Fig. I-2. The most significant difference be-

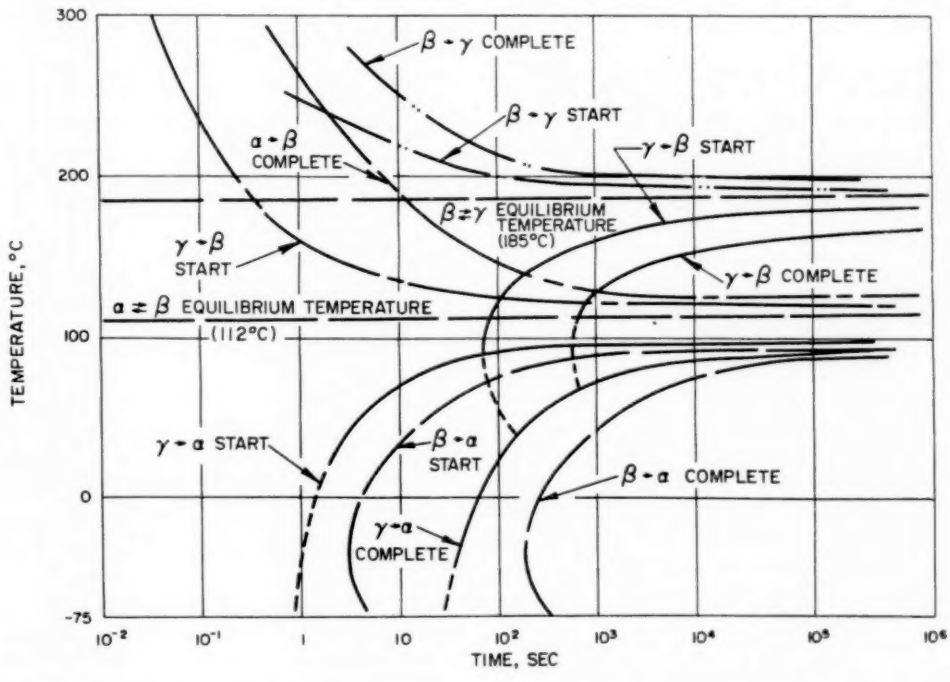

Fig. I-2 T-T-T curves of the $\alpha \rightleftharpoons \beta \rightleftharpoons \gamma$ transformations of plutonium.[13]

Table I-3 ANNEALING HISTORY OF IRRADIATED ALUMINUM–17.3 WT.% URANIUM ALLOY SPECIMENS[11]

Specimen	Burnup		Annealing temp.,* °C	Time at temp., hr	Cumulative time at temp., hr	Weight,† g	Density,† g/cm³	Total % ΔV‡	Dimensions,† in.		
	10^{20} fissions/cm³	% U^{235}							Length	Width	Thickness
W-12-TE	5.9	45.1	550	0	0	10.405	2.856		2.055	1.001	0.111
				94	94	10.430	2.426	+17.7	2.082	0.989	0.112 to 0.219
				1.5	95.5	10.422	2.419	+18.0	2.079	0.986	0.119 to 0.220
				2	97.5	10.434	2.416	+18.2	2.076	0.981 to 1.003	0.107 to 0.209
				3.5	101	10.478	2.413	+18.3	2.076	0.986 to 1.006	0.128 to 0.215
				3	104	10.525	2.386	+19.5	2.087	0.980 to 1.003	0.131 to 0.228
				46	150	10.631	2.360	+20.8	2.074	0.977 to 1.009	0.128 to 0.230
				36	186	10.753	2.352	+21.1	2.088	0.980 to 1.008	0.126 to 0.228
				114	300	10.928	2.321	+22.6	2.094	0.983 to 1.021	0.139 to 0.244
				71	371	11.065	2.308	+23.3	2.101	0.984 to 1.021	0.133 to 0.249
W-12-TES	5.9	45.1	550	0	0	4.986	2.809		2.051	0.497	0.104
				1.5	1.5	4.952	2.791	+0.6	2.054	0.493	0.104
				2	3.5	4.945	2.767	+1.5	2.042	0.491 to 0.505	0.096 to 0.106
				3.5	7	4.944	2.760	+2.4	2.045	0.487 to 0.505	0.098 to 0.105
				3	10	4.944	2.744	+2.5	2.051	0.490 to 0.504	0.098 to 0.105
				94	104	4.997	2.667	+5.3	2.072	0.504 to 0.510	0.101 to 0.133
				46	150	5.020	2.636	+6.6	2.011	0.502 to 0.511	0.098 to 0.124
				36	186	5.033	2.627	+6.9	2.070	0.502 to 0.513	0.095 to 0.117
				114	300	5.058	2.616	+7.4	2.078	0.497 to 0.514	0.104 to 0.114
				71	371	5.071	2.616	+7.4	2.076	0.505 to 0.514	0.097 to 0.133
W-12-6	1.4	10.8	550	0	0	10.415§	2.890‡		1.024	2.001	0.105
				24	24	10.382	2.887	NMC	1.024	1.999	0.106
				69	93	10.367	2.881	+0.3	1.024	2.004	0.105
				115	208	10.353	2.881	+0.3	1.027	2.008	0.103
				115	323	10.364¶	2.865§	+0.9	1.031	2.000	0.103
				94	417	10.354	2.860	+1.0	1.032	2.003	0.102
				94	511	10.356	2.850	+1.4	1.034	2.004	0.102
W-12-5	1.2	8.8	500	0	0	10.141¶	2.889§		1.005	2.000	0.105
				24	24	10.120¶	2.896§		1.004	1.998	0.103
				69	93	10.111	2.895	NMC	1.006	1.998	0.103
				116	209	10.102	2.896	NMC	1.005	1.996	0.103
				115	324	10.103¶	2.891§	+0.2	1.002	1.996	0.103
				209	533	10.093	2.892	+0.1	1.005	1.999	0.103
W-12-4	0.77	5.8	365	0	0	9.897	2.904		0.987	1.996	0.105
				24	24	9.887	2.903	NMC	0.990	1.995	0.104
				72	96	9.887	2.891	+0.4	0.989	1.995	0.104
				144	240	9.885	2.888	+0.6	0.989	1.997	0.104
				120	360	9.883	2.896	+0.3	0.991	1.995	0.104
W-12-1	0.41	3.2	210	0	0	10.293	2.904		1.022	1.993	0.104
				24	24	10.281	2.903	NMC	1.022	1.991	0.105
				72	96	10.380	2.905	NMC	1.022	1.992	0.104
				146	242	10.283	2.898	+0.2	1.022	1.993	0.105
				120	362	10.277	2.897	+0.2	1.022	1.994	0.103

*The temperature did not vary more than ±10°C at any time during test.

†The precision of measurements is: weight, ±0.002 g; density, ±0.003 g/cm³; dimensions, ±0.001 in.

‡Based on the assumption of no weight change and calculated from the expression $\% \Delta V = [(\rho_i/\rho_f) - 1]\,100$, where ρ_i and ρ_f are the initial and final densities, respectively. NMC means no measurable change.

§Average of six measurements.

¶Average of two measurements.

Fig. I
clad
wt. %
nealin
•, alu
wt. %

CHANGE IN DENSITY, %

tween
nium
curve
to lov

Stu
stres
formi
total
tion
and i
tion
Trans
grain
rate
Ar
ture
resul
caus
to a
where
rate
Ch
cryst
decre
from
perat
cally
alum
Th
temp
the h
toniu
Fig.
mens
below

tween these data and data obtained for plutonium containing 1000 ppm impurities is that the curves for the higher quality metal are shifted to lower times.

Studies of the weakening of plutonium under stress during transformation indicate that transformation strain is a significant portion of the total strain. Also, it was found that transformation strain increases with the applied stress and is greater for the alpha-to-beta transformation than for the beta-to-alpha transformation. Transformation strain increases as the initial grain size decreases and is transformation-rate dependent.

Argonne[14] is investigating the effects of moisture on the oxidation of plutonium. Preliminary results indicate that at 190°C, 180 ppm moisture causes the oxidation of plutonium to accelerate to a maximum rate of about 20 $\mu g/(cm^2)(min)$, whereas 20 ppm moisture produces a maximum rate of 1.5 $\mu g/(cm^2)(min)$.

Chalk River[15] studies indicate that single crystals of hexagonal $PuAl_3$ transform to ordered rhombohedral $PuAl_3$ when slowly cooled from 950°C, which is coincident with the temperature at which $PuAl_4$ decomposes peritectically to disordered rhombohedral $PuAl_3$ plus an aluminum-rich liquid.

The effects of postirradiation annealing at temperatures up to 600°C on the density and the hardness of aluminum–5 and 10 wt.% plutonium alloys have been reported.[16] As shown in Fig. I-3, the density of the irradiated specimens increased after annealing at temperatures below 525°C and decreased when annealed above

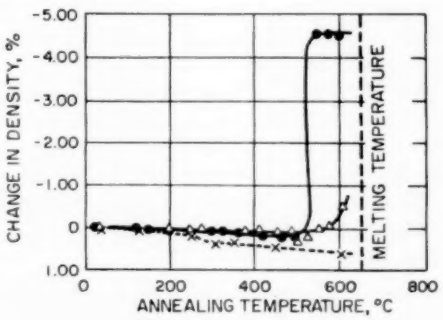

Fig. I-3 Change in density of irradiated aluminum-clad aluminum–5 wt. % plutonium and aluminum–10 wt. % plutonium alloys and of rolled aluminum on annealing 15 min at successively higher temperatures.[16] •, aluminum–5 wt. % plutonium; Δ, aluminum–10 wt. % plutonium; ×, aluminum.

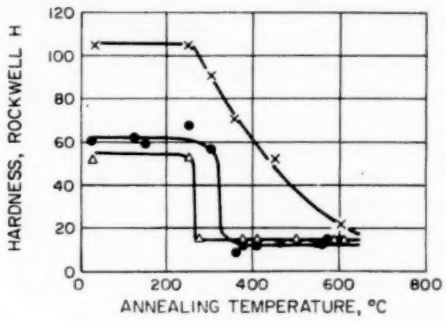

Fig. I-4 Change in the room-temperature hardness of irradiated aluminum-clad aluminum–5 wt. % plutonium and aluminum–10 wt. % plutonium alloys and of rolled aluminum after annealing 15 min at successively higher temperatures.[16] •, aluminum–5 wt. % plutonium; Δ, aluminum–10 wt. % plutonium; ×, aluminum.

525°C. The lower swelling of the aluminum–10 wt.% plutonium alloy is believed to be the result of more uniform plutonium distribution and consequent smaller gas-bubble formation. Room-temperature hardness data plotted in Fig. I-4 show that hardness decreased substantially after annealing at temperatures between 275 and 360°C.

Another report[17] describes the development and manufacture of core IV for the EBR-I. Fuel alloy for core IV is delta-stabilized plutonium–1.25 wt.% aluminum.

Hanford[18] indicates that fuel rods consisting of aluminum–2 wt.% plutonium–2 wt.% nickel alloy injection cast into Zircaloy-2 cladding behaved satisfactorily when irradiated to maximum burnups of 20% of the plutonium atoms. Circumferential grooves in the tubing provided core-to-cladding mechanical bonding.

Mound[19] is continuing studies of low-melting plutonium alloys. The plutonium-cerium-copper ternary system diagram has been revised as shown in Fig. I-5. The previously proposed diagram incorrectly indicated complete solid solubility between $CeCu_6$ and Pu_4Cu_{17}. A range of limited solid solubility has been found to exist between $CeCu_6$ and Pu_2Cu_{11}.

Melting temperatures of plutonium-cerium-nickel ternary alloys of compositions between plutonium–12.5 at.% nickel and cerium–20 at.% nickel vary between 440 and 475°C.

Viscosities of plutonium-iron alloys as a function of composition at various temperatures

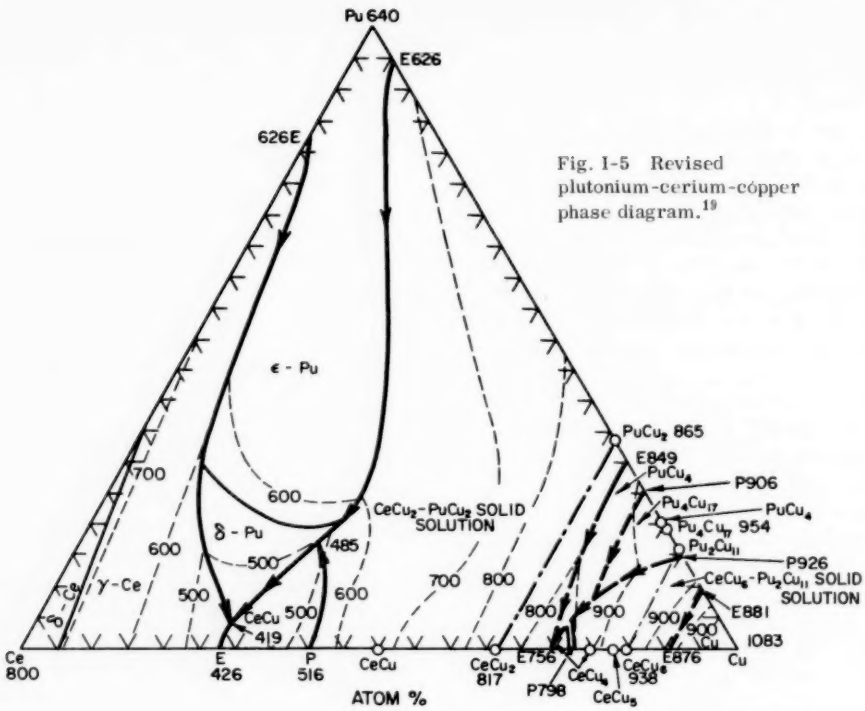

Fig. I-5 Revised plutonium-cerium-copper phase diagram.[19]

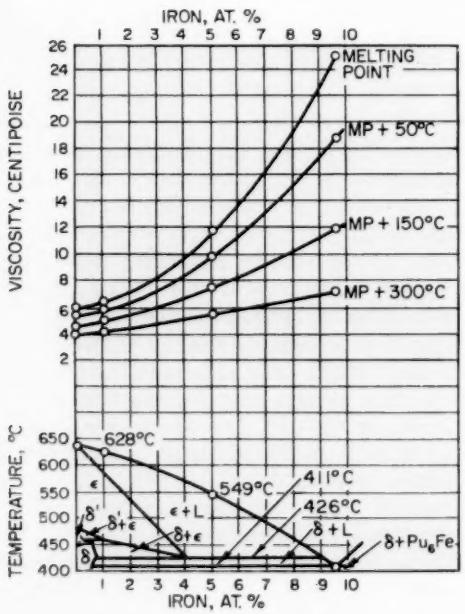

Fig. I-6 Viscosities of plutonium-iron molten alloys as a function of iron concentration and superheating temperature.[19]

are shown in Fig. I-6. The viscosity of 25.3 centipoises for the alloy at the eutectic composition is the highest ever reported for a liquid metal. (V. W. Storhok)

Plutonium Compounds

In the plasma-torch melting of PuO_2 spheres at Mound,[19] central voids that formed were attributed to vapor entrapment, although some unmelted portions were noted. PuO_2–50 wt.% ThO_2 spheres were prepared with a lattice parameter of 5.53 ± 0.01 A, as compared with a theoretical value of 5.49 A. The structure[20] of ZrO_2–27 mole % PuO_2 was identified as solid-solution stabilization of tetragonal ZrO_2, as opposed to previous reports that this composition exhibited a cubic structure.

Hanford workers[21] have located the PuO_2-MgO eutectic at 43 mole % MgO and 2100°C, while substantiating the absence of solid solubility. They also developed a method of air roasting PuO_2 to remove halogen impurities that lead to subsequent corrosion of the fuel cladding. The production of UO_2-PuO_2 fuel elements by alternate loading of UO_2 and mixtures of UO_2 and

PuO_2 in a tube (incremental loading process)[22] provides gross homogeneity in a fuel rod but minor segregation within individual increments. This segregation was accommodated in the thermal design of PRTR fuel rods. Gamma scanning techniques were employed to assure that no plutonium concentration exceeded that which would cause local hot spots in excess of the maximum permissible point surface heat flux. Occasional regions of bulk sintering, columnar grain growth, and void formation were observed. These were not detrimental to the fuel-rod performance. Irradiation tests of capsules containing both sintered (90% T.D.) pellets and non-sintered (65% T.D.) mixtures of UO_2 and PuO_2 showed that fission gas release was more dependent on rod power than on PuO_2 concentration.[22] A European laboratory[23] has determined that sintered densities of PuO_2 are inversely proportional to the calcining temperature, regardless of the preparation technique, and has also confirmed that PuO_2 is the diffusing species in the $(U,Pu)O_2$ system. Corrosion resistance of all $(U,Pu)O_2$ compositions is comparable to that of UO_2 in 680°F water after 1000-hr exposure.[24]

PuO_2 was shown to be compatible with the austenitic stainless steels[24] at 1000°C and was reported[18] to react with molybdenum and tungsten after 8 hr at 1600°C, forming a $PuO_{1.7}$ eutectoid structure. A recent British publication[25] reports thermodynamic data for PuO_{2-x} and $(U,Pu)O_2$ mixtures and also suggests that solid-solution fuels may be more stable under irradiation than UO_2. A single fluorite type

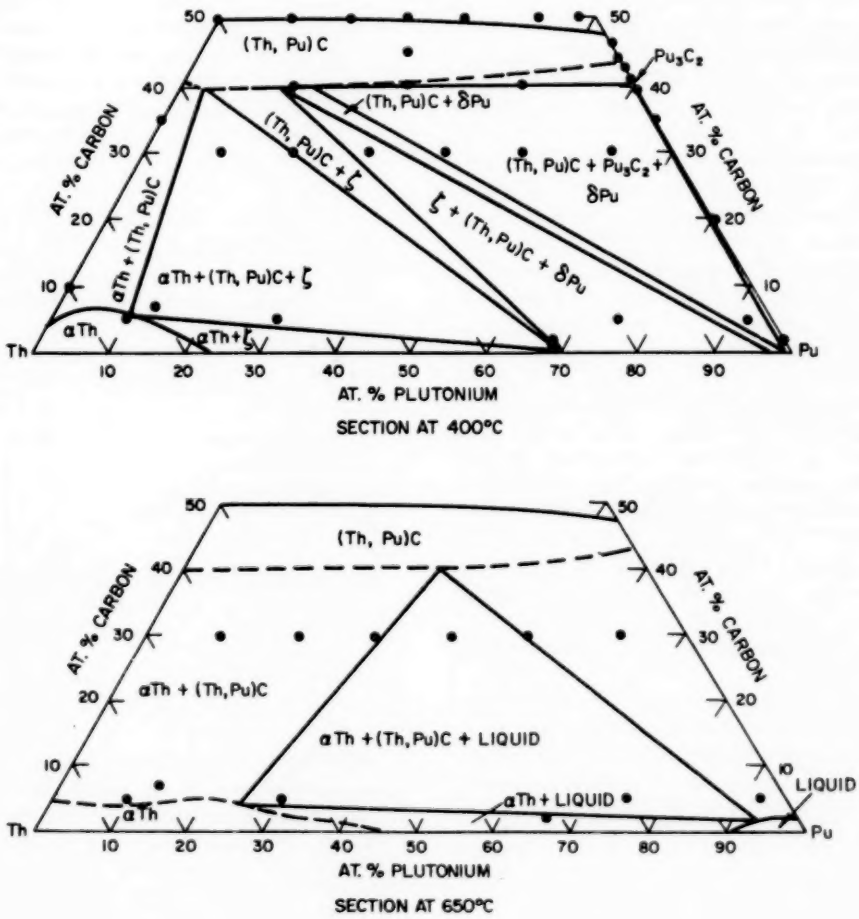

Fig. I-7 Isothermal sections of the thorium-plutonium-carbon phase diagram.[2]

phase[26] was identified in the Eu_2O_3-PuO_2 system between zero and 42 mole % Eu_2O_3.

The British[25] conclude that (U,Pu)C and (U,Pu)N are completely soluble in all proportions, as are U_2C_3 and Pu_2C_3, and that 0.5 wt.% oxygen is soluble in (U,Pu)C at 1500°C. They also maintain that $(U_{0.7}Pu_{0.3})C$ is harder at room temperature than $(U_{0.7}Pu_{0.3})N$, but it is considerably softer and more ductile at temperatures above 600°C. Hanford,[21] in studies of the pseudobinary system (Pu-Zr)C, found a continuous series of solid solutions with melting points ranging from 2900°C for 10 mole % PuC to 2260°C for 63 mole % PuC.

Argonne[27–29] has published reports covering the entire uranium-plutonium-carbon ternary phase diagram. In addition, certain results[2] of an investigation of the thorium-plutonium-carbon system are illustrated in Fig. I-7. Pins of 80% dense UC–20 wt.% PuC were irradiated[14] to burnups of 5.0×10^{20} to 7.1×10^{20} fissions/cm^3 at a mean cladding temperature of 370 to 515°C, with a maximum diametrical change of 1%.

A PuN–50 vol.% tungsten cermet[21] heat-treated 4 hr at 1400°C and 4 hr at 1500°C in vacuum showed 9% weight loss in each case. This behavior was attributed to PuN decomposition, although the dissociation pressure at these temperatures was reported by other sources to be negligible. A PuN–10 vol.% plutonium cermet[18] showed no reaction with an Al_2O_3 crucible after 2 hr at 1000°C in vacuum. PuN pellets heated on molybdenum for 12 hr at 1700°C slumped and flowed drastically, presumably owing to the presence of free plutonium metal. No reaction between PuN and molybdenum, tantalum, tungsten, or niobium was noted by Battelle[30–33] after 50 hr at 1288°C. $(U_{0.8}Pu_{0.2})N$ heated 4 hr at 1000°C in a type 304 stainless-steel crucible showed no reaction visually.[34] There was also no reaction between a 40 vol.% PuC–tantalum compact sintered 11 hr at 1400°C in vacuum.

Attempts to prepare PuP,[30–35] PuAs,[36] and PuS[35] have been achieving partial success in investigations to prepare desirable refractory-fuel compounds other than the oxides, carbides, and nitrides. (W. M. Pardue)

Thorium

Oak Ridge[37,38] is investigating the strengthening of thorium by dispersion hardening, using stable oxide dispersoids. A promising technique for preparing dispersions of ThO_2 in thorium consists of blending and milling powders of thorium hydride and thorium oxide. The hot powders are hot pressed under vacuum which simultaneously compacts and reduces the hydride to thorium metal. The compacts are then extruded. Mixtures of thorium and 10 vol.% AlO(OH) and 10 vol.% ZrO_2 were also investigated. Both the AlO(OH) and ZrO_2 reacted with thorium and formed large agglomerates of thoria. Hot-hardness curves for various mixtures are shown in Fig. I-8. Stress-rupture tests of thorium–10 vol.% ThO_2 were conducted at 800°C. Data from these tests, shown in Table I-4, compare favorably with results obtained for a thorium–2 wt.% uranium–2 wt.% zirconium alloy.

Attempts are being made at Hanford[39] to strengthen a thorium-uranium-zirconium alloy by adding aluminum or beryllium. A thorium–2.5 wt.% uranium–2.0 wt.% zirconium alloy and similar alloys containing 500 to 2000 ppm aluminum or beryllium cracked severely when

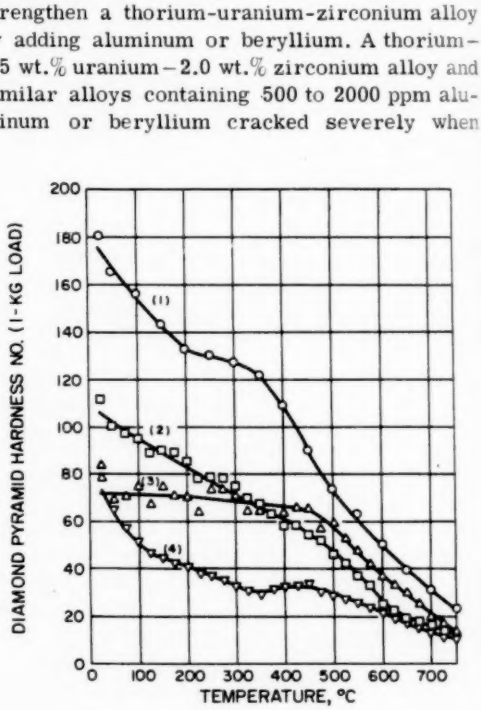

Fig. I-8 Hot-hardness curves of thorium and thorium containing dispersions of hard particles.[37] (1) ○, Th–10 vol. % AlO(OH) hot pressed at 1300°C, extruded at 800°C, and annealed for 1 hr at 800°C; each point is average of two readings; (2) □, Th + ThO_2 obtained from milling; hot pressed at 1000°C and extruded at 700°C; (3) Δ, Th–10 vol.% ZrO_2 hot pressed at 1300°C, heated for 1 hr in vacuum, and extruded at 700°C, (4) ▽, Th arc melted and hot rolled at 800°C.

rolled at 850 to 900°C. A thorium–2.5 wt.% uranium–1.0 wt.% zirconium alloy was rolled at 900°C without cracking.

The thorium-holmium, thorium-neodymium, and thorium-praseodymium alloy systems are being investigated by the Bureau of Mines.[40] Two-phase regions were observed in the thorium-holmium and thorium-neodymium systems, although solidus temperatures in both systems decreased gradually with increasing rare-earth content and no minimum melting point or eutectic was indicated. Hardness of thorium-praseodymium alloys decreased gradually with increasing praseodymium content.

Chalk River[15] data indicate an order-disorder transformation in $ThAl_3$ coincident with the Al-$ThAl_3$ eutectic temperature at 630°C. An unreported orthorhombic phase of composition approximating $Th_{0.93}Al_3$ and a density of 5.3 g/cm³ was found in cast aluminum–16 and 30 wt.% thorium alloys. The phase was partially transformed to hexagonal $ThAl_3$ by heating at 358°C for one week, and the reaction could be reversed by heating for an additional week at 303°C. (V. W. Storhok)

Table I-4 STRESS-RUPTURE RESULTS AT 800°C OF Th-ThO_2 AND Th-U-Zr ALLOY[38]

Stress, psi	Minimum creep rate, %/hr		Rupture time, hr	
	Th–vol.% ThO_2	Th–5 wt.% U–2 wt.% Zr	Th–10 wt.% ThO_2	Th–5 wt.% U–2 wt.% Zr
4000	4.0×10^{-3}	2.5×10^{-2}	69.5*	143.4
5000	2.8×10^{-2}	9.0×10^{-2}†	29.2	40.0†

*Stress increased to 5000 psi after 65.5 hr at 4000 psi.
†Extrapolated data.

Metal-Ceramic Fuels

Dispersions

Hanford[34] pneumatically impacted a series of samples with a 20 vol.% PuO_2–type 304 stainless-steel dispersion. A new split die design was used, and the densified pellets required only finish machining to dimensions.

Argonne[2] has completed irradiation testing of 39 wt.% U_3O_8–aluminum dispersions and found they are resistant to swelling for burnups and temperature levels up to at least 1×10^{20} fissions/cm³ and 550°C, respectively. X-ray diffraction analysis confirmed that a reaction between the U_3O_8 particles and aluminum occurs at temperatures as low as 210°C, with the formation of UO_2 and uranium-aluminum intermetallic compounds. It was not indicated whether Al_2O_3 was also a reaction product. Temperature, time, and particle size were found to be variables that affect the rate of reaction. Oak Ridge's study[38] of the U_3O_8-aluminum system indicated that the presence of trace amounts of stearic acid–CCl_4 lubricant used in compacting the initial dispersions helped promote the reaction of U_3O_8 with aluminum. Their study revealed that chloride behaved as an accelerator for the reactions and suggested that chloride type binders or lubricants should not be used for future compatibility studies.

Samples that contained a 27½ vol.% UO_2–type 347 stainless-steel disperson clad with type 347

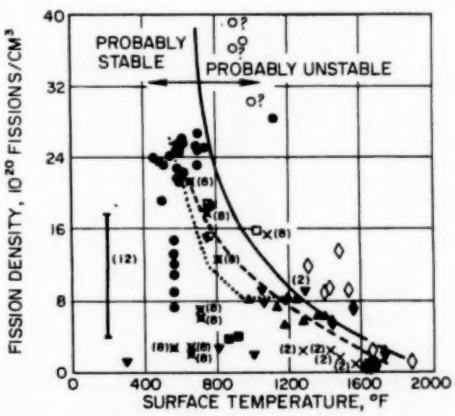

Fig. I-9 Irradiation stability of UO_2–stainless-steel dispersions.[38] ●○, BMI-32; ■□, ORNL-46; ▲△, BMI-33; ◆◇, BMI-GCRE; ▼▽, KAPL; ×, NDA-1; ▪ PWAC; I, ORNL-21; ?, questionable temperature; ( ), number of samples; ——, ORNL-2; .....,KAPL; – – –, BMI (minimum). Open symbols indicate failure; filled symbols indicate nonfailure.

stainless steel were irradiated[38] in the Materials Testing Reactor, with nominal fission burnups of 9, 16, and 26% of the U^{235} atoms. The postirradiation tests indicated that the surface temperatures ranged between 715 and 1220°F for all the samples and that the samples experiencing the nominal 26% burnup of U^{235} atoms swelled approximately 30% in thickness. Figure I-9 shows the temperature-burnup limitations for the UO_2–stainless-steel dispersion fuels. This figure compares the data furnished by the above samples, ORNL-46, with available information where the burnup was measured and temperatures were reasonably well documented. The stable fuels, as listed, often exhibited some swelling with no evidence of blistering or gross dimensional changes. (D. L. Stoltz)

Cermet Fuels

Battelle[33] measured thermal conductivity and electrical resistivity concurrently for an 80 vol.% UO_2 (tungsten-coated UO_2 particles)–tungsten cermet having a density of 98% of theoretical. The results are shown in Table I-5.

Table I-5 INTERPOLATED THERMAL-CONDUCTIVITY AND ELECTRICAL-RESISTIVITY VALUES FOR TUNGSTEN–80 VOL.% UO_2 (VAPOR-DEPOSITED TUNGSTEN) CERMET[33]

Temp., °C	Thermal conductivity, watts/(cm)(°C)	Electrical resistivity, μohm-cm
25		$41._5$
100	0.30_1	$54._5$
200	0.27_2	$72._0$
300	0.25_1	$89._5$
400	0.23_6	108
500	0.22_5	129
600	0.21_7	152
700	0.21_2	172
800	0.21_0	195
900	0.20_9	217
1000	0.20_8	238

At Los Alamos[41] a blend of 80 vol.% PuO_2–20 vol.% type 302B stainless steel was sintered at 1650°C to approximately 90% of theoretical density. Microstructures of the densified samples indicated the formation of a liquid phase which produced a dispersion of stainless-steel particles in a continuous PuO_2 matrix. Similar results were obtained[42] in sintering studies of UO_2–stainless steel when sintering was done above the melting point, apparently as a result of nonwetting of the oxide by the metal matrix.

Workers at Hanford carried out pneumatic impaction of a 65 vol.% UN–35 vol.% molybdenum cermet to 97% of theoretical density.[22] In addition, 90 vol.% PuN–10 vol.% plutonium cermet samples were heat-treated in an alumina crucible for 2 hr at 1000°C in a vacuum. Visual inspection of the contact area between the crucible and the cermet samples indicated no visible melting or reaction.[18] (D. E. Kizer)

Coated-Particle Fuel Materials

Particle Coating

Preparation of zirconium carbide-coated uranium oxide fuel particles has been investigated by Davies et al.[43] The zirconium carbide coatings were prepared at 1500°C from the reactants methane or toluene and zirconium tetrachloride in a hydrogen-fluidized bed or, more satisfactorily, in a rotating crucible. Agglomeration difficulties were encountered with the fluidized-bed technique and, as an alternative, the rotating crucible was used to prepare material for irradiation tests. The results of initial out-of-pile tests have been encouraging. However, the contribution of excess carbon in the coating to the out-of-pile results is not known. The authors advocate the development of a fluidized-bed process for preparation of large quantities of coated product, in spite of early difficulties with the method.

Molybdenum coatings were deposited on UO_2 by hydrogen reduction of $MoCl_5$ in a fluidized bed by Gadiyar and Balachandra.[44] It was determined that the density of the coating and the sintered density of the consolidated material increases as the molybdenum deposition temperature was increased from 550 to 700°C.

In attrition studies on Al_2O_3-coated and uncoated $\frac{1}{8}$-in.-diameter spheres of ThO_2, workers at Oak Ridge concluded that vapor-deposited Al_2O_3 effectively decreased attrition of pellets, providing proper coating conditions are maintained.[37] The ThO_2 pellets were coated with Al_2O_3 at Battelle and then evaluated by Oak Ridge.

Other work reported by Oak Ridge includes a description of metallographic techniques that were developed for examination of coated and

uncoated uranium carbide particles, both in the unsupported condition and as-fabricated in graphite matrices.[45] The structural and compositional variations found in various lots are presented, and the effects of heat-treatments on the particles and coatings are described.

Four experimental pyrolytic carbon coating runs were made by Oak Ridge[46] under conditions designed to deposit a porous carbon layer on uranium carbide fuel particles. The conditions required for formation of a porous deposit are reported to be (1) a relatively low coating temperature (<1400°C) and (2) a high partial pressure of hydrocarbon (1 atm). With acetylene as the source of carbon, much soot was formed during the coating runs. The coated products had random crystallite orientation, good crushing strength, and appeared to be porous. A quantitative measurement of the porosity has not been made.

Fuel for the Peach Bottom High-Temperature Gas-Cooled Reactor will consist of PyC-coated $(Th,U)C_2$ particles, coated at about 1400°C by pyrolysis of CH_4 in a fluidized bed and dispersed in graphite-matrix fuel compacts.[47] A review of research by General Atomic on PyC-coated carbide fuel particles and graphite-matrix fuel compacts through the spring of 1962 is reported.

A topical report on the preparation of pyrolytic carbon coatings has been compiled by workers at Battelle.[48] Fluidized-bed techniques and conditions used to prepare columnar, laminar, porous, and composites of the three types of PyC coatings are described. Several of the conclusions drawn from the work are: (1) the growth structure of PyC coatings deposited at 1400°C by pyrolysis of acetylene can be varied with the deposition rate, with the lower rates favoring the columnar type; (2) a minimum density is obtained at coating temperatures of 1400 to 1500°C; (3) migration of uranium causes contamination of the coating at deposition temperatures of 1600°C and above; and (4) after low irradiation exposure, both monolithic and composite coatings retain fission gases at temperatures up to 1300°C. The more encouraging extended-radiation results were obtained with composites of metal oxide and duplex PyC coatings. It was also determined that PyC-coated UC_2 can be prepared by coating uranium metal with PyC and then reacting the two *in situ*.

Fuel slugs were prepared at Battelle by use of a technique suggested by Nuclear Materials & Equipment Corp.[49] The interstitial voids between PyC-coated particles were infiltrated in a packed bed of the particles with a PyC matrix to form a strong fuel body. In addition, attempts were made to identify the mechanisms that affect the coating properties. Inclusion of carbon dust, formed by the gas-phase decomposition of the hydrocarbon, is the primary factor affecting the properties of the coating. A study has been initiated to determine the role that homogeneously nucleated soot particles play in determining the coating properties.[32,33,50] In addition, coatings are being developed to withstand fuel migration at elevated temperatures. Various combinations of columnar, laminar, and porous PyC are being studied.

The development of BeO coatings on UO_2 is being continued, with emphasis on control of the as-deposited grain structure.[33,50] Recently it was learned that BeO coatings, deposited at 1500°C on dense PyC-coated UO_2, consist of large crystals that grow only in isolated clusters, whereas BeO deposited directly on UO_2 at 1500°C forms large, coherent, nearly equiaxed grains. It was also learned that a porous PyC coating provided a nucleating surface for BeO deposited at 1500°C, which was superior to that provided by dense PyC. An additional improvement was obtained by the deposition of an intermediate porous BeO coating at 600 to 700°C on the porous PyC. The porous BeO was then overcoated with dense BeO at 1500°C. Good coverage by a fine-grained BeO coating on a porous PyC layer was achieved also by rapid deposition (14 μ/hr, as compared to the usual 3 to 7 μ/hr) at 1400 to 1500°C. (N. D. Veigel)

Irradiation and Evaluation of Coated-Particle Fuels

Oxide-Base Fuel. Specimens consisting of 200-μ, 92% dense UO_2 particles coated with 5 μ of Al_2O_3 and overcoated with 118 μ of columnar pyrolytic carbon are currently being irradiated at Battelle.[32,33,50] The purpose of the thin layer of Al_2O_3 is to prevent infiltration of carbon into the porous UO_2 during the coating operation. A specimen of unsupported particles of this type was irradiated at 815°C to an estimated burnup of 1.5×10^{21} fissions/cm^3, or 9 at.%, with no coating failure. The fission-gas-release fractions (R/B) remained in the order

of 10^{-9} throughout the irradiation. A number of thermal cycles to temperatures as low as 50°C occurred with no detrimental effects on the coatings. A graphite-matrix specimen of these particles is being irradiated at 1000°C, and after approximately 2 at.% burnup the coatings are still intact.

An elevated-temperature irradiation of Al_2O_3-coated UO_2 particles is also in progress. The specimen consists of 200-μ, 80% dense UO_2 particles coated with 60 μ of Al_2O_3 and dispersed in a graphite matrix. The temperature in the capsule is achieved by fission heating and is permitted to fluctuate with reactor power. During reactor operation, the specimen temperature has ranged from 770 to 940°C. The equilibrium fission-gas-release fractions have remained about 10^{-7} throughout the first 3 at.% burnup, with no apparent coating failure. This good performance is not surprising, since the use of porous UO_2 particles has been found to prevent the in-pile failure of Al_2O_3 coatings.

Additional irradiation studies of BeO-coated UO_2 particles have been conducted at Battelle, but successful performance has not yet been achieved.[32,33,50] A specimen of 127-μ, 80% dense UO_2 particles coated with 60 μ of BeO was irradiated at 100°C and at 815°C. Essentially complete failure of the coatings occurred during the first 2 hr of irradiation at 100°C. Cracking of the coatings also occurred in the 815°C experiment, but only when the temperature was cycled to 300°C and to 80°C. The poor performance of this material may not be typical of good BeO coatings. Considerable grain growth occurred in the process of depositing the BeO, and the coatings contained grains that extended all the way through the coatings in some cases.

Carbide-Base Fuel. Irradiation data obtained for pyrolytic carbon-coated carbide fuel particles on the Dragon Project have been summarized in a recent report.[51] Sintered, porous fuel particles (50 to 82% of theoretical density) of UC_2, $(Th,U)C_2$, and $(Zr,U)C_2$ were used in addition to high-density melted particles of the type used in all the U. S. work. The porous UC_2 particles coated with double and triple layers of laminar pyrolytic carbon (coating thicknesses in the range of 54 to 77 μ) were irradiated to burnups ranging from 3.3 to 14 at.% at temperatures from 700 to 1500°C. In most cases there was very little coating failure, and the porous UC_2 cores were observed to have densified and shrunk significantly. The densification occurred over the whole temperature range but was most pronounced at the lower temperatures. The sintering was found to be irradiation induced, since an out-of-pile annealing of the particles caused no microstructural change. Swelling of the UC_2 during irradiation at least partially offset the sintering and densification. The effect of the swelling was to cause local expansion of the UC_2 into cracks in the inner layer(s) of the pyrolytic carbon coatings. The sintered $(Th,U)C_2$ and $(Zr,U)C_2$ did not appear to densify as markedly as the UC_2 under irradiation. The melted $(Zr,U)C_2$ particles were essentially unchanged by the irradiation, and the melted $(Th,U)C_2$, which was monocrystalline, either appeared to undergo a phase transformation or cracked, which resulted in cracks also occurring in the coatings. No swelling was observed for the alloyed fuels, but the burnups were lower than for the UC_2 particles. The $(Zr,U)C_2$ cores were coated with a double coating of laminar pyrolytic carbon, a duplex coating of laminar and columnar pyrolytic carbon, or a triplex coating consisting of two 20- to 30-μ layers of laminar pyrolytic carbon separated by a 22-μ layer of SiC. The irradiations were to burnups of 2 to 2.6 at.% of metal at temperatures from 1300 to 1660°C. In most cases no coating failure occurred, but in some of the lower temperature irradiations large fractions of the coatings cracked. Surprisingly, the same coatings performed well at the higher temperatures. The $(Th,U)C_2$ particles were coated with varying thicknesses of the triplex coating containing the SiC. No coating failure occurred in irradiations to burnups of 1.2 to 2.7 at.% of metal at 850 to 1400°C except in two cases, where the fuel cores shattered.

In nearly all the particles irradiated in the Dragon Project studies, "spearhead attack" was observed.[51] Spearhead attack is defined as the formation of V-shaped cracks extending radially outward from the fuel core into the first 20 to 25 μ of the pyrolytic carbon coatings. It has been postulated that this results from shrinkage of the pyrolytic carbon caused by fission-fragment bombardment. Failure of the coatings normally occurred through outward growth of spearhead attack or cracks associated with it. The propagation of cracks from the spearhead attack was often stopped by the interface between two laminar pyrolytic carbon coatings or between the two layers of a duplex coating. The importance of an interface to stop crack

propagation has also been emphasized by Oak Ridge[52] and is inherent in the studies at General Atomic[53] and Battelle.[54]

Because of their superior irradiation performance, duplex and, more recently, triplex coatings have been receiving much attention. Satisfactory performance has been demonstrated at Oak Ridge for duplex coatings that consist of an inner layer (approximately 30 μ) of low-density laminar pyrolytic carbon and an outer layer (70 to 100 μ) of high-density columnar pyrolytic carbon. No broken coatings were detected for a specimen of unsupported $(Th,U)C_2$ particles having this type of coating after a burnup of 15 at.% of heavy metal at 1120°C. Fission-gas-release fractions were below 10^{-10} for a fueled-graphite sphere that contains particles of this type after 5 at.% burnup of heavy metal at 1000°C.[52] Similar results were reported by Battelle[32,33,54] for UC_2 particles coated with 39 μ of porous (approximately 50% dense) sooty carbon and 69 μ of columnar pyrolytic carbon. No failure occurred in an irradiation to 6 at.% burnup at 815°C.

Triplex pyrolytic carbon-coated UC_2 and $(Th,U)C_2$ particles prepared by General Atomic were irradiated at Oak Ridge.[55,56] These coatings contain an inner layer of porous carbon, a layer of laminar pyrolytic carbon, and an outer layer of columnar pyrolytic carbon (total coating thickness of 100 to 150 μ). One specimen was irradiated to a burnup of 9 at.% of heavy metal at 1120°C, with the fission-gas-release fractions (R/B) remaining constant at approximately 10^{-6}. Another specimen was irradiated to 20 at.% burnup at 1370°C, with final R/B values on the order of 10^{-5}. In this case the gas release was constant for the first two weeks and then gradually increased to double the initial value.[56] Graphite-matrix specimens of this type of material are being irradiated at 1370°C, and the R/B values are remaining constant[55] at about 10^{-4}. This high level of release may be a result of coatings being cracked in the process of preparing the specimens.

Fission-product-release data and irradiation results for monolithic pyrolytic carbon coatings which were obtained earlier by General Atomic have been summarized in two recent reports.[47,57] (C. W. Townley)

Compatibility of Coated Particles

In a study of compatibility problems related to the use of carbon-coated ThC-UC fuel particles, workers at General Atomic[47] have discussed and summarized the "amoeba" effect. They found that, although the particles were apparently stable at high temperatures, coatings failed when compacts were heated in a thermal gradient. Metallographic examination indicated that coating failure was due to carbide attack on the coating on the high-temperature side of the particle. In all cases the particles appeared to be moving toward the hottest region of the compact. This behavior is reported to be caused by solution of the carbon coating on the high-temperature side and precipitation behind the particle on the low-temperature side. The amoeba effect has been observed only at temperatures above 1800°C, with a temperature gradient across a particle (~200-μ diameter) of only about 3°C. This same behavior was also observed for carbon-coated UC_2. Carbon-coated high-carbon UC_2 particles presently being made at General Atomic do not show this effect. The same workers also investigated coating-fuel reactions in long-term isothermal tests. They found that at 1700°C after 3100 hr there was some reaction but that particles with coatings deposited from methane gave better results than those coated from acetylene. The same behavior was observed after 7000 hr at 1550°C, where reaction occurred in coatings deposited from

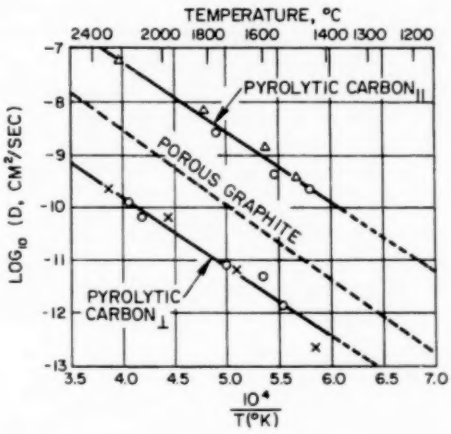

Fig. I-10 Actinide diffusion coefficients as a function of temperature.[52] The porous graphite curve is based on the results of instantaneous-source-layer experiments with thorium and constant-potential experiments with uranium. Δ, U^{235} (as F.P.); ○, Pa^{233} (with Th); ×, Th^{232}.

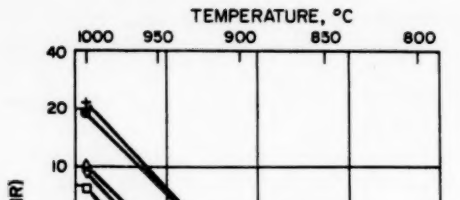

Fig. I-11 Arrhenius plots of the steam reaction with various fueled graphite spheres.[52] +, 3M-S3-15; ●, 3M-S2-23; Δ, GA-S3-6, ▽, NCF-S3-Ri; ■, GA-S4-9; ×, GA-S5-11.

acetylene. However, no reaction was observed for particles with coatings deposited from methane.

The diffusion of uranium in pyrolytic carbon is also being studied at General Atomic.[58] In the course of the investigation, rapid surface diffusion was observed and a value of 10^{-5} cm^2/sec was estimated for the surface diffusion coefficient of uranium in pyrolytic carbon at 954°C.

Oak Ridge[52] has studied the diffusion of uranium, protactinum, and thorium in pyrolytic carbon and porous graphite. The results are summarized in Fig. I-10. They have also studied the compatibility of graphite and carbon-coated fuel particles in steam at 800 to 1000°C. The results for several lots of commercially prepared coated particles are shown in Fig. I-11. The rate of attack on the coated particles was not found to differ significantly from that of unfueled graphite.

Battelle[59] has completed a compatibility study of oxide-coated fuel particles in graphite and has also determined the oxidation resistance of oxide-coated UO_2. The results are shown in Tables I-6 and I-7. On the basis of these data, it was estimated that Al_2O_3-coated UO_2 particles were resistant to oxidation for several thousand hours at temperatures to 1100°C and BeO-coated UO_2 particles to temperatures of 1000°C. In flowing argon, beryllia-graphite mixtures

Table I-6 OXIDATION RESISTANCE OF OXIDE-COATED* UO_2 PARTICLES†[59]

Oxide coating	Time, hr	Temp., °C	Failed particles, %	Est. max. temp. for 10,000-hr service, °C
Al_2O_3	6000	1100	0	1100
	3000	1200	0	
	300	1300	0	
	136	1400	30	
BeO	5000	1000	0	1000
	2000	1100	20	
MgO	45	900	42	
	70	800	47	

*Oxide coatings as follows: (1) 54-μ Al_2O_3 coating deposited at 1400°C on 126-μ UO_2, (2) 60-μ BeO coating deposited at 1000°C on 127-μ UO_2, and (3) 60-μ MgO coating deposited at 1400°C on 127-μ UO_2 (coating was applied in two steps: 22 μ at 1000°C followed by 38 μ at 1400°C).

†Atmosphere was 100% (dried) oxygen, flowing at 250 cm^3/min under a slight positive pressure.

Table I-7 RESULTS OF COMPATIBILITY STUDIES* INVOLVING OXIDE-GRAPHITE MIXTURES[59]

Reactants	Temp., °C	Time, hr	Max. depth of penetration, μ	Remarks
Al_2O_3 + graphite	1700†	25	Complete	Al_4O_4C
	1500	74	25	Al_4C_3
	1400	145	20	Al_4C_3
	1300	2542	<2	
	1200	3169	<2	
	1100	3500	<2	
BeO + graphite	1600	25	<2	
	1500	60	<2	
	1400	1512	<2	
	1300	2500	<2	
MgO + graphite	1300	400	4	
	1100	1000	2	
	1000	3072	6	
	900	2754	<2	
ZrO_2 + graphite	1400	25	6	ZrC
	1200	957	3	ZrC
	1100	1292	2	
	900	2754	<2	

*Test conditions were as follows: (1) Flowing argon (250 cm^3/min) at slight positive pressure, (2) 150 to 200-μ oxide particles and 44-μ carbon particles, and (3) 50 wt.% mixtures of the above particles.

†Tested in flowing hydrogen.

formed the most stable oxide-graphite combination, followed by mixtures of graphite with alumina, magnesia, and zirconia. The results suggest that beryllia-graphite mixtures should be compatible for 10,000 hr at temperatures >1400°C, alumina-graphite to 1350°C, magnesia-graphite to 950 to 1000°C, and zirconia-graphite to 900 to 1000°C. (G. W. Cunningham)

Uranium Oxide Fuel Materials

Properties and Behavior

In a recent article de Halas[60] discusses the various factors that contribute to the thermal conductivity of UO_2 over different temperature ranges. It is postulated that, at low temperatures, internal radiation is a more important means of conduction in large-grain near-stoichiometric UO_2 than it is in small-grain hyperstoichiometric UO_2. Above 800°C heat transfer is expected to increase in large-grain near-stoichiometric UO_2 as conduction by internal infrared radiation increases. At about 1200°C the infrared absorption coefficient has increased to the extent that thermal conduction again decreases until the electronic contribution to heat transfer becomes significant at about 1800°C. Thermal conduction then increases with rising temperature. M. F. Lyons et al.[61] have determined the thermal conductivity of 95% dense polycrystalline UO_2 in the temperature range from 1900 to 2450°C. Their results, along with those of other investigators, are presented in Fig. I-12. These thermal-conductivity values were determined by examining the structural changes occurring across the radii of cylindrical specimens irradiated for short times under well-known thermal conditions.

In other high-temperature studies, J. B. Conway et al.[62] measured thermal expansion and enthalpy (heat capacity) for 95.5% dense sintered UO_2, covering temperatures up to 2200°C. These results are shown in Figs. I-13 and I-14.

Creep deformation tests were performed on sintered uranium oxide in the composition range $UO_{2.00}$ to $UO_{2.25}$ at temperatures from 975 to 1400°C by Armstrong and Irvine.[63] The creep

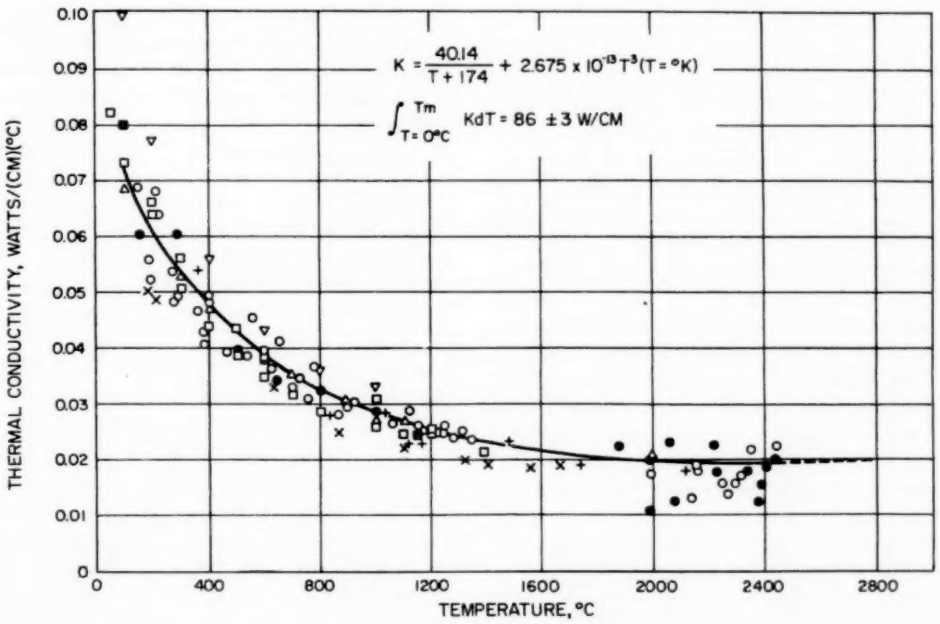

Fig. I-12 The UO_2 thermal conductivity vs. temperature for 95% of theoretical density.[61] ×, Hedge and Fieldhouse; ○, Howard and Gulvin; ∇, Kingery; □, Lucks and Deem; Δ, McElroy and Godfrey; +, Reiswig; ■, Scott; ●, experimental data from this study.

behavior of compositions from $UO_{2.02}$ to $UO_{2.08}$ followed the expression

$$\epsilon = A[(O/U) - 2]\ \sigma \exp(-55{,}700/RT)$$

where ϵ is the unit strain rate for a tensile stress σ, R is the gas constant, T is the absolute temperature, and A is a constant. For the particular material studied, which had a density of 96.0% and grain size of about 6 μ, A has a value of 0.064 poise^{-1}. Metallographic studies disclosed that creep occurs by slippage along grain boundaries. The presence of excess oxygen was found to inhibit the intercrystalline cracking that accompanies creep of stoichiometric UO_2.

A topical report from Hanford[64] describes measurements of the visible and infrared absorption spectra of UO_2 at room temperature. The UO_2 spectrum exhibits the features of a typical semiconductor: opaque in the visible but transparent over much of the infrared. The absorption edge occurs at about 0.6 μ. For single-crystal oxide with an oxygen-uranium ratio from 1.96 to 2.001, the absorption coefficient between 1.5 and 15 μ attains a maximum value of 57 cm^{-1} at 1.70 μ and a minimum value of 6 cm^{-1} at both 2.75 and 8 μ. Below 8 μ the absorption coefficient for 97.5% dense polycrystalline material with an oxygen-uranium ratio of 2.001 is about 10 times larger than for single-crystal UO_2.

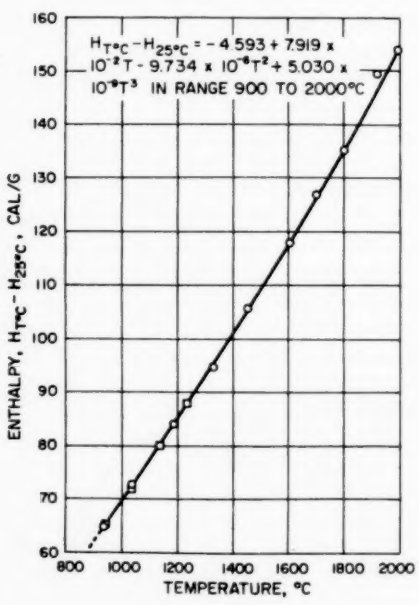
$H_{T°C} - H_{25°C} = -4.593 + 7.919 \times 10^{-2} T - 9.734 \times 10^{-6} T^2 + 5.030 \times 10^{-9} T^3$ IN RANGE 900 TO 2000°C
ENTHALPY, $H_{T°C} - H_{25°C}$, CAL/G
TEMPERATURE, °C

Fig. I-13 Enthalpy-temperature data for sintered UO_2.[62] ○, Conway et al.; □, Moore and Kelley.

The phase structure of the UO_2-Eu_2O_3 system was investigated by Haug[26] using X-ray spectroscopy. For compositions of 38 to 64 mole % $EuO_{1.5}$ annealed at 1100°C, a fluorite structure with lattice constants of 5.406 and 5.391 A was observed. On the uranium-rich side of the system, a second phase appeared that contained $UO_{2.6}$ in a mixed crystal with 38 mole % $EuO_{1.5}$.

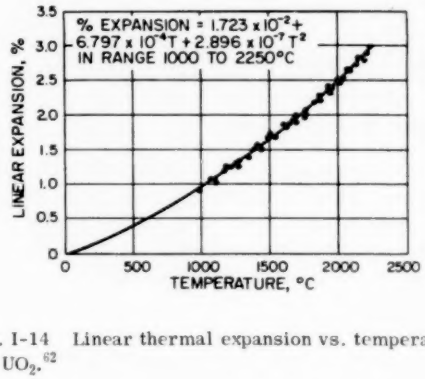

Fig. I-14 Linear thermal expansion vs. temperature for UO_2.[62]

The effects of additions of 0.1 wt.% TiO_2 to UO_2 and 0.4 wt.% Nb_2O_5 to UO_2 on the irradiation characteristics of UO_2 fuel elements were studied at Chalk River.[65] These additives were found to have no influence on fission-gas release or fuel-element dimensions for burnups up to about 1500 Mwd/ton of uranium. However, there was evidence of a low-melting UO_2-Nb_2O_5 eutectic and niobium migration to the hot central-core zone from the surrounding cooler regions.

The diffusion of Pu^{239} in sintered UO_2 was measured by Schmitz and Lindner.[66] Over the temperature range from 1260 to 1575°C, the diffusion coefficient can be represented by

$$D = 0.34 \exp(-97{,}300/RT)\ \text{cm}^2/\text{sec}$$

for 97% dense UO_2. The emanation of thoron (Rn^{220}) from sintered UO_2 powders and plates was measured as a function of temperature at Bettis.[67] For sintered UO_2 with densities from 71 to 85% of theoretical, the diffusion coefficient for thoron can be expressed by

$$D = 1 \times 10^{-8} \exp(-39{,}500/RT)\ \text{cm}^2/\text{sec}$$

for temperatures from 1100 to 1450°C. The diffusion coefficient for 99% dense UO_2 followed the expression

$$D = 0.13 \exp(-79{,}960/RT) \text{ cm}^2/\text{sec}$$

over the temperature range from 1200 to 1450°C. The variation of activation energy over the temperature range from 400 to 1450°C indicates that radon diffusion in UO_2 involves several different processes.

Scott and Harrison[68] have studied the oxidation of UO_2 in air under conditions of linearly increasing temperature up to 800°C. UO_2 powder was found to oxidize in a two-step process: first to a tetragonal phase of composition $UO_{2.35}$ and then to U_3O_8. The activation energy for the oxidation of UO_2 to U_3O_7 was determined to be 19.1 kcal/mole. The UO_2 with low surface area followed only a single-step process in oxidizing from UO_2 to U_3O_8. Oxidation rates were proportional to the heating rate.

Work on uranium oxide-fueled glasses is continuing at Argonne.[2] Density measurements were made on Na_2O-CaO-SiO_2 and Na_2O-K_2O-SiO_2 base glasses fueled with UO_2. The limits of UO_2 solubility were found to be between 60 and 70 wt.% UO_2 for the Na_2O-K_2O-SiO_2 glass and 50 to 60 wt.% UO_2 for the Na_2O-CaO-SiO_2 glass. Results of the density measurements are shown in Fig. I-15. The effect on thermal expansion of a 35 wt.% addition of UO_2 to Na_2O-K_2O-SiO_2 base glass is shown in Fig. I-16.

(R. H. Barnes)

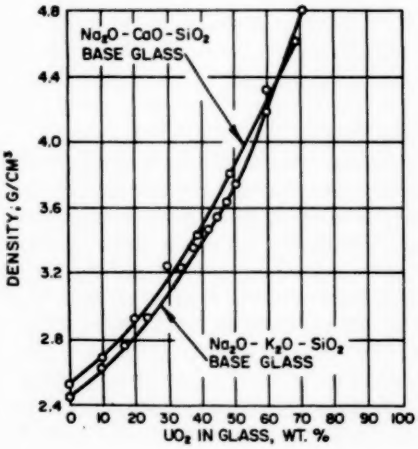

Fig. I-15 Effect of UO_2 on density of base glasses.[2]

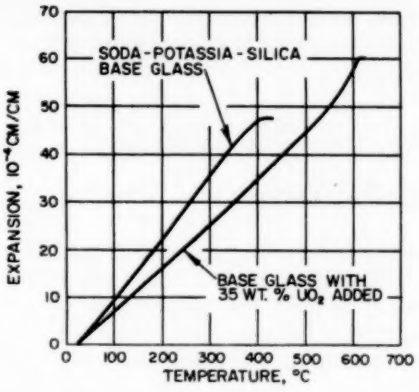

Fig. I-16 Thermal expansion to softening point of base and fueled glasses.[2]

Preparation of Uranium Oxide Fuel Bodies

A final report[69] was issued by FIAT on steam sintering of UO_2. The use of CO_2 in the sintering of UO_2 was also studied at the same site.[70] It was concluded that CO_2 is about as effective as steam as a sintering atmosphere at 1400 to 1500°C. Maximum UO_2 pellet density was achieved with either steam or CO_2 at a temperature approximately 300°C lower than that required with hydrogen.

It was determined by British workers[71] that grain growth in UO_2 pellets can be suppressed by the addition of a second phase of platinum at the 0.1 wt.% level or by sintering for prolonged periods at low temperatures. Densities approaching 10.9 g/cm^3 were obtained by sintering the UO_2 for 70 hr at 1400°C in hydrogen.

A final report has been issued by workers at United Nuclear[72] on the characterization of UO_2 powders. The fabrication and characterization of UO_2 pellets prepared at FIAT is described in a recent topical report.[73] Ceramic-grade UO_2 from three different sources was used in this study.

Thin, uniform plates of uranium dioxide were prepared by a powder rolling process.[74] Continuous strips approximately 4 in. wide and 0.020 to 0.100 in. thick were prepared by this technique. Following sintering at 1700°C in hydrogen, a density of 10.4 g/cm^3 was achieved.

The technique used to fabricate the PWR core 2 seed fuel wafers was reported by workers at Bettis.[75] Approximately 1,300,000 high-density enriched urania-zirconia fuel wafers were man-

ufactured on this program. Techniques used to obtain high-density urania-zirconia wafers are described. (D. E. Rhodes)

Uranium Carbides and Nitrides

Two independent investigations of the uranium-molybdenum-carbon constitution diagram are in agreement that pseudobinary tie lines exist between UC and molybdenum and between $UMoC_2$ and UC, UC_2, graphite, Mo_3C_2, and Mo_2C.[76,77] Rudy and Benesovsky suggest that the composition of a newly discovered ternary phase is near 20 at.% uranium–50 at.% molybdenum–30 at.% carbon.[76] Chubb and Keller suggest that the composition of this same ternary phase is near 33 at.% carbon, 33 at.% molybdenum, and 33 at.% uranium but that it probably contains slightly more than 33 at.% carbon.[77a] Pseudobinary tie lines exist in the thorium-molybdenum-carbon system between ThC and molybdenum, between ThC and Mo_2C, between ThC_2 and Mo_2C, and between ThC_2 and Mo_3C_2.[76]

Many of the refractory metals form monocarbides but not dicarbides. These monocarbides often form solutions with UC which are stable in the presence of excess carbon to form UC_2. This concentration of UC probably always decreases with increasing temperature, since the stability of UC_2 increases with temperature up to its melting point. Rudy and Benesovsky have determined the location of this composition at which the solid solution first reacts with carbon to form UC_2 for a variety of systems as a function of temperature. Their results are shown in Table I-8.[78]

Chubb and Keller have investigated the major features of the systems of uranium and carbon with molybdenum, niobium, rhenium, tungsten, and yttrium.[77a] The uranium-carbon-niobium system shows pseudobinary tie lines between NbC and UC, between NbC and uranium, and between Nb_2C and uranium. Substoichiometric NbC and Nb_2C will dissolve less than 1 at.% uranium. The uranium-carbon-rhenium system contains an orthorhombic ternary phase, $UReC_2$, and shows pseudobinary tie lines between UC and URe_2, between UC and rhenium, between UC and $UReC_2$, between $UReC_2$ and carbon, and between $UReC_2$ and rhenium. The uranium-carbon-tungsten system shows pseudobinary tie lines between UC and tungsten, between UC and UWC_2, and between UWC_2 and U_2C_3, UC_2, carbon, WC, W_2C, and tungsten. The uranium-carbon-yttrium system shows complete solubility between UC_2 and YC_2 and between UC and YC (40 at.% carbon). A pseudobinary tie line exists between YC (40 at.% carbon) and uranium metal.

J. T. Dalton has determined that U_2C_3 and Pu_2C_3 form a complete series of solid solutions and that Pu_2C_3 stabilizes U_2C_3 to appreciably higher temperatures.[77b]

The limit of solubility of "UO" in UC is variously reported as 37 mole % UO,[77c] 35 mole % UO,[77d] 35 mole % UO,[77e] and 25 mole % UO.[79]

Briggs et al. have prepared a revised diagram of the uranium-chromium-carbon system showing pseudobinary tie lines radiating from UC to chromium, $Cr_{23}C_6$, Cr_7C_3, Cr_3C_2, and $UCrC_2$. In studies of the pseudoternary system, UC-iron-chromium, it was found that iron-chromium alloys that contained from about 8 to 98 wt.% chromium reacted with UC to form $Cr_{23}C_6$ and UFe_2.[77f]

Table I-8 THE COMPOSITION OF MONOCARBIDE SOLID SOLUTIONS AT WHICH UC_2 AND GRAPHITE AND MONOCARBIDE CAN EXIST IN EQUILIBRIUM[78]

Temp., °C	Mole % in MC in (U,M)C			
	ZrC	NbC	TaC	HfC
1630	10	10	9	
1720	30	48	49	87
1800	40	57	76	88
1900	60	70	79	88
2000	70	75	81	89
2100	75	77	83	89
2200	78	78	85	89

Nichols and Marples[77g] have determined the eutectic temperatures in the uranium-iron-carbon and plutonium-iron-carbon systems as follows: $UFeC_2$-Fe binary at 1160°C, UC-$UFeC_2$-Fe ternary at 1130°C, UC-Fe binary at 1117°C, UC-Fe-UFe_2 ternary at 1037°C, UC-UFe_2 binary at 1200°C, UC-UFe_2-U ternary at 720°C, PuC-$PuFe_2$ binary at 1081°C, Pu_2C_3-$PuFe_2$ binary at 1100°C, $Pu_2Fe_2C_3$-$PuFe_2$ binary at 1051°C, Pu_2Fe_2C3-$PuFe_2$-Fe ternary at 1037°C, $Pu_2Fe_2C_3$-Fe binary at 1143°C, $PuFeC_2$-Fe binary at 1156°C, and $PuFeC_2$-Fe_3C binary at 1096°C.

Shalek and White find that UC and US do not form a complete series of solid solutions.[77h] UC dissolves up to 4 mole % US and US dissolves up to 40 mole % UC.

Thorpe et al. examined UC–50 mole % ZrC alloy as a possible fuel for thermionic energy converters.[77i] At 1850°C niobium reacted with UC-ZrC and penetrated the UC-ZrC grain boundaries, causing the UC-ZrC grains to split apart. Uranium diffused into the niobium and showed a tendency to concentrate at grain boundaries. Zirconium also diffused into the niobium but at a much slower rate than the uranium. A slight reaction was observed between UC-ZrC and tantalum at 2130°C. No reaction was observed between UC-ZrC and tungsten up to 2200°C.

Alexander et al. have obtained equilibrium-vapor-pressure data for the uranium carbides, using Knudsen effusion techniques. The partial pressures obtained are much higher than those obtained by the Langmuir technique and may be represented by the equations:

$$\text{For UC: } \log P \text{ (atm)} = -27{,}800/T + 6.10$$

$$\text{For } UC_2\text{: } \log P \text{ (atm)} = -27{,}600/T + 5.05$$

The free energies of formation of the various uranium carbides based on the Knudsen vapor-pressure data[77j] are shown in Fig. I-17.

Norreys et al.[77k] find that the thermal-expansion coefficient of U_2C_3 is almost identical to that of UC and equal to 10.5×10^{-6}/°C from 20 to 1000°C.

Norreys[77m] has obtained compressive creep data on uranium carbides and dilute uranium carbide-tungsten alloys at temperatures from 1000 to 1500°C. At 1300°C and 6000 psi, uranium–50.5 at.% carbon and uranium–52 at.% carbon alloys showed strains of less than 2% in 30 hr, whereas a uranium–49.5 at.% carbon alloy showed a strain of over 24%. An addition of 0.9 wt.% tungsten to hyperstoichiometric UC reduced the creep rate at 1400°C by a factor of 50. The activation energy for creep of uranium–50.5 at.% carbon alloy at temperatures from 1200 to 1400°C was found to be 49 kcal/mole.

Bentle et al.[80] have obtained additional data on the deformation of uranium carbide at constant strain rates and at temperatures from 1500 to 2000°C. At a strain rate of 4×10^{-4}/min, hypostoichiometric and stoichiometric uranium carbide supported stresses of about 2200 psi at 1500°C, 1200 psi at 1800°C, and 900 psi at 2000°C at a strain of 0.06%. Hyperstoichiometric uranium carbide supported stresses of about 5000 psi at 1500°C, 2200 psi at 1800°C, and 1500 psi at 2000°C at the same strain.

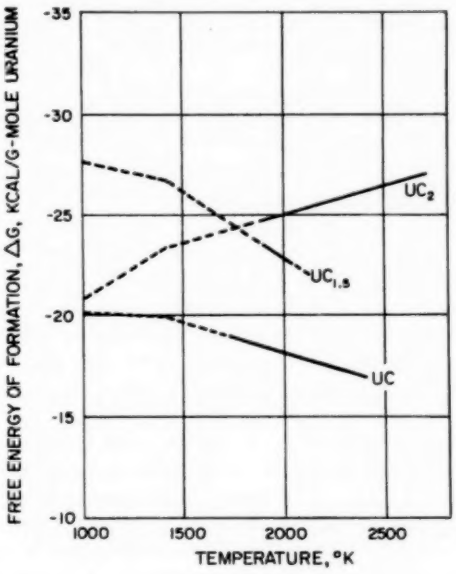

Fig. I-17 Free energies of formation of uranium carbides.[77j]

United Nuclear has reported additional results of its studies on the effect of stoichiometry and fabrication techniques on the irradiation behavior of uranium carbide.[81] The samples were clad in niobium–1 wt.% zirconium and were irradiated at surface temperatures of 700 to 800°C to burnups of 15,000 to 25,000 Mwd/ton of uranium. The results summarized in Table I-9* indicate a pronounced effect of stoichiometry on the irradiation behavior of uranium carbides at these temperatures. The results also suggest that sintered carbides release slightly more fission gas than the dense cast carbides.

S. Rosen finds that thorium and thorium monocarbide in equilibrium with uranium metal at 950°C contain less than 1 at.% uranium.[2]

*Table I-9 is made up of data taken from the tabulation on page 6 of Ref. 81.

Battelle[82] reports that the solubility of nitrogen in liquid uranium is about 0.1 wt.% at 1700°C, about 0.5 wt.% at 2150°C, and about 1.2 wt.% at 2380°C. Uranium mononitride reacted with aluminum in 400 hr at 500°C, with zirconium in 100 hr at 900°C, and with stainless steel in 100 hr at 1300°C.

Wullaert et al.[83] concluded that uranium mononitride has excellent radiation stability on the basis of a series of irradiations at surface temperatures as high as 615°C and centerline temperatures of 1260°C. The production of hydrogen by the (n,p) reaction was not detrimental to the UN at surface temperatures from 65 to 615°C. At the maximum burnup of 3.8 at.% of the uranium, diameter and length changes of about 2% were measured. (W. Chubb)

Table I-9 EFFECT OF STOICHIOMETRY AND FABRICATION TECHNIQUE ON THE IRRADIATION BEHAVIOR OF URANIUM CARBIDES[81]

Carbon content, wt.%	Fabrication method	Fission-gas release, % Kr	Diameter change, %	Density change, %
4.3	Sintered	45	11	26
4.3	Sintered	50	1	15
4.4	Cast	30	11	24
4.4	Cast	43	0.7	14
4.8	Sintered	14		9
4.8	Sintered	16	1	3
4.7	Cast	7		6
4.7	Cast	5	3	6
5.2	Cast	4		7
5.2	Cast	1	3	6

Mechanism of Corrosion of Fuel Alloys

The oxidation of uranium by CO_2 at temperatures above 900°C was investigated by Bessonov and Vlasov.[84] The oxidation rate was found to be dependent on the one-fourth power of the pressure. The rate decreased when the temperature of the uranium was increased from 900 to 1000°C, owing to an increase in density of the UO_2 surface layer. At temperatures below 780°C, oxidation proceeded mostly by oxygen diffusion inward through the oxide layer, but at temperatures greater than 900°C the rate of diffusion of the metal through the scale became significant. (W. E. Berry)

Basic Studies of Irradiation Effects in Fuel Materials

Metallic Fuels

The physical mechanisms deduced from an electron-microscope study of inert gas bubbles are used by Barnes[85] to evolve a model for fuel swelling. The model assumes insolubility of the inert gases and bodily migration of the gas bubbles. The model also utilizes the equation of state for the inert gas, the surface energy, the surface diffusion coefficient, and the lattice parameter of the solid, and some internal driving force, which is believed to be related to the line tension of dislocation lines. With values for these parameters and the irradiation and annealing conditions, estimates for the bubble size and number per cubic centimeter are made. From these the swelling can be calculated, but the effect of grain size and other structural features of the solid must be considered.

The model was tested against experimental results from a variety of solids, with satisfactory agreement. The model is thought to be useful for all solids, including nonmetals, and can account for breakaway swelling and gas release. The limitations of the model are discussed.

An experiment has been performed at Atomics International[86] to test the hypothesis that swelling may be controlled in nuclear fuels containing a fine dispersion of a second phase. The idea is to produce extensive nucleation of small bubbles, whose growth would be restrained by surface tension. It is also hypothesized that small-atom additions to the fuel may tie up the rare gases owing to an attraction between the large gas atoms and the small atoms. In this test, specimens of uranium alloys having either fine dispersions or small-atom additions were irradiated at 300 and 400°C to burnups of 0.4 and 0.6 at.% and were subsequently annealed at temperatures up to 680°C. The density changes occurring in all the alloys during irradiation could be accounted for by the solid fission products produced. No further density changes took place in any of the ternary alloys when annealed at 650 and 550°C, but control samples

of uranium did undergo swelling. Very limited swelling of two groups of specimens did occur after the one group was heated at 600°C and the other at 680°C. Although all the observed effects are not entirely understood, it does appear possible to limit swelling through alloying to produce controlled nucleation of the gases.

At Nuclear Metals[87] the behavior of helium in uranium and in several uranium alloys was studied metallographically after room-temperature irradiation with alpha particles, followed by various heat-treatments. The observed gas bubbles were grouped into two classes, differing in size, concentration, and mechanism of formation. These bubbles appear to resemble those resulting from fission-product gases in neutron-irradiated uranium. The results are believed to be applicable to the understanding of the factors affecting bubble formation and thus to the suppression of swelling in neutron-irradiated materials.

In Belgium[88] studies of swelling of uranium were conducted on zone-refined pure alpha uranium and uranium–1.5 wt.% chromium. Foils were irradiated with alpha particles, and the annealing of damage was examined. It was found that the annealing behavior of alpha-particle-irradiated foils was markedly different from that of foils exposed to fission fragments. Mild annealing below 500°C gave rise to large polygonal loops. Cavities were formed at temperatures above 500°C, where the helium was mobile. These cavities were rather similar in aspect to the cavities observed in quenched foils.

In a study of swelling of uranium conducted in Belgium,[89] damage due to neutron irradiation was identified as dislocation loops, the number being proportional to the irradiation dose. The direction of rows of dots associated with the dislocation loops was in many cases in the three principal axes: [001], [010], and [100]. The [112], [021], and [114] directions were also observed. The loops are irregularly shaped. Some had diameters of 500 A, but most had diameters between 100 and 200 A. In unirradiated uranium, dislocation networks were shown to begin to form in slowly cooled alpha uranium after annealing for 1 hr at 550°C (after deformation by rolling).

Blackburn[90] reports that, when there is a large difference between core and surface temperatures of a fuel, appreciable pressures will build up near the center. The swelling and the ratio of this central pressure to the absolute temperature are functions of the product of the absolute temperature and the creep rate per unit stress and dose, when the unrestrained swelling after a particular dose is given. For a material in the range 410 to 500°C, a small homogeneous specimen of which would swell 20% after 2000 Mwd/ton, this pressure would increase by about 50% in the absence of surface-tension restraint.

The diffusion coefficient and activation energy for diffusion of Xe^{133} in uranium metal were determined at Atomics International[91] for a number of sample conditions, with metals of high purity and commercial purity. Samples were irradiated to burnups in the range of 10^{14} to 10^{17} fissions/cm^3 at ambient temperatures in the General Electric Test Reactor shuttle tube. Samples were annealed at temperatures in the range 600 to 1000°C in evacuated static systems. The Xe^{133} released was measured *in situ* by scintillation counting of the 81-kev gamma emission. The amount of gas released was noted to be dependent on the initial gas concentration. A possible dependence on the metallurgical condition of the material was also observed. The effect of internal precipitation on external release measurements is described.

A review has been made at Battelle[8] for the Radiation Effects Information Center of the effects of nuclear radiation on metallic fuel materials. In the review are data for uranium, alpha-phase uranium alloys, gamma-phase uranium alloys, epsilon-phase uranium alloys, dilute uranium alloys, thorium, thorium-uranium alloys, and plutonium-containing alloys.

Olsen and Vineyard[92] show that the electrical resistivity of single-phase alpha and delta plutonium at 20°K increases with time. The initial rate of increase in resistivity of unalloyed alpha is greater than that in alloyed delta by a factor of about 6. The increase in resistivity is attributed to radiation damage caused by alpha activity in plutonium and is believed to have its origin in lattice defects produced by the alpha particles and their accompanying recoil nuclei. An appreciable fraction of the lattice defects is removed by annealing in the temperature range below 100°K. The self-irradiation behavior of two-phase alloys consisting of alpha-plus-delta phase mixtures is also discussed.

Irradiation Effects in Ceramic Fuels

At Oak Ridge[55] a definite effect of stress on the rate of fission-gas release from UO_2 has been observed. The effect appears to increase with increasing stress or temperature or both and to diminish with increasing time at temperature. There may be a correlation between the motion of dislocations and the release of fission gas. The behavior of ThO_2 + 2 wt.% UO_2, releasing Xe^{133} during cycling to 1450°C, also appears to be consistent with what would be expected if gas release is related to dislocation motion.

A number of current results[93–95] of fission-gas-release experiments are available. In general, no new conclusions have been reached at this time.

A progress report by the Bureau of Standards[96] describes experiments being conducted to determine the solubility of helium in UO_2.

Blank and Amelinckx[97] report that vapor-grown crystals of UO_2 show a dense pattern of precipitates and may contain loops due to quenched-in vacancies. However, they may contain hardly any dislocations. Dislocation networks are produced on annealing the crystals. Irregular patterns of dislocations arise when sufficiently thick parts of the crystal foils are treated with heat shocks in the microscope. After exposure to 10^{16} neutrons/cm^2, the crystal foils show fission tracks, short segments of straight dislocation lines, and black dots which are partly distributed at random and partly aligned on fission tracks. Interaction between fission tracks and dislocations was observed. The findings can be explained by a model of a displacement field around the fission tracks.

A report from Lawrence[98] presents a discussion of diffusion of Xe^{133} in uranium monocarbide. It was found that the diffusion coefficient of specimens consisting of large grains (700 to 1000 μ), in the temperature range 1000 to 2000°C, was best approximated by

$$D = (1.17 \pm 0.16)\ 10^{-6} \exp\left(\frac{-54{,}900 \pm 1200}{RT}\right)$$

where D is in square centimeters per second and RT is in calories per mole. Specimens with small grains (20 to 150 μ) exhibited the same diffusion coefficient above 1500°C. Below 1500°C results varied widely, with the latter specimens showing dependence on grain size, indicating appreciable grain-boundary diffusion. These data are $2\frac{1}{2}$ to 3 orders of magnitude higher than those obtained by Auskern and Osawa (USAEC Report BNL-6012) for UC powders. (F. A. Rough)

References

1. R. B. Russell and A. K. Wolff, Summary Report on the Study of Beta Treatment of Uranium, USAEC Report NMI-2807, Nuclear Metals, Inc., April 1963.
2. Argonne National Laboratory, Metallurgy Division Annual Report for 1962, USAEC Report ANL-6677.
3. Ames Laboratory, Annual Summary Research Report of Chemistry, Engineering, Metallurgy, Physics, and Reactor Divisions, July 1, 1962–June 30, 1963, USAEC Report IS-700, September 1963.
4. A. S. Bufferd, K. N. Swilsky, and N. J. Grant, Dispersion Strengthening in the Uranium-Alumina System, *Trans. Am. Soc. Metals*, 56: 508-512 (September 1963).
5. National Lead Co. of Ohio, Summary Technical Report for the Period July 1 to September 30, 1963, USAEC Report NLCO-890, Oct. 28, 1963.
6. H. Savage and R. D. Seibel, Heat Capacity Studies of Uranium and Uranium-Fissium Alloys, USAEC Report ANL-6702, Argonne National Laboratory, September 1962.
7. A. L. Geary, Fundamental and Applied Research and Development in Metallurgy, Development of Uranium-Base Alloys Strengthened by the SLIS Techniques, USAEC Report NMI-1259, Nuclear Metals, Inc., October 1963.
8. A. A. Bauer, M. S. Farkas, and V. W. Storhok, The Effect of Nuclear Radiation on Metallic Fuel Materials, Report REIC-29, Battelle Memorial Institute, Radiation Effects Information Center, Sept. 30, 1963.
9. B. N. Briggs, Some Experiences in Fabricating Uranium Metal Fuel Rods for Advanced Organic Reactor Concepts, USAEC Report NAA-SR-Memo-8161, Atomics International, Jan. 23, 1963.
10. B. R. Butcher and B. A. Hatt, The Mechanical Properties of Quenched Uranium-Molybdenum Alloys. Part II. A Preliminary Survey of the Deformation Mechanisms, British Report AERE-R-4353, June 1963.
11. C. R. Reinke, Irradiation and Postirradiation Annealing of Some Aluminum-Base Fuels, USAEC Report ANL-6665, Argonne National Laboratory, September 1963.
12. D. R. Stephens, The Phase Diagram of Plutonium, USAEC Report UCRL-7172, University of California, Lawrence Radiation Laboratory, Feb. 8, 1963.
13. Hanford Atomic Products Operation, Metallurgy Development Operation Quarterly Progress Re-

port, April–June 1963, USAEC Report HW-78157, Sept. 18, 1963. (Classified)
14. Argonne National Laboratory, Reactor Development Program Progress Report, October 1963, USAEC Report ANL-6801, Nov. 15, 1963.
15. Atomic Energy of Canada Ltd., 1963. (Unpublished)
16. B. A. Loomis, Swelling of Aluminum-Clad Aluminum-Plutonium Alloys on Postirradiation Annealing, USAEC Report ANL-6651, Argonne National Laboratory, November 1963.
17. W. R. Burt, Jr., A. G. Hins, R. M. Mayfield, and A. B. Shuck, Development and Manufacture of Fuel, Blanket, and Thermocouple Rods for the Experimental Breeder Reactor I, Core IV, USAEC Report ANL-6622, Argonne National Laboratory, September 1963.
18. Hanford Atomic Products Operation, Ceramics Research and Development Operation Quarterly Report, April–June 1963, USAEC Report HW-76302.
19. L. J. Wittenberg and G. R. Grove, Reactor Fuels and Materials Development Plutonium Research, July–September 1963, USAEC Report MLM-1171, Mound Laboratory, Nov. 11, 1963.
20. L. J. Wittenberg, Reactor Fuels and Materials Development Plutonium Research, April–June 1963, USAEC Report MLM-1162, Mound Laboratory, June 30, 1963.
21. F. W. Albaugh, Reactor and Fuels Laboratory Monthly Report, August 1963, USAEC Report HW-78758A, Hanford Atomic Products Operation, Sept. 15, 1963. (Classified)
22. M. M. Hendrickson and J. K. Green (Eds.), Research and Development Programs Executed for the Division of Reactor Development, Quarterly Progress Report, January–March 1963, USAEC Report HW-78118, Hanford Atomic Products Operation, April 1963.
23. BelgoNucléaire and Centre d'Étude de l'Énergie Nucléaire, The Use of Plutonium as Fuel in Nuclear Reactors, *The Joint Research and Development Program Quarterly Digest*, Period from April 1 to June 30, 1963, 3(2): 29 (September 1963).
24. Nuclear Materials & Equipment Corp., Development of Plutonium-Bearing Fuel Materials, Progress Report, April 1–June 30, 1963, USAEC Report NUMEC-P-105, July 1963.
25. United Kingdom Atomic Energy Authority, September 1963. (Unpublished)
26. H. Haug, On Investigations in the Systems Uranium Oxide–Europium Oxide and Plutonium Oxide–Europium Oxide (Thesis), Report NP-13003, Munich University, 1963.
27. S. Rosen, M. V. Nevitt, and J. J. Barker, The U-Pu-C Ternary Phase Diagram Below 50 Atomic Per Cent Carbon, *J. Nucl. Mater.*, 9(2): 128-136 (July 1963).
28. S. Rosen, M. V. Nevitt, and A. W. Mitchell, The Uranium Monocarbide-Plutonium Monocarbide System, *J. Nucl. Mater.*, 9(2): 137-142 (July 1963).
29. S. Rosen, M. V. Nevitt, and A. W. Mitchell, Metallographic and X-Ray Observations of Pu-C Alloys, USAEC Report TID-17867, Nov. 8, 1962.
30. R. W. Dayton and R. F. Dickerson, Progress Relating to Civilian Applications During July 1963, USAEC Report BMI-1642, Battelle Memorial Institute, Aug. 1, 1963. (Classified)
31. R. W. Dayton and R. F. Dickerson, Progress Relating to Civilian Applications During August 1963, USAEC Report BMI-1644, Battelle Memorial Institute, Sept. 1, 1963. (Classified)
32. R. W. Dayton and R. F. Dickerson, Progress Relating to Civilian Applications During September 1963, USAEC Report BMI-1650, Battelle Memorial Institute, Oct. 1, 1963. (Classified)
33. R. W. Dayton and R. F. Dickerson, Progress Relating to Civilian Applications During October 1963, USAEC Report BMI-1655, Battelle Memorial Institute, Nov. 1, 1963. (Classified)
34. F. W. Albaugh, Reactor and Fuels Laboratory Monthly Report, October 1963, USAEC Report HW-79377A, Hanford Atomic Products Operation, Nov. 15, 1963. (Classified)
35. Argonne National Laboratory, Reactor Development Program Progress Report, September 1963, USAEC Report ANL-6784, Oct. 15, 1963.
36. G. R. Grove, F. D. Lonadier, and R. E. Vallee, Summary Report on Isotopes Development: July 1, 1962, to June 30, 1963, USAEC Report MLM-1164, Mound Laboratory, Aug. 30, 1963. (Classified)
37. D. E. Ferguson (Comp.), Status and Progress Report for Thorium Fuel Cycle Development for Period Ending December 31, 1962, USAEC Report ORNL-3385, Oak Ridge National Laboratory, Oct. 28, 1963.
38. Oak Ridge National Laboratory, Metals and Ceramics Division Annual Progress Report for Period Ending May 31, 1963, USAEC Report ORNL-3470, Nov. 11, 1963.
39. F. W. Albaugh, Reactor and Fuels Laboratory Monthly Report—September 1963, USAEC Report HW-79046A, Hanford Atomic Products Operation, Oct. 15, 1963. (Classified)
40. Bureau of Mines, Quarterly Metallurgical Progress Report No. 20, July 1–September 30, 1963, USAEC Report USBM-U-1082.
41. W. C. Pritchard, K. A. Johnson, and J. A. Leary, Compaction and Sintering of PuO_2-Type 302B stainless Steel Powder Mixtures, USAEC Report LAMS-2898, Los Alamos Scientific Laboratory, Jan. 3, 1963.
42. S. J. Paprocki, D. L. Keller, G. W. Cunningham, and D. E. Kizer, Preparation and Properties of UO_2 Cermet Fuels, USAEC Report BMI-1487, Battelle Memorial Institute, Dec. 19, 1960.
43. W. J. K. Davies, A. G. Thomas, J. B. Huffadine, and N. C. Moore, Zirconium-Carbide-Coated Uranium-Oxide Fuel Particles, *Trans. Brit. Ceram. Soc.*, 62: 269-279 (March 1963).
44. H. S. Gadiyar and J. Balachandra, Vapor-Phase

Deposition of Molybdenum on Uranium Dioxide Particles Using Fluidized-Bed Technique, *Trans. Indian Inst. Metals*, 15: 168-176 (September 1962).

45. C. K. H. DuBose and R. J. Gray, Metallography of Pyrolytic Carbon Coated and Uncoated Uranium Carbide Spheres, USAEC Report ORNL-TM-91, Oak Ridge National Laboratory, Mar. 21, 1963.
46. Oak Ridge National Laboratory, Dec. 12, 1963. (Unpublished)
47. W. V. Goeddel, High-Temperature Gas-Cooled Reactor Fuel Materials Development, USAEC Report GA-4562, General Atomic Division, General Dynamics Corp., September 1963.
48. M. F. Browning, J. M. Blocher, Jr., V. M. Secrest, and A. C. Secrest, Coating Fuel Particles with Pyrolytic Carbon, USAEC Report BMI-1643, Battelle Memorial Institute, Aug. 16, 1963.
49. L. P. Pepkowitz, B. L. Vondra, and F. Shipko, Development of Protective Metal Coatings for UO_2 and Uranium Particles, Second Conference, Gatlinburg, Tennessee, October 10–12, 1961, USAEC Report TID-7622 (pp. 98-107), Oak Ridge National Laboratory, July 1962.
50. R. W. Dayton and R. F. Dickerson, Progress Relating to Civilian Applications During November 1963, USAEC Report BMI-1657, Battelle Memorial Institute, Dec. 1, 1963. (Classified)
51. J. B. Sayers, K. S. B. Rose, J. H. Coobs, G. P. Hauser, and C. Vivante, The Irradiation Behavior of Coated Particle Fuel, British Report DP-Report-227, October 1962.
52. W. O. Harms, Development of Fueled Graphite Containing Pyrolytic-Carbon-Coated Carbide Particles for Nonpurged, Gas-Cooled Reactor Systems, *Trans. Am. Nucl. Soc.*, 6(2): 378 (November 1963).
53. W. V. Goeddel, Development and Utilization of Pyrolytic-Carbon-Coated Carbide Fuel for HTGR, *Trans. Am. Nucl. Soc.*, 6(2): 379 (November 1963).
54. C. W. Townley, N. E. Miller, R. L. Ritzman, and R. J. Burian, Irradiation Studies of Ceramic-Coated Nuclear Fuel Particles, *Trans. Am. Nucl. Soc.*, 6(2): 378 (November 1963).
55. Oak Ridge National Laboratory Status and Progress Report, September 1963, USAEC Report ORNL-3517, Oct. 9, 1963.
56. Oak Ridge National Laboratory, Nov. 11, 1963. (Unpublished)
57. L. R. Zumwalt, E. E. Anderson, and P. E. Gethard, Fission-Product Retention Characteristics of Certain (Th,U)C_2-Graphite Fuels, USAEC Report GA-4551, General Atomic Division, General Dynamics Corp., Sept. 17, 1963.
58. General Atomic Division, General Dynamics Corp., Advanced Graphite Matrix, Dispersion Type Fuel Systems, July 1, 1963, Through September 30, 1963, USAEC Report GA-4617 (Pt. V), Nov. 30, 1963.
59. W. H. Pfeifer, G. W. Cunningham, D. C. Carmichael, and E. S. Hodge, Resistance of Ceramic Fuel-Particle Coatings to Reactions with Oxygen and Graphite, USAEC Report BMI-1647, Battelle Memorial Institute, Sept. 6, 1963.
60. D. R. de Halas, Understanding UO_2 Thermal Conductivity, *Nucleonics*, 21(10): 92-94 (September 1963).
61. M. F. Lyons, R. L. Straley, D. H. Coplin, B. Wiedenbaum, and T. J. Pashas, UO_2 Thermal Conductivity at Elevated Temperature, *Trans. Am. Nucl. Soc.*, 6(1): 152 (June 1963).
62. J. B. Conway, R. M. Fincel, Jr., and R. A. Hein, The Thermal Expansion and Heat Capacity of UO_2 to 2200°C, *Trans. Am. Nucl. Soc.*, 6(1): 153 (June 1963).
63. W. M. Armstrong and W. R. Irvine, Creep Deformation of Non-Stoichiometric Uranium Dioxide, *J. Nucl. Mater.*, 9: 121 (July 1963).
64. J. L. Bates, Visible and Infrared Adsorption Spectra of Uranium Dioxide, USAEC Report HW-79033, Hanford Atomic Products Operation, September 1963.
65. R. D. MacDonald, The Effect of TiO_2 and Nb_2O_5 Additions on the Irradiation Behavior of Sintered UO_2, Canadian Report CRFD-1012, April 1963.
66. F. Schmitz and R. Lindner, Diffusion of Plutonium in UO_2, *Radiochim. Acta*, 1: 218 (August 1963).
67. J. C. Clayton and S. Aronson, The Emanation of Radon-220 from Sintered UO_2 Powders and Plates, USAEC Report WAPD-276, Westinghouse Electric Corp., Bettis Atomic Power Laboratory, October 1963.
68. K. T. Scott and K. T. Harrison, Some Studies of the Oxidation of Uranium Dioxide, *J. Nucl. Mater.*, 8: 307 (May 1963).
69. I. Amato and R. Columbo, Steam Sintering of Uranium Dioxide, Final Report, September 1960–March 1962, USAEC-Euratom Report EURAEC-411, FIAT. Sezione Energia Nucleare, June 30, 1962.
70. I. Amato, R. L. Columbo, and A. M. Protti, Sintering of UO_2 in Carbon Dioxide Atmosphere, *Nucl. Sci. Eng.*, 16: 137-140 (May 1963).
71. C. A. Elyard, B. M. Gibbs, and H. Rawson, Effect on Uranium Oxide of Controlling Grain Growth During Sintering, *Trans. Brit. Ceram. Soc.*, 62: 127-137 (February 1963).
72. J. F. Carpenter, C. W. Kuhlman, and R. A. Nelson, Characterization of Uranium Dioxide Powders, USAEC Report UNC-1004, United Nuclear Corp.
73. I. Amato, Fission Gas Release from Uranium Dioxide. Topical Report on UO_2 Pellets Fabrication and Characterization, USAEC-Euraton Report EURAEC-701, FIAT. Sezione Energia Nucleare, May 1, 1963.
74. J. J. Fargo, Fabrication of Thin Uranium Dioxide Plates by a Powder Rolling Process, Report CONF-50-3, International Pipe & Ceramics Corp.
75. Westinghouse Electric Corp., Bettis Atomic Power Laboratory, Bettis Technical Review. Reactor Technology, USAEC Report WAPD-BT-29, October 1963.

76. E. Rudy and F. Benesovsky, Investigations in the Systems: Th-Mo-C and U-Mo-C, *Monatsh. Chem.*, 94: 85-98 (1963).
77. Proceedings of the Conference on Carbides on Nuclear Energy, Harwell, England, November 5-7, 1963.
    a. W. Chubb and D. L. Keller, Constitution of the Systems of Uranium and Carbon with Mo, Nb, Re, W, and Y, Preprint A-15.
    b. J. T. Dalton, Equilibria in the System: U-Pu-C, Preprint A-8.
    c. P. Magnier, J. Trouvé, and A. Accary, The Solubility of Oxygen and Nitrogen on UC, Preprint A-9.
    d. F. Anselin, G. Dean, R. Lorenzelli, and R. Pascard, On the System: (U, Pu) (C, N, O), Preprint A-11.
    e. N. H. Brett, H. J. Hecger, and J. S. Pottinger, Solubility of Oxygen in UC and (U, P)-C Alloys, Preprint A-12.
    f. G. Briggs, S. K. Dutta, and J. White, Phase Relations in the Systems U-Cr-C, U-Ni-C, and U-Fe-Cr-C, Preprint A-16.
    g. J. L. Nichols and J. A. C. Marples, An Investigation of the U-Fe-C and Pu-Fe-C Ternary Phase Diagrams, Preprint A-17.
    h. P. D. Shalek and G. D. White, The System: UC-US, Preprint A-19.
    i. T. Thorpe, J. W. Harrison, J. C. Riviere, and J. Adam, (U, Zr)C for Thermionic Converters, Preprint B-27.
    j. C. A. Alexander, J. J. Ward, J. S. Ogden, and G. W. Cunningham, Thermodynamics for Compatibility Studies of Metal-Clad Uranium Carbide, Preprint A-14.
    k. J. J. Norreys, M. J. Wheeler, and E. Gillam, Preparation and Some Properties of U_2C_3, Preprint A-3.
    m. J. J. Norreys, Compressive Creep of UC, Preprint C-14.
78. E. Rudy and F. Benesovsky, The Stability of UC_2 and the Carbon-Stable Regions in the Systems of UC with ZrC, HfC, NbC, and TaC, *Monatsh. Chem.*, 94: 204-224 (1963).
79. R. F. Stoops and J. V. Hamme, Uranium Interstitial Phases, Quarterly Report, USAEC Report NCSC-2663-13 (EURAEC-766), North Carolina State College, June 1963.
80. G. G. Bentle, F. E. Ekstrom, and R. Chang, Plastic Deformation of Uranium Carbide Crystals, USAEC Report NAA-SR-8108, Atomics International, Sept. 30, 1963.
81. J. Crane, United Nuclear Corp., Oct. 15, 1963. (Unpublished)
82. D. L. Keller, Battelle Memorial Institute, July 1963. (Unpublished)
83. R. A. Wullaert, J. F. Lagedrost, J. Bugl, and J. E. Gates, Radiation Stability of Uranium Mononitride, USAEC Report BMI-1638 (EURAEC-760), Battelle Memorial Institute, June 28, 1963.
84. A. F. Bessonov and V. G. Vlasov, On the Question of the High Temperature Oxidation of Metallic Uranium, *Fiz. Metal. i Metalloved.*, 15(3): 477-478 (1963).
85. R. S. Barnes, A Theory of Swelling and Gas Release for Reactor Materials, British Report AERE-R-4429, October 1963.
86. D. Kramer and W. V. Johnston, Postirradiation Annealing of Uranium-Molybdenum Ternary Alloys, *J. Nucl. Mater.*, 9: 213-215 (July 1963).
87. H. M. Green, A Metallographic Study of Gas Behavior in Uranium Irradiated with Alpha Particles, USAEC Report NMI-7009, Nuclear Metals, Inc., Sept. 28, 1962.
88. Centre d'Étude de l'Énergie Nucléaire, Swelling of Uranium. Quarterly Report No. 5, October 1–December 31, 1961, USAEC-Euratom Report EURAEC-274.
89. Centre d'Étude de l'Énergie Nucléaire, Swelling of Uranium. Quarterly Report No. 11, April 1–June 30, 1963, USAEC-Euratom Report EURAEC-745.
90. W. S. Blackburn, Estimation of the Effect of Differential Fuel Swelling, *J. Nucl. Energy*, 17: 253-255 (August 1963).
91. J. W. Savage, Diffusion of Fission Gas in Uranium, USAEC Report NAA-SR-6761, Atomics International, Aug. 15, 1963.
92. C. E. Olsen and G. H. Vineyard, Self-Irradiation and Annealing of Plutonium and Plutonium-Aluminum Alloys, *Acta Met.*, 11: 1129-1138 (October 1963).
93. FIAT. Sezione Energia Nucleare, Fission Gas Release from Uranium Dioxide. Quarterly Progress Report No. 9, January–March 1963, USAEC-Euratom Report EURAEC-656.
94. P. Schmeling, Evaluation of Gas Release Curves Attained During PAD Experiments. I. Multi-Temperature Anneals with F < 0.2, Technical Report No. 3, November 11, 1961–March 12, 1962, USAEC-Euratom Report EURAEC-359, Hahn-Meitner-Institut für Kernforschung.
95. FIAT. Sezione Energia Nucleare, Fission Gas Release from Uranium Dioxide. Quarterly Report No. 10, April–June 1963, USAEC-Euratom Report EURAEC-774.
96. S. Hasko and R. Szwarc, Noble Gas Solubility and Diffusion in UO_2, Period Covered, September 1, 1962, to June 30, 1963, USAEC Report TID-19229, National Bureau of Standards, Aug. 6, 1963.
97. H. Blank and S. Amelinckx, Some Preliminary Results on Defects in Irradiated UO_2 Single Crystals as Revealed by Transmission Electron Microscopy, *J. Appl. Phys.*, 34: 2200-2209 (August 1963).
98. University of California, Lawrence Radiation Laboratory, Inorganic Materials Research Division Annual Report, 1962, USAEC Report UCRL-10706, Feb. 28, 1963.

Section II

Reactor Materials

Moderator Materials

Graphite

Further experimental data on irradiation-induced creep in graphite has been obtained at Harwell.[1] Test specimens of grade A graphite were subjected to 500-psi tensile stress during irradiation at 300°C in the high-flux reactor PLUTO at Harwell. The specimens showed steady-state creep rates of 1 to 2×10^{-7} $(psi)^{-1}$ per 10^{20} neutrons/cm^2 for specimens loaded parallel to the extrusion direction and 4 to 5×10^{-7} $(psi)^{-1}$ per 10^{20} neutrons/cm^2 for specimens loaded perpendicular to the extrusion direction. There was no evidence that the creep strain could be removed by annealing (up to 1000°C) either with or without stress. The experimental results were consistent with an interpretation of creep in terms of the removal of dislocation barriers.

An informative electron-microscopy study of graphite oxidation has been conducted at Glasgow University.[2] Ultrathin sections of a synthetic graphite were examined in the electron microscope before and after oxidation in air at a temperature of 500°C. In unirradiated material the photomicrographs of individual areas showed that oxidative attack occurred at grain boundaries and at pores between individual crystallites. Parallel experiments on material that had been irradiated to a dose of 8.7×10^{19} neutrons/cm^2 again showed etching at pores and at grain boundaries, but, in addition, the majority of specimens exhibited a shallow surface pitting of the entire (0001) faces of the individual crystallites. The density of these shallow pits varied from 5×10^{10}/cm^2 to 5×10^{11}/cm^2. Variations in reaction rate were observed and were traced to impurities that appeared to be absorbed only at pores and intercrystallite boundaries, oxidation effects being observed only at these sites. In irradiated material impurities were also absorbed at sites on the (0001) crystal faces, where oxidation produced etch pits of widely varying depth and density. Channeling of the (0001) layer nets occurred in both irradiated and unirradiated specimens. Annealing of the irradiated graphite at 650°C for 1 hr produced no significant change in the pattern of attack by oxygen. The observed etch-pit density measured on the (0001) layer nets was 8×10^{10}/cm^2.

A kinetic study of the exchange of normal and radioactive Br_2 in graphite-Br_2 lamellar compounds was made at temperatures[3] of 30 to 50°C. The compositions studied were approximately $CBr_{0.08}$ and $CBr_{0.10}$ in natural graphite powders and $CBr_{0.05}$ and $CBr_{0.07}$ in artificial graphite powders. Of the two alternative mechanisms considered for exchange, volume diffusion and surface exchange, the data agreed better with the diffusion mechanism. Diffusion coefficients of 10^{-9} to 10^{-8} cm^2/sec were calculated for the natural powders, and an activation energy of 11 to 14 kcal/mole was calculated.

(M. C. Brockway)

Beryllium Metal and Alloys

Reduction, Purification, and Analysis of Beryllium

A modification of the electrorefining cell developed by the Bureau of Mines[4] at Boulder City permits easier and more rapid removal of the beryllium crystals that are deposited on the cathode. Raising the cathode through a die situated above the cell, after insertion of a basket to catch the stripped-off beryllium crystals, made it unnecessary to disassemble the equipment. An atmosphere lock was provided

to permit inspection and withdrawal of the basket without loss of vacuum in the cell.

A vacuum-induction-melting process in which a reactive metal, such as beryllium, is placed on a water-cooled stool (without side walls) and surrounded by an induction coil has been developed at Lawrence Radiation Laboratory.[5] The melt is supported on the bottom by the stool and on the sides by the pinch effect of the coil. This arrangement allows melting and remelting repeatedly, without contamination from a crucible. After six remelts of Pechiney SR flake under a pressure of about 5×10^{-6} mm Hg, the chlorine, oxygen, and carbon levels were much reduced and nitrogen was at about 1 ppm. The beryllium loss from volatilization was about 25% of the charge weight. This melting method, combined with various casting procedures, will no doubt find numerous applications in research laboratories.

Schaub and Cabane[6] stated that beryllium bars that had been obtained by fusion under ultrahigh vacuum by electron bombardment of foils of electrolytic beryllium were further purified by floating-zone fusion under argon. After six zone passes the metal had the analysis shown in Table II-1. Removal of iron is poor; copper is not affected at all by zone melting, and nickel is concentrated at the otherwise pure end. However, the floating-zone fusion process gave beryllium bars, after the third pass, that could easily be bent by hand at room temperature, regardless of the quality of the starting material.

Table II-1 IMPURITIES IN ZONE-REFINED BERYLLIUM[6]

Element	Impurities, ppm: At start	After six passes	Element	Impurities, ppm: At start	After six passes
Al	5	<0.05	Si		
Ca		2	Ta	≥4	<0.01
Co	<0.1	<0.1	W	0.1	0.04
Cr	3	<0.03	Zn		1
Cu	3	4	B		<0.01
Fe	15	10	F		0.1
K		1.5	P		0.1
Li		0.15	O	30	5
Mg		0.15	C	40	10
Mn	2	<0.02			
Na	1	0.04	N	30	≤2 <10 17†
Ni	15	80* 2*			

*Upper figure is at head, lower at two lengths further down the bar.

†Sometimes <2.

The preceding paragraph showed the ultimate purity of beryllium which has recently been achieved in a laboratory in France. Also from France, Syre and Logerot[7] stress that the commercial metallurgy of beryllium has made notable strides in the recent past. They single out: the increased purity of the starting material (flake); the practice of appropriate melting techniques; the development of low-temperature transformation processes; and a better comprehension of the metallurgical mechanisms of brittleness, both hot and cold. The outstanding gains in purity of both commercial and refined (SR) flake are shown in Table II-2.

Still other French scientists[8] have described the use of neutron activation in a flux of approximately 5×10^{12} neutrons/(cm^2)(sec) to determine traces of impurities in beryllium and beryllium acetate. All the measurements were made by gamma spectrometry. Certain elements (manganese, copper, sodium) could be determined nondestructively, whereas others (rare earths, chromium, silicon, iron, cobalt, zinc, tantalum, nickel) required chemical separations first.

Fabrication of Beryllium

At Nuclear Metals[9] comparison was made of the bend and tensile properties of material fabricated by extrusion which had a range of impurity levels never before studied in polycrystalline beryllium. Preliminary results indicated that the high-purity beryllium produced by extrusion of powder made from double-distilled stock had superior bendability, compared to either Brush QMV or Pechiney materials. The tensile properties, however, showed elongations (~9%) about equivalent to extrusions prepared from QMV metal but with much lower strengths (64,000 vs. 111,000 psi ultimates). Comparisons of these materials were rather difficult, since the grain sizes were quite different.

Reports on redrawing of extruded beryllium channel[10] indicate that considerable difficulties are being encountered in carrying out the process, but note that 10-ft lengths can be drawn to at least a 6% reduction in thickness. Preliminary evaluation of warm redrawn channel by bend and tensile tests of specimens cut from the channel webs suggested that about 9%

Table II-2 PECHINEY BERYLLIUM[7]

	BeO	Cl	C	Fe	Al	Ni	Si	Mg	Ca	Na	Zn	Cr	Mn	Cu	Ti	Ag	Pb	Mo	B
Commercial production, 1958		1100	700	500	500	100	500	300	500	300									
Commercial production, 1961	4000	800	300	300	300	150	200	50	200	200	100	20	30	50					
Commercial, typical, January 1963	3750	328	255	200	110	90	55	20	45	<100	<80	<10	7	5		8	<15	<15	1
Specification, SR	800	700	150	50	60	30	30	30	30	175	50	5	30	10	5				
SR, typical, 1962	690	500	150	30	<30	10	15	10	<30	150	<80	<10	<5	<5	<25				
SR, typical, Lot 64*	440	700	110	5	<30	5	<10	<10	<30	<100	25	2	<2	<5	<2				

* The last lot before submission of paper, presented Jan. 16, 1963.

reduction in thickness provided a nearly 50% increase in yield strength without sacrifice of ultimate strength. However, there was some loss in ductility. Heavier reductions and annealing resulted in material with strengths equal to or less than those of as-extruded channels and with impaired ductility.

Still another report[11] indicated that shaped-die extrusions of finned beryllium tubes were made successfully. Inspections by Dye-Check penetrant techniques and the helium-leak detector did not reveal any abnormalities in the tubing as a result of the fabrication methods. The short-time elevated-temperature burst strength was determined for beryllium tubing that had been hot extruded with a reduction in area of 23×. The hoop stresses at rupture varied linearly from 27,000 to 10,000 psi in the temperature range 800 to 1300°F. The strength of tubing extruded with a 28× reduction was similar.

The final technical report[12] of Brush Beryllium's project on the development of a process for the production of ultrafine beryllium wire was received. Conventional warm drawing by the methods reported earlier for drawing 0.062-in. beryllium rod to below 0.005-in. diameter at 700 to 800°F with a MoS_2 lubricant was the most successful process found. Wire with usable structural qualities was produced at diameters down to ~0.00185 in. The tensile properties did not improve as the wire became finer, however. The two best lots reported had the mechanical properties shown in Table II-3 (both lots had the last anneal at 0.062 in. diameter).

Beryllium supplied both by the Commissariat à l'Énergie Atomique (CEA) of France and by Oak Ridge was successfully joined with a magnetic-force welder at Hanford.[13] The French beryllium tube was counterbored to obtain a cross-sectional area of 0.025 sq in. (within the capacity of the welder) and welded using approximately 50,000 amp, 1-cycle weld time, and a forging force of 1400 lb. The recrystallized grain size was the same or slightly smaller than that in the parent metal. The Oak Ridge tubing (extruded beryllium, warm drawn from hot-pressed block), with a cross-sectional area of 0.028 sq in., was welded with the same parameters as the French beryllium, except for a current reduction to 45,000 amp. Again the recrystallized grains appeared smaller than those in the parent method.

Best results were obtained by Hamilton Standard[14] in electron-beam welding of beryllium by using moderately high power densities and slow welding speeds. The resultant welds were sound, crack-free, and exhibited good joint strengths. At high welding speeds or extremely high power densities, columnar grain growth

Table II-3 STRENGTH OF FINE BERYLLIUM WIRE[12]

Drawn diameter, in.	Reduction ratio from last anneal	Room-temperature tensile strength		
		Ultimate, 1000 psi	Yield, 1000 psi	Elongation, %
0.00502	152 to 1	202	162	1.8
0.001848	1120 to 1	203	153	1.3

led to weld cracking. The room-temperature tensile strength of electron-beam-welded 0.040-in. sheet was consistently about 65% of the base-metal strength; the elongation of the weldments was lower than that of the base metal. At 1000°F the ultimate and yield strengths of the base metal and weldments were essentially the same. The ductile-to-brittle transition temperature of the weld metal was estimated to lie at 1040°F, compared to 400°F for the base metal.

A group from Aeronca Mfg. Corp.[15] report that beryllium performs better in sandwich structures than as sheet material because the honeycomb structure stabilizes the beryllium faces and reduces brittle fracture. The group found that sterling silver with 0.5% lithium added was the best alloy for brazing the beryllium face sheets to cores of type 302 stainless steel, Inconel, or A-286 alloy.

Details of the dust-collecting system, aided by clear reproductions of photographs of specific machines, distinguish an article by Titus[16] on the machining of beryllium in a West Coast shop. The beryllium parts consist mostly of precision components for aircraft, missiles, and satellite installations. Tolerances down to 50 μin. are commonly specified on diameters and to 20 μin. on concentricity and normality. Tolerances to 10 millionths of an inch have been held by honing and lapping. Surface finishes of 8 μin. on lathe work and 2 μin. on honing and lapping are said to be maintained consistently.

Physical Metallurgy of Beryllium

An investigation by Garber et al.[17] of the mechanical properties of beryllium single crystals in which the basal plane was at right angles to the compression revealed unusually high strength in the temperature range 4.2 to 900°K. At the temperature of liquid helium the maximum compressive strength reached a value of 746,500 psi (532 kg/mm^2). At higher temperatures (500 to 900°K) the crystals possessed some plasticity due to slip along the second-order pyramidal planes. At low temperatures plastic deformation was not observed, and practically all the deformation before fracture was elastic.

It has been established (during the past year), says a report from Nuclear Metals,[18] that the addition of iron to zone-refined crystals [critical resolved shear stress (CRSS) for basal slip = 300 psi] at the 1500-ppm level results in an increase in CRSS for basal slip to 2000 psi, the value observed in a single crystal of commercial purity. At the same time, the high basal glide capacity (100 to 200%) found for high-purity zone-refined crystals is retained after the iron addition.

Another report[19] indicates that critical resolved shear stress for prism slip in beryllium is strongly temperature dependent, whereas critical resolved shear stress for basal slip is almost independent of temperature. Purification by zone refining markedly increases the capacity for basal glide and reduces the rate of work hardening. Fracture of the purified crystals still occurs by basal cleavage at room temperature, but at elevated temperatures, brittle fracture by cleavage is eliminated. Flow characteristics of beryllium single crystals strengthened by iron additions, as measured by work hardening, are but little affected.

According to Munro and Hill,[20] the results of hot and cold bend tests on beryllium sheet, and of the deformation of beryllium tubes by the application of internal and external pressure, showed that under complex stressing at elevated temperatures, beryllium can develop considerable ductility. There was a large scatter in the tube properties at 620°C, where the diametral expansions ranged from 0.2 to 11%, and the elapsed times to failure ranged from 1 to 220 min under a pressure of 1000 psi. The scatter within each tube was less than the overall scatter, but it was great enough to mask any differences produced by varied fabrication techniques.

The macroscopic mechanical properties of beryllium, it is well known, are very sensitive to the nature of its surface finish. Bonfield et al.[21] reported that the stress to cause a permanent microstrain of 2×10^{-6} in./in. also is very sensitive to surface condition. The initiation of plastic flow in as-machined specimens, which contain a high density of twins and large residual compressive stresses to a depth of about 0.010 in. from the surface, occurred by the nucleation of slip from high-stress fields around twin tips in the surface layers. Removal of the damaged surface by chemical polishing resulted in an increase by almost a factor of 2 in the microscopic yield stress. This increase was attributed to the removal of stress-raising twins, rather than to the release of residual stress.

During a microscopic examination of the polished surface of a cylindrical plate during extension under load, Bastien and Pointu[22] studied the behavior of two variations of commercial beryllium between ambient temperature and 900°C before and after precipitation for 110 hr. One specimen, *A*, showed a ratio in weight of Al/Fe of 3.5, and a second specimen, *B*, had a ratio of 0.67. After annealing following precipitation, specimen *A* always showed the liquid phase above 500°C, whereas specimen *B* did not. The liquid phase appeared, therefore, to be the cause of hot brittleness. Independently of the liquid phase and of the decohesion of grain boundaries, the intragranular deformation of the raw material showed some bands of great slip in separated areas at temperatures between 150 and 300°C.

Hot-stage microscopic observation by Pointu et al.[23] of beryllium during a tensile test revealed diverse modes of deformation. It showed, at about 500°C, a liquid phase in the grain boundaries that led to their general decohesion. This can be avoided by thermal treatment if there is a suitable ratio between iron and aluminum in the beryllium. Annealing for 110 hr at 650°C brought out a face-centered cubic precipitate, in which $a = 6.07$ A, that contained both iron and aluminum. After annealing, if the ratio of Al/Fe was less than about 5 to 1 by weight, no liquid phase appeared on reheating, and the ductility of the beryllium at 600°C was greatly improved.

The thermal evaporation of single crystals of beryllium of commercial purity (Brush QMV) has been studied by Bastien and Pointu.[24] At temperatures between 650 and 1000°C, evaporation generates plane facets (whose indices were determined) and leaves structures of threadlike forms in relief. The threadlike forms contain a high percentage of transition elements; their orientation is related to that of the crystalline matrix. Microprobe analysis of these structures showed, at the nodes after an evaporation at 750°C, an average of 5 wt.% iron and 5 wt.% nickel, whereas after an evaporation at 950°C, the average analysis was 15 wt.% iron, 3 wt.% nickel, 1 wt.% chromium, and 1 to 8 wt.% manganese. The threads between the nodes showed much lower impurity content: ~ 1.5 wt.% iron, 1.5 wt.% nickel, and 1 wt.% manganese. Magnesium and other elements of lower atomic number could not be found. (Presumably the light elements had all distilled away.)

MacKay and Hill[25] determined the lattice parameters of small crystals of vacuum-distilled beryllium of 99.9% purity, which contained only 250 ppm of oxygen, at 20.5°C. The values found, $a_0 = 2.2858 \pm 0.0002$ A, $c_0 = 3.5843 \pm 0.0003$ A, agree closely with the results obtained by Gordon* for 97% beryllium containing 2 wt.% oxygen and a much greater weight percent of metallic impurities. Since no measurable change was found by reducing the total impurity content from 3 to 0.1 wt.%, it is suggested that either both specimens were saturated with respect to oxygen and the other impurities or at least oxygen in these proportions does not significantly affect the dimensions of the beryllium lattice.

Arzhanyi et al.[26] studied the diffusion saturation of 98.8% pure niobium by beryllium at 900 to 1300°C and determined the diffusion layer thickness, its microstructure, lattice structure, microhardness, and solubility. Consideration was given to the existence of $NbBe_{12}$, $NbBe_8$, $NbBe_5$, and $NbBe_2$ compounds and their heats of formation. They show a phase diagram for the beryllium-niobium system.

Diffusion-barrier coatings on beryllium were described in a Pratt & Whitney[27] report. Beryllium strips were plasma-arc sprayed with chromium, iron, titanium, and beryllium oxide. Additional strips were electroplated with gold. The coated strips were exposed to temperatures of 1400°F and pressures in the range of 10^{-5} to 10^{-7} mm mercury for periods of 150 and 500 hr. After exposure all the coated strips except those coated with BeO were analyzed by X-ray diffraction to determine the extent of diffusion. Only the BeO coatings remained intact for the duration of the exposure. The chromium and iron coatings separated completely, and the titanium coating spalled in localized areas. Interdiffusion between the gold coating and the beryllium substrate resulted in a blistered, nonadherent, unidentified phase.

Various authors have reported the presence of an impurity phase which is face-centered cubic (fcc), $a \approx 6.07$ A, in commercial beryllium. The phase is generally thought to be associated with an aging process and to contain beryllium and the transition elements, particularly iron. Carrabine[28] isolated an impurity product in commercial beryllium, identified as

* P. Gordon, *J. Appl. Phys.*, 20: 908 (1949).

fcc, a = 6.04 A, which contained aluminum, iron, manganese, and beryllium as the major constituents. By synthesis he prepared $AlMnBe_4$, $AlNiBe_4$, and $AlFeBe_4$, all fcc phases with the lattice parameters 6.11, 6.01, and 6.06, respectively. He suggests that the fcc phase found in aged commercial beryllium is correctly described as $AlMBe_4$, where M is a transition metal.

Weisz et al.[29] made studies on synthetic aluminum-beryllium-silicon alloy containing 10 wt.% aluminum and 3 wt.% silicon to determine the temperature of the appearance of the liquid phase in the grain boundaries of commercial beryllium. The fusion point of the eutectic was found by X-ray diffraction. The diffraction chamber used permitted the sample to be heated in a vacuum. A Debye-Scherrer diagram at ambient temperature showed the lines (5 1 1-3 3 3) and (4 2 2) and some spots due to the large crystal of the beryllium matrix. When the temperature was raised to 460°C, the lines disappeared, which indicated that at 460°C the eutectic was in the liquid stage. When the eutectic was chilled to 430°C or below, the intense lines of aluminum reappeared. Hence they concluded that the temperature of solidification of the ternary eutectic of aluminum-beryllium-silicon is between 440 and 430°C.

A corrosion-resistant beryllium-base alloy is described in a British patent.[30] The alloy consists of 0.1 to 3.0 wt.% calcium, 0.1 to 2.0 wt.% zirconium, niobium, vanadium, or titanium, and the remainder beryllium, including unavoidable impurities. The preferred composition is 1 wt.% calcium and 0.5 wt.% zirconium, niobium, vanadium, or titanium. This alloy is claimed to have high neutron transparency and greater strength than the beryllium-calcium alloys. It can be made by conventional powder-metallurgy techniques or by consumable-electrode arc melting followed by direct fabrication.

Reich et al.[31] studied the electrical resistance of four beryllium samples of different purity. They found that the ideal resistivity in the case of the purest metal varies as a function of the temperature from 4 to 1.5 at temperatures from 55 to 500°K. The Debye temperature is given as 1240°K. They also found that, at low temperatures, both the ideal resistance and the residual resistance depend on the purity of the metal, which is not in accord with Matthiessen's rule. In the expression $\rho_i = KT^n$, the exponent n is greatest and the coefficient K is least, in the case of the purest (double electrolyzed) metal. However, the authors conclude that the laws of Bloch* and of Grüneisen,† based on free-electron models, apply not only to metals that are electrically isotropic but also to metals electrically anisotropic like tin and beryllium.

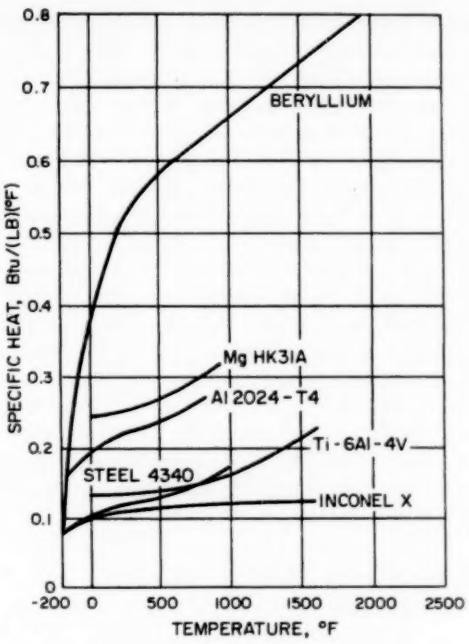

Fig. II-1 Specific heat vs. temperature for beryllium and several metals.[32]

Weismantel and Fisher[32] point out that, although the specific heat of beryllium is approximately equal to that of other construction alloys at room temperature, it is several times that of the more common alloys at 2000°F. This high specific heat, combined with high thermal conductivity, allows beryllium to be used where structures of equal weight, made of stronger and more refractory materials, would melt. Figure II-1 shows the variation in specific heat of beryllium and other materials with temperature.

According to Levine et al.,[33] beryllium sheet rolled to reductions of 83% at 1400°F exhibits considerably higher transverse ductility than

Z. Physik., 52: 555 (1928); 59: 208 (1930).

†*Ann. Phys.*, 16: 530 (1933).

sheet conventionally rolled to about 96% reduction at higher temperatures. The yield and tensile strengths of sheet prepared by either method are quite similar, and elongations in the plane of the sheet appear to be identical. The addition of 1 wt.% copper by electroless plating of the beryllium powder before its consolidation had a strong solid-solution strengthening effect. The beryllium-copper alloy was too stiff to roll at 1400°F, but rolling 77% at 1500°F produced sheet having 65,000 psi yield and 82,500 psi ultimate strengths. The highest strength values Levine et al. obtained for unalloyed beryllium were 59,000 psi yield and 77,800 psi ultimate. The ductility of the two materials in the plane of the sheet was identical; however, the transverse ductility of the 1 wt.% copper alloy sheet was a little less than that of the unalloyed sheet.

Chemical and Nuclear Properties of Beryllium

The oxidation behavior of beryllium sheet and extruded disks prepared from both Brush and Pechiney powders was examined by Menzies.[34] Oxidation appeared to occur in at least three stages: (1) thin-film formation, (2) nonuniform film thickening, and (3) localized intergranular penetration. Stage 3 was observed only in specimens with weight gains greater than 0.1 mg/cm^2. Extruded materials in disk form had greater resistance to oxidation than sheet at all temperatures. Breakaway oxidation occurred in some specimens of all the materials within the 7000-hr testing period. In general, at 600 and 650°C the Brush material resisted corrosion better than the purer Pechiney material, and the corrosion rate was higher in the gas containing more moisture. However, Pechiney disks (which contained 2.8 wt.% oxygen) showed greater resistance to corrosion at 700°C in CO_2 gas containing 300 ppm water vapor than they did at 600°C. The author characterized the corrosion resistance at 700°C of these Pechiney disks as outstanding.

An investigation at Nuclear Metals[35,36] of the corrosion behavior of beryllium showed that commercial-purity beryllium will survive in 343°C water without significant attack for prolonged periods. The presence of a minute amount of copper in the water has a deleterious effect on corrosion resistance. High-purity beryllium exhibited poor corrosion resistance in high-temperature water. Its corrosion resistance could be improved by alloying with small amounts (0.4 wt.%) of nickel or nickel plus iron. Individual alloy additions to high-purity beryllium of aluminum, magnesium, manganese, silicon, iron, nickel, or chromium in amounts comparable to their content in commercial-purity beryllium had no effect on corrosion resistance.

After a study of the chromic acid anodizing process, Whitby et al.[37] decided that the corrosion protection gained by beryllium with anodized coatings is due to the physical barriers interposed by the BeO coating between the base metal and the corrosive environments.

Beryllium, fabricated in six different ways was irradiated by fast-neutron doses of 3.5 to 5.5 $\times$ 10^{20} neutrons/cm^2 at temperatures of 450, 550, and 650°C in British tests.[38] Volume changes in the irradiated specimens, due to the accumulation of helium gas into bubbles, were very slight. Irradiation caused a marked decrease in elongation, combined with an increase in proof stress and ultimate tensile stress. The effect of irradiation was the worst for irradiation and testing at 650°C. Irradiation caused a reversal of the effects of heat-treatment, i.e., a decrease of elongation and, at lower temperatures, an increased proof stress and ultimate tensile stress. The loss of ductility was particularly marked at 650°C, where elongations of all materials were between 1 and 3.5% after irradiation.

Although stainless steel will be used for the first set of fuel cans in the French heavy-water reactor EL4, writes Cabane,[39] it is expected that beryllium will be used in the second set. These fuel cans are subjected to irradiation at temperatures of 550 to 650°C and exposed on the outside to CO_2 under 60 atm pressure. The corrosion from CO_2 depends on the amount of moisture present and to attack along grain boundaries parallel to the extrusion direction. At these sites it is believed that microcracks existed before the exposure or that there was present an inadmissible concentration of impurities. The irradiation of beryllium produces both helium and tritium dispersed in the atomic lattice. At sufficiently elevated temperatures, helium is concentrated into bubbles that add to the brittleness of the beryllium when the metal is cooled. Cabane shows that increasing the purity of the metal decreases the number of sites at which bubbles form. This, together

with the elimination of aluminum and other impurities from the grain boundaries, is expected to make even irradiated beryllium sufficiently ductile to withstand cooling without cracking the cans.

An Australian report[40] concludes that all the observed property changes from irradiation of beryllium can be interpreted in terms of distribution of helium that is produced by fast-neutron transmutation reactions, and that the damage from defect production is negligible for irradiation temperatures of 75°C and above. Density changes caused by helium-bubble formation are shown to be very small, although serious deterioration of mechanical properties can occur. These changes in mechanical properties are very dependent on material history and irradiation temperature. Serious loss of low-temperature ductility occurred with irradiation temperatures below 500°C and particularly in the range 300 to 500°C. The nucleation of gas bubbles at precipitated particles is the only satisfactory explanation of the wide variations in behavior of beryllium metal fabricated by various methods.

Beryllium Hygiene

In the Soviet Union[41] the maximum permissible concentration of beryllium in the air at production facilities has been established at 0.001 mg/m^3. In building plants for obtaining and using beryllium, a sanitary-protective zone with a radius of 2 to 3 km (1.24 to 1.86 miles) is considered necessary. Regulations state that the waste reservoirs for production wastes should be surrounded by a sanitary-protective zone of not less than 1 km (~$\frac{5}{8}$ mile), and its several sections should be covered with fresh dirt as they start to fill up. Concentrations of beryllium greater than 0.5 mg/l retard the processes of biochemical consumption of oxygen. This can interfere with the operation of equipment intended to accomplish the biological purification of waste water and disrupt the processes of self-purification of waters from the organic substances of ordinary waste. (W. Hodge)

Beryllium Oxide

Measurements of the expansion of the lattice parameters of irradiated BeO have shown that each of the reflections used with CuK α-radiation to define the c axis-(1 0 5), (2 0 3), (2 1 1) follows

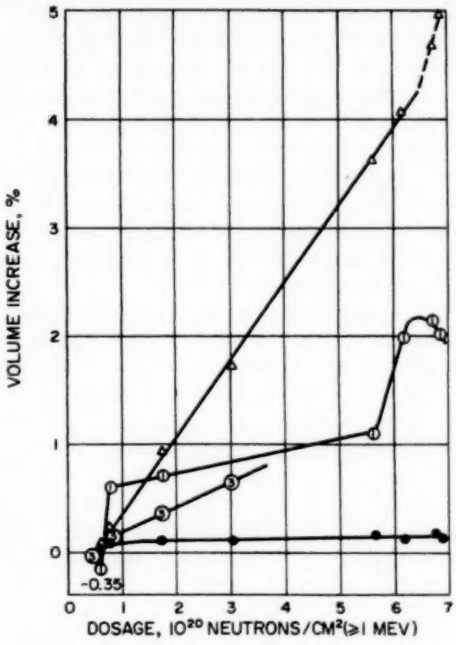

Fig. II-2 Expansion of individual X-ray reflections as a function of dosage in 5-μ grain size BeO irradiated at approximately 100°C.[42] ①, (2 1 1) X-ray line; ③, (2 0 3) X-ray line; ●, (3 0 0) a axis; Δ, macroscopic volume.

an individual pattern of change with irradiation dose.[42] The (2 1 1) reflection, which normally is the least precise measure of the c axis, appears to be fair indicator of the onset of grain-boundary separation. Figure II-2 illustrates the pattern of the c-axis expansion with dosage as defined by the individual lines in specimens of 5-μ grain size. The marked increase in the c axis at approximately 6×10^{20} neutrons/cm^2, as defined by the (2 1 1) reflection, occurs at dosages at which grain-boundary separation begins as evidenced by porosity and/or strength measurements.

Preliminary results were obtained on the irradiation stability of polycrystalline BeO, Al_2O_3 (single crystal), and MgO (single crystal) under test at Harwell.[43] Figure II-3 summarizes the test data at < 150°C for both hot-pressed and cold-pressed and sintered BeO of various grain sizes and densities. The coarse-grained hot-pressed BeO grew very rapidly with increasing dose and ultimately disintegrated at between 1.1 and 4×10^{20} neutrons/cm^2 exposure.

Cold-pressed and sintered UOX BeO of slightly smaller grain size grew at approximately the same rate, but some specimens were still intact after exposure to 3×10^{20} neutrons/cm^2. Lower density material of very fine grain size grew to a marginally smaller extent but generally retained some mechanical strength even after a dose of 6×10^{20} neutrons/cm^2. In contrast to polycrystalline BeO, the growth of magnesia and alumina single crystals showed signs of saturation.

The effects of annealing irradiated specimens are shown in Fig. II-4. The full effect of heating at any given temperature was closely approached in about 30 min; therefore 1-hr anneals at temperature were used. The anneal of hot-pressed BeO irradiated at 150°C to 1.1×10^{20} neutrons/cm^2 (>1 Mev) showed a recovery similar to that of Fig. II-4.

Hot-pressed BeO of >2.98 g/cm^3 density and 40 to 45-μ grain size was irradiated at approximately 1000°C to a dose of about 4×10^{20} neutrons/cm^2 (>1 Mev). The fractional growth was 680×10^{-5}, about the same as that produced by irradiation at 150°C to a dose of 1.1×10^{20} neutrons/cm^2. Although the specimens withstood normal handling, they showed noticeable distortion. Some of the specimens were annealed at temperatures ranging from 800 to 1780°C. No effect of annealing was observed at temperatures up to 1300°C, and only about 38% recovery was realized at 1780°C.

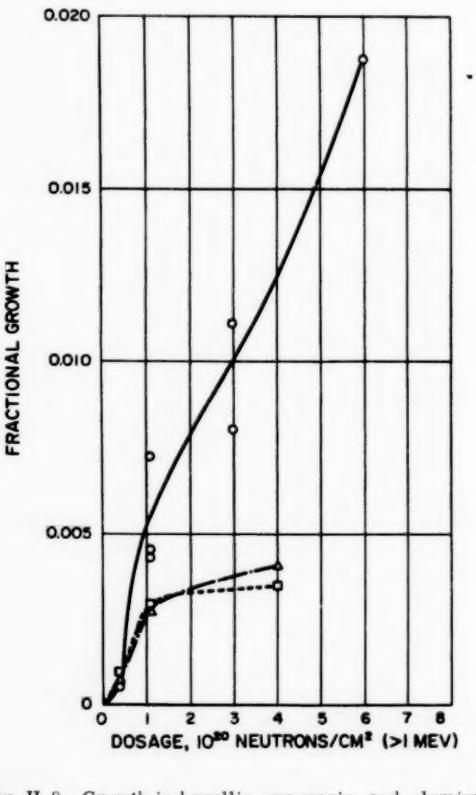

Fig. II-3 Growth in beryllia, magnesia, and alumina on irradiation at about 150°C, as a function of dose.[43] —○—, beryllia; -·△-·, alumina; ---□---, magnesia.

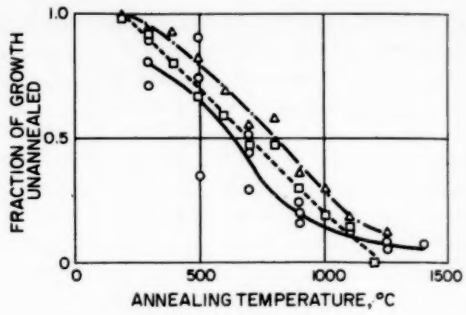

Fig. II-4 Recovery on annealing of specimens irradiated at 150°C to 4×10^{19} neutrons/cm^2 (>1 Mev).[43] —○—, beryllia (mean); ---□---, magnesia; -·△-·, alumina.

British investigators[44] have examined the influence of residual strain on the fracture stress-temperature relation of BeO. Using the theoretical relation

$$\frac{\sigma_2}{\sigma_1} = \left\{ \frac{2\gamma - (E/12)\,[\epsilon_2^2/(1-\nu^2)]\,(r - c_0)}{2\gamma - (E/12)\,[\epsilon_1^2/(1-\nu^2)]\,(r - c_0)} \right\}^{1/2}$$

where σ = fracture stress
ϵ = residual strain (subscripts 1 and 2 refer to two temperatures)
E = Young's modulus, taken as 45×10^6 psi
$2r$ = average grain diameter
c_0 = average pore diameter
ν = Poisson's ratio, taken as 0.34
γ = surface energy in the absence of residual strain, taken as 750 ergs cm^{-2}

they found good agreement between theory and experimental data up to about 700°C, as shown in Fig. II-5. The results indicate that, in the absence of other mechanisms, the magnitude of the residual strain is sufficient to account

for the shape of the fracture stress-temperature curve in this temperature range.

Carniglia et al.[45] have reported in detail on hot pressing of BeO. Of particular interest, they have reported process conditions for preparing uniform, high-purity BeO bodies of simultaneously high density (99.7 to 100% of theoretical) and fine grain size (to a limit of 10-μ average). The routine consists in a dwell

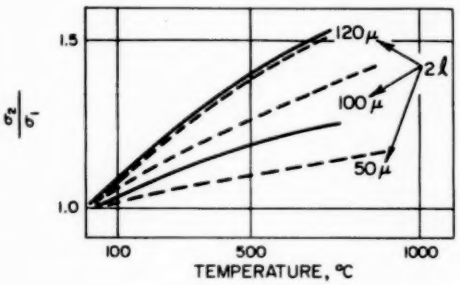

Fig. II-5 Theoretical and experimental forms of σ_2/σ_1 against temperature. Dotted curves are the theoretical values for three different grain sizes.[44] ——, experimental; ---, theoretical.

at temperature without the application of pressure, an optimized time-temperature-pressure cycle, and rapid heating and cooling ramps. Techniques for the controlled preparation of BeO of ultrafine grain size at somewhat less than full density are also discussed.

Anionic impurities of fluorine, phosphorus, sulfur, or silicon in BeO powders were found to be of primary importance in determining required processing parameters for a given final hot-pressed density. The persistence of high modulus-of-rupture strength (48,000 psi) to 1500°C has been demonstrated for anion-free BeO hot pressed to full density. It is estimated that a strength of 60,000 psi at 1500°C may be achieved by present techniques of hot pressing pure BeO.

A useful discussion of BeO properties, fabrication, and radiation stability is contained in a report by Rothman.[46]

X-ray diffraction studies were performed at Oak Ridge[47] on BeO single crystals after irradiation at 100, 650, and 1050°C to integrated fast-neutron doses of over 10^{21} neutrons/cm^2. At 100°C the radiation debris appeared to be distributed in small agglomerates (about 10 to 100 defects per agglomerate), which do not affect the coherent scattering of X rays from the crystal lattice. At 650°C there appears to be microscopic (>10,000 A diameter) agglomeration of the debris, and the crystal is severely fractured on basal planes. Irradiation at 1050°C produces less drastic changes in the optical, physical, and X-ray scattering properties of BeO single crystals. Basal-plane fracture or unambiguous regions with microscopic debris agglomerates are no longer observed. The conclusion was that defect agglomerates are unstable at that temperature and that in-pile annealing occurs. (M. C. Brockway)

Beryllium Compounds

The Seebeck coefficients were measured by General Electric[48] for $ZrBe_{13}$ and $NbBe_{13}$. For $ZrBe_{13}$ the coefficient reached maximum values of 12 to 13 μv/°C in the 900 to 1100°C temperature range. For $NbBe_{13}$ the peak value of 19 μv/°C was reached at 1100°C. The authors judged these values too low to be of interest, and so the materials were dropped from their experimental research program.

Evaporation data were obtained at the Denver Research Institute[49] for $ZrBe_{13}$, $NbBe_{12}$, and Nb_2Be_{17} in the temperature range from 900 to 1200°C. The standard enthalpies of sublimation in kcal/gram atom of beryllium were determined from van't Hoff plots as 85.0 for $ZrBe_{13}$, 19.9 and 59.5 for $NbBe_{12}$, and 98.0 and 55.8 for Nb_2Be_{17}. The authors postulate that there are two enthalpies of sublimation for the niobium beryllides because of a heretofore unknown beryllide intermediate in beryllium content between Nb_2Be_{17} and $NbBe_3$. Thus $NbBe_{12}$ and Nb_2Be_{17} decompose on evaporation to this intermediate species which subsequently decomposes to $NbBe_3$. (R. W. Getz)

Solid Hydrides

Strontium Hydride

The strontium-hydrogen system was studied at Iowa State.[50] The maximum solubility of SrH_2 in strontium metal is 38 mole % at the peritectic temperature of 880°C. Strontium metal undergoes an allotropic transformation at 555°C and melts at 768°C. A second transformation was found at 240°C in samples con-

taining hydrogen. SrH_2 was found to have an allotropic transformation at 855°C.

(H. H. Krause)

References

1. A. J. Perks and J. H. W. Simmons, Radiation Induced Creep in Graphite, British Report AERE-R-4372, August 1963.
2. I. M. Dawson and E. A. C. Follett, The Oxidation of Graphite. I. The Observation of Oxidation of Synthetic Graphite Before and After Irradiation, *Proc. Roy. Soc. (London), Ser. A,* 274: 386-394 (July 30, 1963).
3. J. H. Reynolds (Ed.), Nuclear Engineering Department Progress Report, September 1–December 31, 1962, USAEC Report BNL-782, Brookhaven National Laboratory, May 1963.
4. W. L. Robinson and F. W. Drosten, The Electrorefining of Beryllium — Novel Features in Molten Salt Extraction, paper presented at AIME Meeting, Cleveland, Ohio, Oct. 22, 1963.
5. R. F. Bunshah and R. S. Juntz, A Crucibleless Vacuum Induction Melting and Casting Process for Consolidation and Purification of Reactive Metals, USAEC Report UCRL-7388, Lawrence Radiation Laboratory, 1963.
6. B. Schaub and G. Cabane, Purification of Beryllium by Zone Melting (in French), *Compt. Rend.*, 257(2): 444-447 (July 8, 1963).
7. R. Syre and J. M. Logerot, Recent Advances in the Metallurgy of Beryllium (in French), *Rev. Met. (Paris)*, 60(7/8): 684-691 (July–August 1963).
8. J. Laverlochere and S. May, Determination of Several Impurities in Beryllium by Neutron Irradiation (in French), *Bull. Soc. Chim. France*, 3: 457-462 (March 1963).
9. S. Gelles, V. Nerses, and J. Siergiej, Beryllium as a Structural Material, *J. Metals*, 15(11): 843-848 (November 1963).
10. R. G. Jenkins and J. M. Siergiej, Development of Improved Fabrication Methods, Process, and Techniques for Producing Typical Aircraft Shapes from Beryllium. Interim Progress Reports, February 1, 1963–April 30, 1963, Report NMI-9701.9, and May 1, 1963–July 31, 1963, Report NP-13072, Nuclear Metals, Inc.
11. T. A. Tarpey, I. B. Roll, V. Nerses, and J. M. Siergiej, Final Report to Union Carbide Nuclear Company, Beryllium Tubing Program, USAEC Report NMI-4971, Nuclear Metals, Inc., Feb. 27, 1962.
12. E. A. Murphy and R. G. O'Rourke, Fabrication of Ultrafine Beryllium Wire. Final Report. Technical Report 318-240, Brush Beryllium Co., Aug. 1, 1963.
13. Hanford Atomic Products Operation, Ceramics Research and Development Operation, Quarterly Report, April–June 1963, USAEC Report HW-76302.
14. W. I. Kern and L. E. Lubin, Electron-Beam Welding of Aerospace Materials, Report ASD-TDR-63-132, Hamilton Standard Division, United Aircraft Corp., February 1963.
15. J. N. Krusos, A. S. Kjelby, J. Borosie, and F. B. Eck, Fabrication and Properties of Beryllium-Faced Sandwich Structures, *Mater. Res. Std.*, 3(10): 825-831 (October 1963).
16. D. Titus, One Shop's Experience in Machining Beryllium, *Machinery (N. Y.)*, 69(8): 109-112 (April 1963).
17. R. I. Garber, I. A. Gindin, and Yu. S. Shubin, Compression of Beryllium Single Crystals along the Hexagonal Axis in the Temperature Range 4.2-900°K, *Soviet Phys.-Solid State, (English Trans.)*, 5: 315-320 (August 1963).
18. Nuclear Metals, Inc., Fundamental and Applied Research and Development in Metallurgy, Progress Report to United States Atomic Energy Commission for Month of July 1963, USAEC Report NMI-2119, Sept. 12, 1963.
19. D. F. Kaufman, E. D. Levine, J. J. Pickett, and L. R. Aronin, The Effect of Zone Refining on the Purity and Mechanical Properties of Beryllium Single Crystals, Report NMI-TJ-54, Nuclear Metals, Inc., Aug. 7, 1963.
20. W. Munro and N. A. Hill, The Deformation of Beryllium under Complex Stressing, *Metallurgia*, 66(395): 105-110 (September 1962).
21. W. Bonfield, J. A. Sartell, and C. H. Li, The Effect of Surface Condition on the Microstructure of Beryllium, *Trans. AIME*, 227(3): 669-673 (June 1963).
22. P. Bastien and P. Pointu, Microscopic Examination of Beryllium in the Course of Deformation in the Zone of Hot Brittleness (in French), *J. Nucl. Mater.*, 10: 63-66 (September 1963).
23. P. Pointu, P. Azou, and P. Bastien, Microscopic Observation of the Deformation of Beryllium in the Embrittlement Zone (in French), *Compt. Rend.*, 256: 4419-4421 (May 20, 1963).
24. P. Bastien and P. Pointu, Thermal Evaporation and Impurities of Commercial Beryllium Between 650 and 1000°C (in French), *J. Nucl. Mater.*, 9(2): 185-196 (July 1963).
25. K. J. H. MacKay and N. A. Hill, Lattice Parameter and Hardness Measurements on High Purity Beryllium, *J. Nucl. Mater.*, 8(2): 263-264 (March/April 1963).
26. P. M. Arzhanyi, R. M. Volkova, and D. A. Prokoshkin, Investigation of the Cb-Be System (in Russian), *Dokl. Akad. Nauk SSSR*, 150(1): 96-98 (1963).
27. J. J. Koziol, Summary Report, Beryllium Diffusion Barrier Coatings, Report PWA-2184, Pratt & Whitney Aircraft Division, 1962.
28. J. A. Carrabine, Ternary Phases in Commercially Pure Beryllium, *J. Nucl. Mater.*, 8(2): 278-280 (March/April 1963).

29. M. Weisz, J. Mallen, and J. L. Baron, Possibility of the Appearance of the Liquid Phase Beginning at 430°C in Commercial Beryllium (in French), *J. Nucl. Mater.*, 10: 56-59 (September 1963).
30. T. Raine and J. A. Robinson, Beryllium Alloys, British Patent 933,408, Aug. 8, 1963.
31. R. Reich, Vu Quang Kinh, and J. Bonmarin, Study of the Electrical Resistance of Beryllium Samples as a Function of Temperature and Determination of Their Debye Temperature (in French), *Compt. Rend.*, 256(26): 5558-5561 (June 24, 1963).
32. E. E. Weismantel and H. J. Fisher, Beryllium, *Machine Design* (Nonferrous Book Issue), 35(22): 55-57 (Sept. 19, 1963).
33. E. D. Levine, L. R. Aronin, and S. H. Gelles, Low-Reduction Rolling of Beryllium and Beryllium-1% Copper Alloys, *Trans. Am. Soc. Met.*, 56(3): 540-549 (September 1963).
34. I. A. Menzies, Observations on the Oxidation of Beryllium in Carbon Dioxide at 600–700° (in English), *Corrosion Sci.*, 3(1): 35-49 (January–March 1963).
35. Nuclear Metals, Inc., Beryllium Corrosion in High-Temperature Water and Steam, *The Joint Research and Development Program Quarterly Digest*, Period from April 1 to June 30, 1963, 3(2): 40 (September 1963).
36. D. S. Kneppel, Beryllium Corrosion, Final Technical Report to United States Atomic Energy Commission, April 25, 1962 to April 24, 1963, USAEC Report NMI-1911, Nuclear Metals, Inc., Mar. 24, 1963.
37. L. Whitby, E. Gowen, and D. J. Levy, Chromic Acid Anodizing of Beryllium: Process Parameter, paper from 48th Annual Technical Proceedings, American Electroplaters' Society, Newark, N. J., 1961.
38. B. S. Hickman, G. Bannister, J. H. Chute, J. G. McCracken, R. Smith, and J. C. Bell, Irradiation of Beryllium at Elevated Temperatures. Part I. Irradiation of RIG X-17 in HIFAR, British Report TRG-Report-540, July 31, 1963.
39. G. Cabane, Beryllium in Nuclear Applications (in French), *Rev. Mét. (Paris)*, 60(7-8): 691-696 (July–August 1963).
40. B. S. Hickman and G. T. Stevens, The Effect of Neutron Irradiation on Beryllium Metal, Australian Report AAEC/E-109, June 1963.
41. V. M. Kozlov and V. D. Turovskiy, Beryllium: Toxicology, Clinical Aspects of Diseases, Labor Hygiene, U. S. Dept. of Commerce, Office of Tech. Services, Tech. Translation 63-13366; Report JPRS 16496, Dec. 3, 1962.
42. General Electric Company, Advanced Technology Services, High-Temperature Materials Program Progress Report No. 28, Part A, USAEC Report GEMP-28A, Nov. 11, 1963.
43. J. A. Desport and J. A. G. Smith, Irradiation-Induced Growth in Oxides of Beryllium, Magnesium, and Aluminum, British Report AERE-R-4443, September 1963.
44. T. W. Baker, P. J. Baldock, and F. J. P. Clarke, Residual Strains and the "Fracture Stress-Temperature" Relation in Beryllium Oxide, British Report AERE-R-4437, September 1963.
45. S. C. Carniglia et al., Hot Pressing for Nuclear Applications of BeO: Process, Product, and Properties, USAEC Report NAA-SR-Memo-8988, Atomics International, October 1963 (to be published).
46. A. J. Rothman, Beryllium Oxide for Nuclear Propulsion Application, USAEC Report UCRL-7428, University of California, Lawrence Radiation Laboratory, July 1, 1963.
47. Oak Ridge National Laboratory, Nov. 11, 1963. (Unpublished)
48. General Electric Company, Advanced Technology Services, High-Temperature Materials Program Progress Report No. 29, Part B, USAEC Report GEMP-29B, Dec. 6, 1963. (Classified)
49. C. B. Magee, M. J. Pool, W. D. McMullen, R. C. Jerner, and D. G. Ellis, Investigation of the Characteristics of Intermetallic Compounds as Thermionic Emitters, First Annual Technical Summary Report, USAEC Report DRI-2079, Denver Research Institute, Dec. 31, 1962.
50. Ames Laboratory, Annual Summary Research Report of Chemistry, Engineering, Metallurgy, Physics, and Reactor Divisions, July 1, 1962–June 30, 1963, USAEC Report IS-700, September 1963.

Section

III

Reactor Materials

Nuclear Poisons

Metallic Poisons

Mechanical properties of hafnium sheet were determined[1] at 2000°F after the specimens had oxidized 3 hr at that temperature. The following properties were found: ultimate tensile strength, 4790 psi; 0.2% offset yield strength, 4000 psi; and elongation, 21%. The specimens were very brittle at room temperature. The oxygen diffusion constants[2] in hafnium were 3.8×10^{-11} and 7.6×10^{-10} cm^2/sec at 800 and 950°C, respectively. (M. Kangilaski)

Dispersion Poison Materials

Recent studies at Oak Ridge[3] have been concerned with the evaluation of cadmium-bearing materials for use as a burnable poison in the High-Flux Isotope Reactor fuel plates. For this application it is necessary for the candidate materials to be compatible with the filler-section constituents in the fuel plates, aluminum, and B_4C. Specimens containing several cadmium materials along with aluminum and B_4C were heat-treated for 24 hr at 600°C. A low-silica glass containing 19 wt.% CdO exhibited the best stability, although $CdSO_4$ also showed promise. Subscale fuel plates containing the CdO and $CdSO_4$ materials were fabricated, and prototype fuel plates were later produced using the low-silica glass material.

The irradiation behavior of bulk B_4C and B_4C + SiC burnable-poison control plates was reported[4] in studies conducted at Bettis. Zircaloy-clad elements of these materials were irradiated in pressurized hot-water loops and in the Materials Testing Reactor process water to depletions as high as 97% burnup of the B^{10} atoms present. The B_4C showed first a linear volume swelling rate, followed by more rapid swelling as a result of B_4C cracking. Elements containing B_4C-SiC showed greater thickness changes as a result of SiC cracking. A severe decrease in hot-water corrosion resistance for the B_4C and B_4C-SiC during irradiation was noted as disintegration of these poison cores occurred.

A study of the oxidation of B_4C powder showed measurable reactions at temperatures as low as 250°C with H_2O vapor and 450°C in dry air.[5] The presence of the oxidation product, B_2O_3, on the surface of B_4C was found to inhibit the oxidation by H_2O but not by air. Oxidation by dry air occurs at a lower rate than with H_2O vapor until approximately 700°C.

Efforts to cast hafnium carbide have not been successful, according to a recent report[6] issued by the U. S. Bureau of Mines. Castings that appear externally to be sound were found to have numerous internal cracks when radiographed and sectioned. The cracks are believed to have resulted from thermal-shock effects during solidification. (E. G. Smith, Jr.)

References

1. University of California, Lawrence Radiation Laboratory, 1963. (Unpublished)
2. G. R. Wallwork, The Diffusion of Oxygen in Hafnium, *J. Electrochem. Soc.*, 110: 943-944 (August 1963).
3. T. D. Watts and K. K. Sinha, Compatibility of Cadmium-Bearing Materials with the High Flux Isotope Reactor Fuel Plate Constituents, USAEC Report ORNL-TM-647, Oak Ridge National Laboratory, Oct. 1, 1963.
4. R. G. Gray and L. R. Lynam, Irradiation Behavior of Bulk B_4C and B_4C-SiC Burnable Poison Plates, USAEC Report WAPD-261, Westinghouse Electric Corp., Bettis Atomic Power Laboratory, October 1963.
5. L. M. Litz and R. A. Mercuri, Oxidation of Boron Carbide by Air, Water, and Air-Water Mixtures at Elevated Temperatures, *J. Electrochem. Soc.*, 110: 921-925 (August 1963).
6. Bureau of Mines, Quarterly Metallurgical Progress Report No. 20, July 1–September 30, 1963, USAEC Report USBM-U-1082.

Section

IV

Reactor Materials

Cladding and Structural Materials

Corrosion

Zirconium Corrosion

General. On the basis of a statistical analysis of corrosion results for a number of zirconium alloys after 3000 hr exposure to 300, 400, and 500°C steam, Vallecitos[1] has concluded that a zirconium alloy containing about 1.2 at.% copper, 1.4 (or higher) at.% chromium, and 0.3 at.% iron shows promise of significant improvement in corrosion behavior over that of Zircaloy-2. However, preliminary results of hydrogen analysis now in progress indicate that this alloy composition may not be optimum from the standpoint of hydrogen absorption.

Studies on the corrosion behavior and hydrogen pickup in zirconium-niobium binary alloys containing up to 4.2 wt.% niobium have been summarized by Klepfer.[2,3] Optimum corrosion resistance was obtained in samples heat-treated to produce the equilibrium niobium content in the matrix at the test temperature. Zirconium-niobium alloys performed better than Zircaloy-2 in steam at 482°C but had higher corrosion rates than Zircaloy-2 in 288, 360, and 400°C water and steam. Total hydrogen weight gains (from pickup of corrosion-released hydrogen) were less than for Zircaloy-2. Hydrogen solubility apparently was higher in the zirconium-niobium alloys than in Zircaloy-2, since mechanical tests revealed a low susceptibility to corrosion-hydrogen embrittlement in alpha-phase alloys.

The effect of carbon in the range of 167 to 983 ppm on the aqueous corrosion behavior of Zircaloy-2 has been reported by Bettis.[4] Results of studies in 680°F water and 750°F, 1500-psi steam indicate that the corrosion resistance of Zircaloy-2 with alpha or beta microstructures decreases with increasing carbon content. However, carbon additions reduced the deleterious effects on corrosion resistance of cooling through the alpha-plus-beta phase region. Carbon additions also reduced the ratio of hydrogen absorbed to that generated from the corrosion reaction but did not reduce the total amount of hydrogen absorbed.

Radiation Effects. Studies at Hanford[5] continue to reveal a marked effect of radiation on the corrosion behavior of Zircaloy-2. Specimens receiving a total fast-neutron exposure of 8.2×10^{20} neutrons/cm^2 during 125 days' exposure to water at 540°F exhibited an average weight gain of 121 mg/dm^2, as compared with 8.8 mg/dm^2 for out-of-reactor exposure to the same conditions. The fractional pickup (but not the total quantity) of hydrogen theoretically available from the corrosion reaction was less for in-reactor specimens than for those exposed out-of-reactor.

Zircaloy-cladding failures in two compacted UO_2-PuO_2 Plutonium Recycle Test Reactor (PRTR) Mark I fuel elements have been reported by Hanford.[6] A hole, approximately $^3/_{16}$ by $^3/_{32}$ in., in the side of one rod resulted in only a small amount of fuel washout, no water-logging of the fuel, limited in-reactor sintering of the fuel, and embrittling and cracking of the cladding. Failures in the second fuel element occurred as the result of internal corrosion at the heat-affected zone of the top end-cap weld. The cause of the failures has not been determined, although 30 ppm fluoride and 350 ppm chloride have been detected in the same batch of UO_2-PuO_2 fuel as that used in the elements with the end-cap weld failures.

Oxide Films. Variations in the impedance of oxide films, preformed anodically or thermally in water vapor and dry oxygen, on zirconium and some of its alloys have been studied at Chalk River.[7] Electrolytic evolution of hydrogen

on the oxide surfaces resulted in lowering of the resistance, with a corresponding increase in capacitance for all oxides. The initial oxide impedance value on unalloyed zirconium was recovered as soon as the cathodic charging ceased. The impedance changes in the oxides on Zircaloy-2, Zircaloy-4, and zirconium–2.5 wt.% niobium persisted after the cathodic treatment and after washing in distilled water. Initial values for these alloys were recovered after only a few seconds at anodic potentials large enough to remove hydrogen but too small to cause oxide growth.

The effect of pressure on the oxidation rate of Zircaloy-2 in steam and oxygen at 300 to 600°C has been studied by Cox.[8] Under constant-pressure conditions, the oxidation rate was found to be relatively insensitive to pressure. However, a sudden increase in pressure during posttransition oxidation resulted in a rapid increase in the instantaneous oxidation rate, which was then followed by a recovery to the rate existing prior to the change in pressure. This effect was explained by porosity in the posttransition oxide film which, upon a pressure increase, allowed an increased flow of reactant to the metal-oxide interface, thereby increasing the production of nonstoichiometric oxide. The increasing thickness of this nonstoichiometric oxide then tended to restrict the access of further reactant. This proceeded until the equilibrium between production of nonstoichiometric oxide and its oxidation to stoichiometric oxide was set up again (the latter is believed to be the reaction during posttransition behavior).

(W. E. Berry)

Oxygen in Zircaloy-2

Harwell[9] has reported a study in which predetermined amounts of oxygen were added to Zircaloy-2 by three methods that were expected to give widely different distributions of the oxygen in the metal. Subsequent oxidation of these specimens in steam showed increases in the oxidation rate, as illustrated by Fig. IV-1.

In the reported work, the specimens in which the oxygen was most inhomogeneously distributed were those containing a fine distribution of ZrO_2 particles, and these showed pretransition rates similar to those of low-oxygen material (up to 1 wt.% oxygen) but with the time to transition decreasing, as expected, with increasing oxygen content.

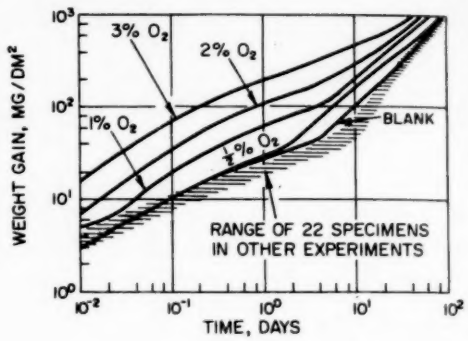

Fig. IV-1 Oxidation of 0.030-in.-thick Zircaloy-2 containing oxygen added by annealing for 24 hr at 1000°C.[9]

The high weight gains (an order of magnitude higher for 3 wt.% of oxygen added) of some of the specimens annealed at 1000°C (in both the pretransition and posttransition periods) were due to the segregation of some of the oxygen at the grain boundaries, as a result of the method of preparation. With improving surface finish (by elimination of microcracks), the oxidation rates approached those of low-oxygen material. However, it was only in specimens in which the oxygen at the surface was uniformly distributed (prepared by annealing at 800°C) that the oxidation rate was indistinguishable from that of low-oxygen Zircaloy-2. Thus the breakdown of the oxide film on Zircaloy-2 is not affected by the presence of oxygen uniformly distributed in the metal, or present as a concentration gradient through the metal. It is affected by the inhomogeneous distribution of oxygen in the surface, and particularly by the limiting case of this where the oxygen is present as particles of ZrO_2 in the metal. (A. W. Lemmon, Jr.)

Aluminum Corrosion

In-reactor studies at Hanford[10] have determined the effect of radiation on the corrosion of 1245 aluminum in treated *p*H 7 Columbia River water at 90°C. In exposures of up to 147 days, the amount of film adsorbed and the corrosion rates were three to five times greater with radiation than with little or no radiation.

(W. E. Berry)

Corrosion of Iron- and Nickel-Base Alloys

Steam. There appears to be little or no effect of pressure on the corrosion behavior of

iron- and nickel-base alloys in deoxygenated steam, on the basis of studies being conducted by Hanford.[11] After 72 days' exposure to 550°C, 5000-psi steam, alloys exhibited the corrosion behavior indicated below.

Weight gain, mg/dm²			
8.0 to 9.4	12.0 to 47	57 to 68	144 to 248
Hastelloy X	Hastelloy N	Fe–25 Cr–3 Al–0.5 Y	Stainless steels
Incoloy	Type 446 stainless steel	Nichrome V	Type 304L
Inconel X	17-4 PH	R-27	Type 406
			Type 316L
			Type 430

The above corrosion results are virtually the same as those obtained in 550°C, 3000-psi steam for the same length of time. After 35 days in atmospheric steam at 550°C, weight gains ranged from 6 to 201 mg/dm², with almost the same alloy grouping as indicated above.

Corrosion studies in flowing steam at 730°C and 3 atm pressure are being conducted by General Electric.[12] Average weight-gain rates after exposures of up to 1279 hr are 10 mg/(dm²)(month) for iron–25 wt.% chromium–4 wt.% aluminum–1 wt.% yttrium alloy, 25 mg/(dm²)(month) for niobium–modified 80 wt.% nickel–20 wt.% chromium, and 27 mg/(dm²)(month) for type 304 stainless steels. Annealed and vapor-blasted specimens exhibited lower weight gains than annealed and pickled specimens (pickled type 304 stainless-steel specimens were the only ones studied which spalled and lost weight).

Water. Results of stress-corrosion studies in tilting autoclaves have been reported by Knolls.[13] The exposure cycle consisted of two 100-hr periods in aerated boiler water (500 ppm chlorides) at 500°F, followed by two 336-hr periods in aerated seawater at 550°F. No cracking was observed in wrought strips of Inconel 600, Inconel X, Inconel C, Zircaloy-2, or Zircaloy-4 or in three-layer deposits of nickel-chromium-iron weld overlays on carbon steel. Stress-corrosion cracking was observed in type 308 stainless-steel three-layer weld overlays on carbon steel and in wrought type 304 stainless-steel strips.

Corrosion studies in simulated N-Reactor secondary have been conducted at Hanford.[14] Average water conditions were 3 to 5 ft/sec, 160°C, 10 to 70 ppb N_2H_4, 5 ppm solids, less than 0.5 ppm chloride, *p*H 8.6, and specific resistivity 192,000 ohm-cm. Corrosion rates are summarized below.

Material	Penetration rate, mil/year
A-212 carbon steel	0.08
Type 304 stainless steel	0.015
70-30 copper-nickel	0.05
Admiralty metal	0.11
Silicon bronze (type A)	0.15

Aqueous Solutions. As a relative indication of possible performance of nuclear superheater materials, General Electric[15] has conducted stress-corrosion tests on a number of candidate materials in boiling $MgCl_2$. Approximate exposure times at which cracking was first noted in U-bend specimens are indicated below.

Material	Time to cracking
Stainless steels	
Type 304	35 min
Type 347	50 min
Type 316	60 min
Type 310	90 min
Type 304 (vacuum melt)	10 hr
Incoloy	288 hr
Ni-O-Nel	336 hr
Inconel 625	584 hr
Hastelloy X	585 hr

A rapid test for determining intergranular corrosion in nickel-molybdenum and nickel-molybdenum-chromium alloy has been described by Graefen.[16] Hastelloy C bars or strips were exposed 24 hr to boiling 10% hydrochloric acid and then bent. Intergranular corrosion was evidenced by tearing in the area of grain boundaries on bending.

Oxidation. A mixed parabolic rate has been observed for the oxidation of TD (thoria dispersion) nickel at Hanford.[5] This suggested that a phase-boundary reaction partially controlled the oxidation rate. Although thoria particles accumulating at the metal-oxide interface might affect kinetics, it was believed that a reaction at the oxygen-oxide interface was more likely, on the basis of the observed pressure dependence of oxidation.

Candidate materials for cladding and structural components of the High-Temperature Lattice Test Reactor (HTLTR) are being exposed to 1000°C purified nitrogen (5 ppm oxygen, 10 ppm argon, and 1 ppm hydrocarbon) at Hanford.[17] The hot gas was passed through graphite and then over the specimens. After 10 days' exposure, A-nickel and TD nickel exhibited no weight change. Weight gains for Inconel 600, Inconel 625, Hastelloy X-280, Hastelloy B, and molybdenum specimens in contact with graphite ranged from 400 mg/dm^2 (molybdenum) to 700 mg/dm^2 (Inconel 600). Specimens not in contact with graphite had slightly smaller weight gains. (W. E. Berry)

Corrosion of Stainless Steels

Steam. Intergranular attack observed in austenitic stainless steel in a superheat loop has been duplicated by General Electric in out-of-pile studies.[18] Types 304 and 316 stainless steels exhibited intergranular attack in a so-called $FeCl_3$ superheat cycle that employed 0.5 ppm chloride (as $FeCl_3$) in the water and 20 ppm oxygen and 2.5 ppm hydrogen in 1000-psi steam. High superheat was not required to cause localized corrosion under these conditions. Intergranular attack occurred at or near boiling operation temperature within 44 hr of exposure.

The factors that influence chloride deposition from high-temperature steam have been investigated by General Nuclear.[19] Sodium chloride containing radioactive Cl^{36} was injected into steam at pressures of 800 to 900 psig. Moisture in the steam was found to have the most pronounced effect on deposition. Dried and superheated steam reduced chloride deposition by a factor of 10, as compared to steam containing moisture. Surface defects, including pits and corrosion films, increased deposition. Steam or heater-surface temperatures in the range of 530 to 1100°F had no effect. The degree of superheat in dry steam also had no effect. Greater deposition occurred at low steam velocities.

Intergranular attack has been observed in austenitic steels exposed 2500 hr to oxygenated steam containing up to 0.5 wt.% moisture and flowing at 250 ft/sec at 489°F and 600 psi in experiments conducted by Allis-Chalmers.[19] Penetration rates to 0.0045 in./year were observed. Increased intergranular penetration was observed with increasing moisture in the steam. Types 304L and 316L stainless steels possessed about equal corrosion resistance and were more resistant than the normal carbon grades of these alloys.

Water. The intergranular stress-corrosion cracking in type 304 stainless-steel nozzles in the high-purity heavy-water moderator of the Savannah River reactors has been attributed to low concentrations of chloride ions in the water and to insidious intergranular pickling damage in sensitized material.[20] Laboratory studies on sensitized material possessing some intergranular attack from an HNO_3-HF pickle indicated that as little as 2 ppm chloride would cause mixed transgranular and intergranular stress-corrosion cracking in *p*H 4.5 water at 90°C.

An effect of surface preparation on the corrosion of type 304 stainless steel in static water at 300°C has been reported.[21] In exposures ranging up to 84 days, metal corrosion on electropolished samples (as determined by hydrogen reduction of the oxides at 800°C) was only about one-third of that observed on samples that were rough machined, fine machined, or abraded with 600-grit paper. The results of short-time tests indicate that the reverse is true in steam at 400°C and 200 kg/cm^2 pressure. (W. E. Berry)

Corrosion of Refractory Metals

Oxidation of molybdenum from 550 to 1700°C in 5 to 76 torrs oxygen pressure is described by Gulbransen et al.,[22] in a recent publication. The changes in rate-controlling processes with temperature and pressure are shown in Table IV-1. The transition temperature refers to the temperature for a given pressure (other factors such as specimen size and environmental conditions can also affect transition temperature) below which chemical-reaction processes are rate controlling and above which gaseous transport is rate controlling. Figure IV-2 indicates schematically the temperature-reaction rate curves for a given pressure and specimen size and illustrates the significance of the transition temperature. Figure IV-3 shows the effect of specimen size on transition temperature at a given pressure, as determined by Gulbransen. The effect of pressure on reaction rate is shown in Table IV-2. At 800°C the effect of pressure on the rate of reaction is large, whereas at 1600°C there is little effect.

Table IV-1 CLASSIFICATION SCHEME: OXIDATION OF MOLYBDENUM[22]

Class	Reaction conditions	Oxidation phenomena	Rate-controlling process
1	Below 450°C	Adherent oxide films or scales form	Wagner type diffusion of metal or oxygen through oxide
2	500 – 700°C	Oxide scales form; also oxide volatilizes; low pressure favors volatility of oxide	Oxide scales not protective; probably chemical type processes on metal interface
3	801°C to transition temperature	Liquid oxide can form; volatilizes as soon as oxide forms	Chemical processes on metal interface
4	Above transition temperature	Oxide volatilizes as fast as it forms	Transport of oxygen to metal interface; turbulence in gas phase important

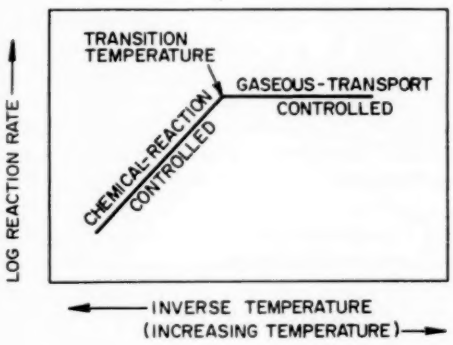

Fig. IV-2 Schematic presentation of effect of rate-controlling processes on temperature dependence of oxidation rate of molybdenum.[22]

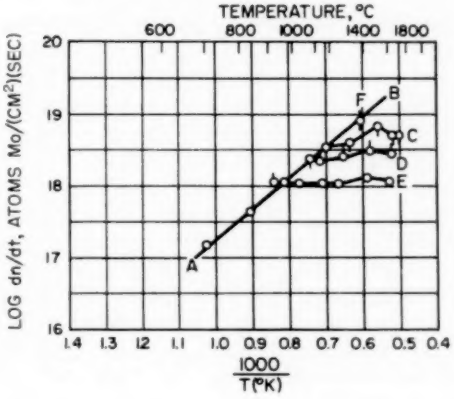

Fig. IV-3 Log dn/dt vs. $1/T$, oxidation of molybdenum, 600 to 1704°C, 76 torrs O_2: line AB, chemical control (ΔH_{AB} = 19.7 kcal/mole); area to right of AB, diffusion control; areas of samples: C, 0.304 cm^2; D, 0.604 cm^2; E, 1.215 cm^2; F, 0.12 cm^2.[22]

Table IV-2 EFFECT OF PRESSURE ON INITIAL RATES OF OXIDATION[22]

(Surface area = 1.215 cm^2)

Nominal temp., °C	Pressure, torrs	dw/dt, mg/(cm^2)(sec)	dn/dt, atoms/(cm^2)(sec)*	log dn/dt
800	76	0.0684	4.30×10^{17}	17.63
800	38	0.0180	1.13×10^{17}	17.05
800	19	0.00733	4.60×10^{16}	16.66
800	5	0.00327	2.05×10^{16}	16.31
1200	76	0.167	1.049×10^{18}	18.02
1200	38	0.150	9.42×10^{17}	17.97
1200	19	0.116	7.28×10^{17}	17.86
1200	5	0.044	2.76×10^{17}	17.44
1600	76	0.177	1.112×10^{18}	18.05
1600	38	0.156	9.80×10^{17}	17.99
1600	19	0.141	8.85×10^{17}	17.95
1600	5	0.127	7.98×10^{17}	17.90

* Atoms of molybdenum reacting/(cm^2)(sec).

Recent developments in protective coatings for refractory metals have been reviewed in a Defense Metals Information Center Newsletter.[23] Much of the experimental work in this area consists of developing manufacturing methods for coating large refractory-alloy parts. Pfaudler,[24] Thompson Ramo Wooldridge,[25] and General Telephone and Electronics[26] are presently scaling up their coating processes for molybdenum, niobium, and tantalum alloys, respectively. (J. J. English)

Corrosion of Liquid Metals

Also, research has been directed toward establishing the suitability of modified 2.25 wt.% chromium–1 wt.% molybdenum steels for sodium service in the 1000 to 1200°F range.[27] Resistance to decarburization by sodium, mechanical strength, weldability, and cost were the selection criteria. Emphasis on the former stemmed from the fact that, although ferritic steels of this type containing 2.25% or more of chromium have adequate resistance to decarburization by sodium, this characteristic is not retained if type 304 stainless steel is included in the system. In this bimetal case, the chromium must be increased to at least 5% to prevent decarburization. The increased chromium content results in several problems, particularly in the area of welding and weld ductility. The investigation established that alloying additions of vanadium, niobium, and/or titanium were effective in reducing the tendency for decarburization. A total of 11 different modifications based on these additions were thoroughly evaluated with the result that two, 4S8 (2.25 wt.% chromium–1 wt.% molybdenum–0.6 wt.% vanadium–0.1 wt.% niobium) and 4S4 (2.25 wt.% chromium–1 wt.% molybdenum–6 wt.% vanadium), were judged to possess the best all-around combination of properties.

The compatibility of 650°C sodium and UO_2, PuO_2, and mixtures of these fuel oxides (all in pellet form) was investigated by General Electric's Atomic Power Equipment Department.[28] Of four materials (UO_2, PuO_2, 20 wt.% PuO_2–80 wt.% UO_2, and 28 wt.% PuO_2–72 wt.% UO_2) tested in 20-hr exposures, only one, the 20 wt.% PuO_2–80 wt.% UO_2, demonstrated any degree of resistance to degradation. One specimen of this material, having an estimated ratio of oxygen atoms to metal atoms of 1.97 and a density of 10.56 g/cm^3, did not change significantly as a result of the exposure. However, another specimen of the same material, this one having an estimated oxygen atom–metal atom ratio of 2.04 and a density of 10.54 g/cm^3, crumbled severely.

Battelle workers are investigating the corrosion of tungsten and five commercially or semicommercially available refractory-metal alloys in 2500 to 3400°F cesium vapor atmospheres and in 2500°F liquid lithium.[29] In the 100-hr static experiments that are performed, these materials are present in the form of claddings on UC, UO_2, or UN cores. The high points of the information thus far gained can be summarized as follows:

Cesium Vapor at 2500°F. The following are quite resistant except in isolated cases involving weld areas or surface defects: tungsten, tungsten–15 wt.% molybdenum, tungsten–25 wt.% rhenium, tungsten–0.9 wt.% niobium, and TZM (molybdenum–0.5 wt.% titanium–0.08 wt.% zirconium). Tantalum–12 wt.% tungsten exhibits grain-boundary attack. The specimen weight changes* are quite variable and, in most cases, little can be concluded from them. Some consistency occurs, however, insofar as weight gains with tungsten–0.9 wt.% niobium and weight losses with tantalum–12 wt.% tungsten.

Cesium Vapor at 2800°F. Attack of the six materials has not been significant, and weight changes are generally small.

Cesium Vapor at 3100°F. Except in the case of tungsten–0.9 wt.% niobium, sample weight grains have generally prevailed. Tungsten–0.9 wt.% niobium shows slight surface attack with the weight losses, suggesting dissolution.

Cesium Vapor at 3400°F. The few data available indicate a trend of small weight losses. Extreme grain growth is apparent with tungsten–15 wt.% molybdenum and with TZM.

Liquid Lithium at 2500°F. Weight gains are generally large, with attack localized in weld zones. Only tantalum–12 wt.% tungsten exhibits a distinct surface reaction zone.

In a lower-temperature cesium-vapor-corrosion investigation,[30] (500, 800, and 1200°F) conducted at National Aeronautics and Space Administration Lewis Research Center, it was

* Except for isolated cases, the weight changes reported are in the ±4 mg/cm^2 range.

found that the following materials were attacked in varying degrees: copper, brass, bronze, gold, silver, aluminum, magnesium, Mycolex, Mykroy, and lava (the latter three are electrical insulating materials, the Mycalex and Mykroy being glass-bonded composites). Materials not attacked were tungsten, molybdenum, tantalum, iron, nickel, cobalt, platinum, Morganite, and sapphire. The observation is made that the compatible materials are all transition elements with unfilled inner shells. (J. H. Stang)

Selected Mechanical Properties of Cladding and Structural Materials

Refractory Metals

Creep data for a number of refractory-metal alloys have been obtained at General Electric.[31] Creep properties are compared for a number of different materials in Fig. IV-4.

A Defense Metals Information Center[32] summary report on the effect of fabrication history and microstructure on the mechanical properties of refractory metals and alloys has been issued by Battelle. This report summarizes the present knowledge concerning the above relation for the refractory metals niobium, tantalum, molybdenum, tungsten, and their alloys. In addition, descriptions of the metallurgical principles involved are included, with suggestions for optimizing mechanical properties by controlling metallurgical structure where possible.

The influence of carbon additions on the properties of niobium–10 wt.% tungsten–5 wt.% vanadium–1 wt.% zirconium (B-77) has been investigated by workers at Westinghouse.[33] Carbon additions of 0.077 and 0.15 wt.% were found to refine the as-cast grain size and to increase the hardness. Heat-treatment studies did not show any evidence of precipitation-hardening effects; however, solution-annealed and cold-rolled B-77 + 0.15 wt.% carbon material gave significantly higher hot-hardness values than solution-annealed material, suggesting that carbide precipitation on dislocations was contributing to high-temperature strength. Preliminary data showed that grain-boundary sliding occurred in B-77 during creep testing at 1205°C (2200°F).

Several Defense Metals Information Center reports covering the state of the art of refractory metals have been issued. The reports, reviewed briefly by subject material here, contain detailed coverage of physical, mechanical, and metallurgical properties of niobium, tantalum, tungsten, and molybdenum alloys.

The first of these reports deals with research on the following niobium-base[34] alloys (wt.%): unalloyed niobium, Nb–1 Zr, Nb–5 Zr, Nb–5 V, Nb–10 Hf–1 Ti–0.5 Zr, Nb–10 Ta–10 W, Nb–28 Ta–10 W–1 Zr, Nb–33 Ta–1 Zr, Nb–10 Ti–5 Zr, Nb–10 Ti–10 Mo–0.1 C, Nb–5 W–1 Zr, Nb–10 W–1 Zr–0.1 C, Nb–10 W–2.5 Zr, Nb–10 W–10 Hf, Nb–15 W–5 Mo–1 Zr, Nb–15 W–5 Mo–5 Ti–1 Zr, Nb–20 W–1 Zr, Nb–20 W–10 Ti–6 Mo, and Nb–5 V–5 Mo–1 Zr.

The coverage for tantalum[35] alloys includes unalloyed tantalum, Ta–10 W, Ta–12.5 W, Ta–30 Nb–7.5 V, Ta–5 W–2.5 Mo, Ta–8 W–2 Hf, Ta–10 W–2.5 Hf, and Ta–10 W–2.5 Mo.

The properties of molybdenum,[36] Mo–1.5 Nb, Mo–0.05 Zr, Mo–0.5 Zr, Mo–0.5 Ti, Mo–0.5 Ti–0.08 Zr–0.03 C, Mo–1.2 Ti–0.25 Zr–0.15 C, Mo–25 W–0.1 Zr–0.03 C, Mo–30 W, and Mo–50 W are reviewed in considerable detail.

The coverage for tungsten[37] is quite complete for the following materials: tungsten, "doped" tungsten, W–0.38 TaC, W–1 ThO_2, W–2 ThO_2, W–0.6 Nb, W–2 Mo, W–15 Mo, W–3 Re, W–5 Re, and W–26 Re.

The creep properties of a number of niobium-base alloys which are commercially available

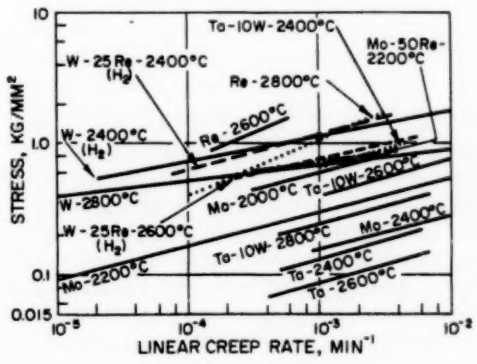

Fig. IV-4 Stress vs. creep rate for refractory metals and alloys.[31]

have been collected by the Defense Metals Information Center.[38] The creep properties presented are for temperature ranges from 1000 to 3000°F, depending upon the material tested. Data are presented for niobium, Nb–1 Zr, Nb–32 Ta–0.8 Zr, Nb–15 W–5 Mo–1 Zr–0.05 C, Nb–27 Ta–11 W–1 Zr, Nb–10 Ti–10 Mo, Nb–10 W–2.5 Zr, Nb–5 Mo–5 V–1 Zr, Nb–5 W–1 Zr–0.06 C–Y, Nb–5 V, Nb–10 Ta–10 W, Nb–10 W–10 Hf, Nb–10 Ti–5 Zr.

(J. A. DeMastry)

Selected Metallurgical Aspects of Cladding and Structural Materials

Refractory Metals

Investigators at ManLabs, Inc.,[39] have arrived at the following conclusions from their program on substructure and mechanical properties of refractory metals:

1. The effective surface energy for fracture of molybdenum strip is about 3000 ergs/cm^2.
2. Tensile ductility transition in molybdenum appears to be associated with the occurrence of necking.
3. Fibering in tungsten involves formation of ribbonlike grains containing a dislocation cell structure in which fine platelets occur.
4. Discontinuous yielding in tantalum single crystals is correlated with a decrease in the shearing strain in the principal slip system to zero, whereas that in the secondary system continues to increase.
5. The binding energy between oxygen atoms and dislocations in tantalum is about 0.54 ev.
6. Dissociation of screw dislocations along three intersecting symmetrically located planes may account for the strong lattice-friction stress in body-centered cubic (bcc) metals.

A literature search has been published[40] covering 1910 references through September 1962 on the metallurgy of molybdenum, niobium, and binary molybdenum–niobium alloys. The references deal with extractive metallurgy, refining and purifying base metals, fabrication methods, physical properties over a wide range of temperatures, and corrosion behavior of the pure metals and the binary alloys.

The solid solubility of boron and beryllium in tungsten (together with the attendant problems concerning the tungsten-rich borides and beryllides in equilibrium with tungsten, and which are liable to precipitate) is dealt with in investigations by the British.[41] Brief supplementary data are given on the tungsten-carbon system. Boron was found to be soluble to the extent of approximately 0.2 at.% in tungsten at 2500°C, its solubility decreasing with temperature. The atomic nature of this solution presents a special, and it is believed, novel problem in that it can be interstitial and substitutional. Tungsten–W_2B forms a eutectic system, the eutectic temperature being about 2600°C. A high-boron compound, WB_4, was observed.

In the tungsten-beryllium system (which presented some special hazards), the solubility of beryllium in tungsten is found to be approximately 5 at.% at the eutectic temperature (~ 2100°C). The solubility limit does not vary appreciably down to 1800°C and decreases to about 3 at.% beryllium in the 1000 to 1300°C range. The solid solution is substitutional, and lattice-spacing variations are described. The equilibrating phase is WBe_2 (hexagonal Laves structure). The diberyllide precipitates from the primary (W, Be) solution and is shown to have a significant homogeneity range itself.

A recent Defense Metals Information Center[42] report has been issued by Battelle covering the objectives of government-sponsored research on tungsten and tungsten alloys. Nine major areas, including preparation of metal, consolidation, primary and secondary working, joining, fabrication and performance of rocket nozzles, oxidation and other high-temperature reactions, protective coatings, properties, and physical metallurgy, are covered.

Zirconium

Investigators at the University of Florida[43] report the existence of two heretofore unrecognized phases, Zr_4Fe and Zr_2Fe, in the zirconium-iron system. A tentative revision of the zirconium-iron phase diagram is given.

(J. A. DeMastry)

Diffusion Studies

A useful bibliography with abstracts has been compiled by Sandia[44] on the permeability to hydrogen and helium of steel, nickel, copper, aluminum, gold, platinum, and their alloys. The

241 references abstracted are to reports and journals published from 1947 to 1963. Author and metal indexes are included.

An investigation of the diffusion and precipitation of helium in aluminum and zirconium was made by Materials Research Corporation,[45] using helium introduced by neutron irradiation and transmutation. In zirconium it is reported that the alpha phase showed the expected behavior, with helium-bubble formation and very low diffusivities and amounts of gas release. However, when heated in the beta phase, the zirconium exhibited a large gas release and high helium diffusivities which followed an Arrhenius relation. It is indicated that, in this temperature range, the helium can escape by ordinary solid-state diffusion without bubble formation. In aluminum a refined bubble distribution was achieved by recrystallizing a cold-worked structure at 350°C, with gas-bubble nucleation occurring during the heating. However, only small amounts of gas were involved, and behavior upon subsequent heating to higher temperatures was not investigated.

In another study, diffusion coefficients of hydrogen in beta zirconium were calculated from experimental hydrogen sorption curves by General Electric workers.[46] They give the relation

$$D = 5.32 \times 10^{-3} \exp(-8320/RT)$$

for temperatures between 760 and 1010°C and consider it to be independent of hydrogen concentration (to 41 at.%) and oxygen concentrations (to 4.2 at.%) in the beta zirconium.

In an investigation at Argonne[47] of the diffusion of iron and chromium in beta uranium, diffusivity constants were determined which indicated anisotropic diffusion in the tetragonal, beta-uranium lattice. A correlated vacancy mechanism is postulated for diffusion in these systems and, in a companion study, for diffusion of various impurities in gamma uranium. Included in the latter investigation have been the diffusion of chromium, manganese, cobalt, iron, nickel, copper, and niobium, and self-diffusion in gamma uranium. Also being conducted are studies of tracer diffusion of palladium in silver, copper, and palladium and of the effects of magnetic ordering on diffusion in copper-zinc and cobalt-manganese alloys.

Diffusion data from Oak Ridge[48] on various body-centered cubic metals indicate that the Arrhenius type equation does not apply to these systems over the temperature range studied. Nonlinear plots of D vs. $1/T$ for V^{48} in vanadium crystals, N^{95} in zirconium, V^{48} in titanium, Ti^{44} in titanium, and Zr^{95} in zirconium were obtained over a temperature range of 900 to 2000°C. The investigators suggest that dislocation-pipe short circuiting enhances the diffusion rate at lower temperatures, causing the deviations from linearity. Also studied has been the diffusion of Nb^{95} in UO_2 over the temperature range of 1096 to 2100°C. It is shown that the diffusivity of the Nb^{95} in pressed and sintered UO_2 pellets increases with increasing temperature from 1265 to 1600°C but remains nearly constant at 2×10^{-8} cm^2/sec from 1700 to 2100°C. In fused UO_2 the diffusivity increases with increasing temperature from 1100 to 2100°C, but an actual relation for the temperature dependence has not yet been determined.

The diffusion of zirconium, molybdenum, vanadium, and oxygen in titanium, and self-diffusion in titanium have been investigated[49] in the temperature range of 600 to 1300°C. Used in the experiments were electron-microprobe analysis for the metallic elements, vacuum-fusion analysis for oxygen, and tracer methods for the self-diffusion of titanium. The following values are reported:

Diffusion couple	$\ln D_t$
Zr in α Ti	$-27.14-11{,}800/RT$
Zr in β Ti	$-4.01-40{,}000/RT$
Mo in α Ti	$-17.19-28{,}400/RT$
Mo in β Ti	$-9.00-33{,}100/RT$
V in α Ti	$-31.39-3100/RT$
V in β Ti	$-4.38-41{,}400/RT$
O in α Ti	$-14.94-16{,}200/RT$
O in β Ti	$+8.37-66{,}800/RT$
Self-diffusion	$\ln D_t$
α Ti	$-21.08-5700/RT$
β Ti	$-8.40-28{,}600/RT$

The values determined for molybdenum and vanadium in alpha titanium and for the self-diffusion of titanium are considered by the investigators to be preliminary. Also, diffusivities and solubilities of uranium and plutonium in magnesium from 365 to 534°C have been determined[50] using electron-microprobe analysis. It is suggested that the diffusion of these elements in magnesium and the solubility of uranium in magnesium are not necessarily

negligible in reactor systems. The relatively large solubility of plutonium in magnesium, as previously known, was confirmed in this work.

(D. C. Carmichael and A. N. Ashurst)

Ceramic Technology

The formation and properties of solid solutions in the ZrO_2-CeO_2, ZrO_2-Y_2O_3, and ZrO_2-La_2O_3 systems[51] have been studied by Leler and Andreeva. Fully stabilized zirconias were produced in each system. The solid solutions of ZrO_2-Y_2O_3 exhibited the highest thermal and chemical stability. Several of the solid solutions have a lower thermal-expansion coefficient and a higher thermal stability (at 1200°C) than ZrO_2 stabilized with CaO or MgO.

The thermal expansion, thermal diffusivity, and elasticity over a range of temperatures of zirconia bodies[52] modified by additions of MgO, Al_2O_3, CeO_2, CaO, Ti, and Zr have been determined by Materiadyne.

Arthur D. Little[53] has reported thermodynamic and kinetic data pertinent to the chemical behavior of zirconium and hafnium carbides and borides at temperatures to 3000°K and in various atmospheres.

In the second year of a continuing program on ceramic oxide materials for use as high-temperature thermal-energy-storage materials[54] for space power systems, General Electric has established containment life expectancies. Corrosion tests indicate that containment is feasible up to one year. The oxide mixture, 3 parts BeO – 2 parts MgO, appears to be the most stable of the mixtures studied. Combinations of BeO with MgO, Al_2O_3, and CaO were included. The best choices of container materials are tungsten-rhenium and rhenium. Considering fabrication, rhenium is the better choice of these two. Longer-time corrosion tests are continuing.

The magnitude of preferred orientation in Al_2O_3 and BeO as affected by the forming technique[55] used has been studied by Melpar. Slip-cast Al_2O_3 had a most pronounced preferred orientation of the 001 planes parallel to the mold face. Dry-pressed Al_2O_3 exhibited less orientation. Dry-pressed BeO showed orientation of the crystallites with the *c* axis perpendicular to the applied pressure.

Lynch and Krochmal[56] have reported a general survey on the problems of purity and phase control in refractory inorganic nonmetallic materials. A number of specific examples of the effects of impurities on the properties of the materials are given. Research programs to obtain high-purity well-characterized materials are described.

A study of the phenomena associated with the fracture of ceramic oxides is continuing at Illinois Institute of Technology.[57] They have reported the nature of strength and failure of MgO and Al_2O_3 for various environments and temperatures. Both hot-extruded and sintered specimens have been studied.

A bibliography of the phase relations of molybdenum, niobium, and tungsten borides, carbides, and silicides[58] has been prepared by Lockheed. The information came primarily from the period 1955 to 1962.

A refractory-ceramics selection handbook[59] has been prepared by Battelle. Property data are given on nonmetallic inorganic crystalline materials with melting points above 1500°C. Detailed properties of nearly 600 materials are presented.

(D. J. Bowers)

Radiation Effects in Nonfuel Materials

Defects: Structure and Properties

Metals. An accurate electrochemical technique for the removal of extremely thin (10 to 1000 A) uniform layers of metal from a tungsten target analogous to that used previously for range studies in aluminum has been developed.[60] This technique has been used to obtain the range distributions of Xe^{133} and Ar^{41} ions in rolled tungsten foils as a function of energy over the region 2 to 200 kev. The distributions consist of an asymmetric peak followed by a point of inflection and a very penetrating tail. Unlike the earlier distributions in aluminum, the tail in tungsten is exponential only over a limited region. It eventually decreases in an approximately Gaussian manner. Comparison with theory shows that, in tungsten, the median range is about a factor of 2 larger than that predicted by the Lindhard theory. A range distribution has also been obtained for 40-kev Kr^{85} ions in amorphous WO_3. This distribution shows no penetrating tail. A result that is in accordance with recent computer studies by Robinson

and Oen, who suggest that the tails observed in crystalline (metallic) targets are due to channeling of the incoming ions by the crystal lattice. Also, in WO_3 the median range is in reasonable agreement with theory. Observations of focused-collision sequences have also been made in UO_2 (along ⟨1 1 0⟩, ⟨1 0 0⟩, and ⟨1 1 1⟩ crystal axes)[61] and in the ⟨1 1 0⟩ axis of gold.[62] Another report[63] indicates observations of the radioactivity of copper crystals bombarded with Kr^{85} ions of well-defined energy within the range from 10 to 150 kev. Measurements were made with a GM tube after progressive controlled sputterings with nonradioactive krypton ions of 2.5 kev energy. For ion doses of the order of $10^{14}/cm^2$, such measurements have been used to provide the variation of radioactivity (concentration) with depth perpendicular to (1 1 1), (1 1 0), and (1 0 0) planes. It is supposed that channels, observed in the [1 0 0] and and [1 1 0] directions, are due to a focusing of fast krypton particles into such directions. Especially in the direction perpendicular to (1 1 0), this effect leads to the super-ranges, and appreciable concentrations of krypton atoms have been detected to depths of 4000 A, i.e., up to 20 times the most probable range.

Analysis of the defect clusters in molybdenum,[64] which had been exposed to fission fragments and annealed at 950°C, showed the defects to be composed of interstitials. This means that vacancies that had formed during the irradiation either remained in the lattice as point defects or escaped.

The recovery of zone-refined aluminum and 99.995% pure aluminum samples,[65] irradiated to 1.4×10^{18} neutrons/cm^2 (>1 Mev), took place, mainly, in two stages; the first, at −150°C with an activation energy of 0.3 ev, is sensitive to impurity content and is ascribed to the release of trapped interstitials, and the second, at −60°C with an activation energy of 0.59 ev, follows complex kinetics. Some evidence suggests that this second stage is the annihilation of a multiple vacancy type defect (quadrivacancy) by recombination with an immobile interstitial aggregate.

An investigation was made with a high-resolution (up to 7 A) electron microscope of the interaction of the U^{235} fission fragments with fine-grained cathode-sputtered metal samples[66] (grain size as small as 10 A). It was found that, in samples with grain size of less than 40 A, the fission fragments form hollow channels of 20 to 200 A diameter, which last a long time. The channels do not remain in crystal samples with a grain size of more than 100 A, but self-heal by collective rearrangement of the atoms. Uranium or aluminum layers produce tracks of both the heavy fragments (thick tracks 100 to 200 A diameter) and the light fragments (thin tracks 20 to 50 A diameter).

Defects in Metal Alloys. Recent results again illustrate that ZrO_2 alloyed with certain materials will transform as a result of neutron irradiation.[67] The system studied was the transformation from monoclinic ZrO_2, grown at 300°C on a zirconium−5 wt.% vanadium alloy, to cubic ZrO_2. Recovery is also discussed.[68] Another series of experiments covers the influence of reactor irradiation on the special structural state in nickel−20 wt.% chromium alloy, known as the K state, investigated on the basis of electrical-resistivity measurements. It is shown that two opposite processes may take place in the alloy under irradiation: destruction and formation of the K state. Depending on the initial state, one or the other process predominates. After a cold-worked and quenched alloy is irradiated, its annealing promotes further transformation of the K state, whereas the annealing after irradiation of a tempered alloy causes it to revert to the same state.

Resistivity measurements were also made on aluminum alloys[69] with copper, manganese, silicon, zinc, silver, tin, and magnesium that were annealed after neutron irradiation. The isochronal annealing curves show that each soluble element affected the lower-temperature annealing stage in a characteristic way, whereas foreign atoms had little effect on most of the upper stage. Evidence was obtained that vacancy type defects move in the upper stage, and interstitials are released in the lower stage.

Thin films of gold, copper, silver, and nickel were irradiated, and the structure before and after irradiation was examined by electron diffraction or by electron microscopy.[70] The neutron doses were in the range of 10^{17} to 10^{18} neutrons/cm^2. The films were deposited on glass and quartz substrates as well as on copper and nickel grids and were irradiated in evacuated phials or in phials filled with oxygen or inert gases. As a result of irradiating thin films of gold on copper grids in vacuum or inert gases, different alloys such as AuCu and $AuCu_3$ were formed. No alloys were observed on thin films deposited on nickel grids. Radia-

tion effects in thin films irradiated in oxygen resulted in a thorough oxidation associated with the phenomenon of alloy formation for the thin films deposited on copper grids. By irradiating copper, silver, and nickel films, diffraction patterns of Cu_2O, CuO, and (CuO), Ag_2O_3, and NiO were formed. By irradiating gold films on copper and nickel grids, different diffraction patterns very similar to those observed by Shishakov were observed. These may arise from the oxidation of impurities either in the specimens or in the grid. Some order-disorder phenomena were also observed: a hexagonal structure of nickel, the colloidal form of gold as reported elsewhere, and a hexagonal structure of silver very similar to the structure reported by Boublick. The order-disorder and the alloy-formation mechanisms may be due to enhanced diffusion associated with thermal-spike phenomena as a result of irradiation.

Defects in Other Materials. Fission fragments were recoiled into flat Al_2O_3 specimens, and the height of the expansion step formed at the boundary between irradiated and unirradiated regions of the surface measured by interferometry techniques.[71] Expansion normal to the surface was found to be independent of crystal orientation for specimens cut along three different axes. Expansion was not a linear function of fission-fragment concentration, as a factor of 10 increase in exposure produced only a factor of 3 increase normal to the specimen surface. Expansion coefficients calculated from measurements normal to the surface were at least three times larger than expansion coefficients calculated from the bending moment of thin, fission-fragment-irradiated Al_2O_3 disks. This result indicates that fission-fragment-induced expansion is not isotropic but that the stresses are preferentially relieved by expansion normal to that free surface.

Single crystals of MgO irradiated to a dose of 4×10^{19} neutrons/cm^2 at < 2000°C become very brittle.[72] From the density of damage clusters, which was observed with the electron microscope, and the smallness in the increase of the lattice parameter, 0.09%, it is concluded that most of the ions that had been displaced subsequently returned to normal lattice sites during irradiation. On annealing, the damage coarsens and can be identified as prismatic dislocation loops of ⟨1 1 0⟩ Burgers vector lying on 1 1 0. A crystal, irradiated to a dose of 5.4×10^{19} neutrons/cm^2 at 650°C, contained similar dislocation loops, the majority, if not all, of which were of the interstitial type. The damage in this crystal was homogeneous except for a narrow surface zone < 1 μ deep. However, when exactly similar crystals were annealed in air at 1200 and 1350°C, the loops disappeared from a surface zone many microns deep while coarsening in the center of the crystal.

Thin films of metastable amorphous germanium (700 ± 100 A thick), prepared by evaporation on rock salt, were bombarded with either fast neutrons or monoenergetic Xe^+ ions at room temperature.[73] Subsequent examination by bright- and dark-field transmission electron microscopy revealed that small discrete crystallized regions (ranging up to several hundred A in size) were produced throughout the amorphous matrix by the irradiation. The fast-neutron irradiation resulted in a linear increase in the density of crystallized regions with neutron doses ranging from 0 to 5.1×10^{16} neutrons/cm^2, and a most probable crystallized region size of 190 A. The monoenergetic Xe^+-ion bombardment (covering a range of incident energies) resulted in a most probable crystallized region size very closely equal to the calculated ion range for incident ion energies from 40 to 90 kev. Also, a low (<40 kev) and a high (≥ 140 kev) Xe^+-ion energy cutoff for the production of crystallized regions were observed. Other furnace-annealing experiments with similar amorphous films showed that they crystallized completely near 400°C as a result of ordinary homogeneous heating. The results were explained on the basis of "displacement spike crystallization," where the concentration of kinetic energy in the displacement cascade region was capable of inducing crystallization of the amorphous structure. A body of experimental evidence was presented, which indicated, in general, that the crystallization was confined to the displacement cascade region and therefore required the intense atomic agitation characteristic of the early stages of a displacement spike.

Woolley[74] suggests that observation of the thermal resistance of irradiated polycrystalline graphite can be explained if the grain boundaries are regarded as a sink for interstitial clusters which then produce the extra phonon scattering. Brocklehurst and Weeks[75] suggest that irradiation-induced dimensional behavior of new crystalline graphites can be

effectively predicted by observing the changes produced by bromine adsorption.

Another paper[76] first reviews previous work on spin resonance in neutron-irradiated single crystals of graphite. On irradiation, acceptors or electron traps are produced, i.e., mobile holes are set free. This results in a marked g_{11} shift, a decrease in line width, and an increase in intensity of the carrier resonance. The number of traps derived from the increase in intensity is compared with the number of displaced carbon atoms as estimated from electron-microscopy pictures of Bollmann. The ratio found is almost unity. This is discussed in terms of an amorphous region model where, due to the energy release of primary or secondary ionized carbon atoms, amorphous regions of up to 60 A in diameter are formed. The traps would be due to broken bonds within the amorphous regions. A study of the annealing of two single crystals irradiated at room temperature with 1×10^{19} and 5×10^{20} neutrons/cm^2 (thermal), shows that the recrystallization of the amorphous regions takes place at about 200°C. The two nearly identical annealing curves show that the annealing is independent of the dosage, unless the irradiation reaches the critical dosage where the amorphous regions become so dense as to overlap each other. The critical dose for irradiations at 20 to 30°C is near 5×10^{20} neutrons/cm^2. The so-called "radiation annealing" at 300°C with two single crystals is also reported. (T. G. Knorr)

Theories of Radiaton Effects

A theory of irradiation damage in graphite at power-reactor temperatures is developed,[77] on the basis of the interactions of three types of defects: single sessile vacancies, small mobile interstitial clusters, and large sessile interstitial clusters. Reactions between the mobile and sessile defects occur at random and lead to expressions for recombination, nucleation, and cluster growth. They also lead to equations for the concentration of the various types of defects as a function of temperature, dose, and flux. These equations are consistent with experimental data on total stored energy and cluster size reported by other workers.

The various investigations involving computer calculations of the interaction of charged particles with idealized lattices have produced considerable results in the last few months. General Electric workers have published a number of reports. Their results include calculations of the ratio of tunnel ranges to normal ranges in BeO.[78] Damage calculations have now been extended to include an arbitrary potential in either the bcc or fcc structure, rather than being restricted to a hard-sphere approximation to the Bohr potential as in the past.[79] In addition, they find that the size of the damage clusters produced in a metal by neutron bombardment depends on the size of the sample and, in some respects, on the geometry of the neutron flux.[80] For example,[81] in iron the density of clusters believed to be sufficiently large to increase the yield strength at elevated temperature (~623°K) decreased with sample size for irradiation with isotropically incident neutrons but increased with sample size for irradiation with normal incident neutrons. When isotropic neutron scattering in the center of mass system was assumed, the cluster density was about 2.3 times that obtained for anisotropic neutron scattering. They state, even more generally, that neutron damage in large samples is essentially different from that produced in small samples, the spread in the size distribution being greater. In addition, the absolute number of large clusters produced per incident neutron in large samples greatly exceeds that produced in small samples. These circumstances lead to questioning the direct application of irradiation data and test results for small samples in the design of large structural parts for a reactor. The Oak Ridge[82] results are summarized in their annual report. Robinson and Oen[83] have also published a paper that discusses the slowing down of 1- to 10-kev copper atoms in various structures. They find an orientation dependence of the range which can be explained in terms of channeling. The order of the ranges is

fcc	[011] > [001] > [111] ~ isotropic
bcc	[111] > [001] > [011] > isotropic
Diamond	[011] > [001] > [111] > isotropic

They also discuss experimental evidence for channeling and some of its implications for radiation-damage theory. Sigmund[84] (Danish AEC) published a note commenting on the assumptions used by Robinson and Oen when discussing the effects of channeling in displacement cascade theory.

Calculations, carried out at Brookhaven,[85] on the basis of a many-body lattice model of alpha iron, indicate that the cubic lattice shows particular anisotropy to radiation damage when directions lying in the symmetry planes are compared with interior directions not lying in such planes. In addition, they report that kinetic energy is not conserved in collisions between pairs of atoms in a crystal lattice, since the range of the interatomic forces is not small with respect to the interatomic distances. As a result, a significant fraction of the total energy of a cascade resides as potential energy in lattice bonds. As a rule any displaced atom ends its history at a replacement collision. Since many of these replacements take place in a cascade, this constitutes an important loss of energy that is not available for displacements. Thus the efficiency of a high-energy cascade in which an appreciable number of such replacement sequences occur is expected to be low compared to a low-energy cascade. Additional contributions to the theory of focusing have been reported by Frere.[86] He uses the focusing in $\langle 1\,1\,\bar{2}\,3\rangle$ rows in the hcp metal structure for his illustrations. (T. G. Knorr)

Surveys on Radiation-Induced Defects

The effects of radiation on solids are discussed in a recently published survey containing 138 references.[87] The topics considered are the interaction of radiation and solids, calculation of the number of radiation defects produced, other defects produced by elastic energy transfer, modification of the properties of irradiated materials, and annealing of radiation effects. Dakin and Wallace[88] have gathered together theoretical and experimental data on the range-energy relations and stopping power for heavy ions in a variety of metals.

Clarke, Bowen, and Wilks[89] have collected the available data concerning irradiation damage in nonfissile ceramics, particularly MgO and BeO. A theoretical discussion of the defect production is also included. A survey has appeared concerned with the effects of neutron irradiation on the lattice parameter and dimensions of graphite.[90] Wigner energy stored in irradiated graphite and annealing at various temperatures to obtain recovery effects are also discussed.

A symposium on radiation damage[91] was presented at the Cambridge Conference on Electron Microscopy in July 1963. (T. G. Knorr)

Effects of Radiation on Mechanical Properties

The effect of temperature and neutron irradiation on the yield point and work hardening in pure iron is discussed by Mogford and Hull.[92] They report a lower work-hardening rate for the irradiated iron than for the unirradiated. A comparison is made between the decrease in work-hardening rate with increasing strains and the decrease in work-hardening rate produced by irradiation. In other English work reported from Harwell,[93] the effect of irradiation on mild and low-alloy steel is described. Irradiations were carried out at 30°C to exposures of 1.72×10^{18} neutrons/cm^2 and results were discussed in terms of the Petch relation. The lower yield increased after irradiation and was a maximum after irradiation and a 1-hr anneal at 100°C. The workers believe the results show clearly that radiation hardening in mild and alloy steel is a form of dispersion hardening and similar to age hardening.

Westinghouse (Bettis)[94] investigators have studied the effect of irradiation on the impact properties of two pressure-vessel steels, A-212B and A-302B. Irradiation produced an increase in ductile-to-brittle transition temperature which varied with exposure for both materials. There was only a slight effect of irradiation on the transition temperature at exposures up to 1.0×10^{17} neutrons/cm^2 (> 1 Mev), but a rapid increase occurred in the neighborhood of 1×10^{20} neutrons/cm^2. The maximum increase in transition temperature was reported to be 410°F. It was also noted that a postirradiation anneal at 650°F produced a recovery of radiation damage. When the annealed samples were reirradiated, they exhibited a higher transition temperature than they did in the annealed condition. The results of a Russian[95] investigation on the irradiation of low alloy steels and stainless steels are reported. The irradiation-induced property changes are similar to those in other steels with similar composition. They report a redistribution and a change in shape of the carbide phase in some of the ferritic steels.

The workers at Culcheth[96] have studied the effect of neutron irradiation on three 20 wt.% chromium–25 wt.% nickel stainless steels. Two contained niobium and titanium, respectively, for stabilizers, and the third contained low carbon (0.005 wt.%). The effects of exposure to

1×10^{20} neutrons/cm^2 (>1 Mev) at two irradiation temperatures, 590 and 750°F, were shown by tensile tests made over the 500 to 900°C range. The major effect was a large reduction in the ductility of all three steels and a change in fracture characteristics after irradiation to an intercrystalline type fracture. No structural differences between the irradiated and the unirradiated steels were noted. Battelle[97] researchers have tested in fatigue a type 347 stainless-steel specimen irradiated to 1.1×10^{22} neutrons/cm^2 for 1×10^6 cycles without failure. General Electric[81] personnel have continued to investigate the creep properties of A-286 stainless steel irradiated to 4.9×10^{19} neutrons/cm^2 (>1 Mev). They found that heats containing lower boron content (0.00085 wt.%) showed consistently lower rupture life and ductility than did the material containing 0.01 wt.% boron at test temperatures of 650°C.

Nickel and nickel-base alloys have been studied by Oak Ridge[82] workers. A commercial type 330 nickel alloy was irradiated in the 1/4 to 1/2 hard temper and cold-rolled condition to 7.8 to 11.3 $\times 10^{20}$ neutrons/cm^2 (>1 Mev) at ambient temperature. Smooth and notched speci-

Table IV-3 TENSILE PROPERTIES OF IRRADIATED TYPE 330 NICKEL[82]

Heat	Condition*	Specimen type†	Irradiation flux,‡ 10^{20} neutrons/cm^2 (>1 Mev)	Yield strength,§ psi	Ultimate tensile strength, psi	Total elongation, %	No. of tests
N6906A1	As received	S	None	45,800	63,400	36	5
N6906A1	As received	S	7.8	95,600	¶	10	1
N6906A1	As received	S	9.0	98,600	¶	11	4
N6906A1	As received	S	11.3	101,300	¶	8	1
N6906A1	As received	N	None	52,500	66,500		2
N6906A1	As received	N	7.8	108,600	¶		2
N9185A1	As received	S	None	67,200	87,500	34	2
N9185A1	As received	S	11.3	145,000	¶	5	5
N9185A1	As received	N	None	80,000	97,400		2
N9185A1	As received	N	11.3	163,000	¶		2
N9185A1	Cold worked	S	None	80,500	82,300	8	1
N9185A1	Cold worked	S	None	45,500	84,100	29	2
N9185A1	Cold worked	S	7.8	146,000	¶	3	4
N9185A1	Cold worked	N	None	53,200	84,100		2
N9185A1	Cold worked	N	7.8	149,000	¶		2
Weld-metal specimens		S	None	37,300	61,800	30	2
Weld-metal specimens		S	9.0	98,000	¶	7	5
Weld-metal specimens		N**	None	49,600	84,700		2
Weld-metal specimens		N**	11.3	118,000	129,800		2
N6906A1	Heat-affected zone	N††	None	<40,000	63,000		1
N6906A1	Heat-affected zone	N††	9.0	104,000	¶		1
N9185A1	Heat-affected zone	N††	None	43,000	82,000		1
N9185A1	Heat-affected zone	N††	9.0	118,000	¶		1

* The as-received condition is cold rolled 1/4 to 1/2 hard temper. The cold-worked condition is cold rolled an additional 75%. The heat-affected-zone condition is the heat-affected zone of a weldment, and weld-metal specimens contain base plate of both heats and weld metal.

† S indicates smooth sheet tensile specimens, and N indicates deep-edge-notched specimens.

‡ Based on the $Ni^{58}(n,p)Co^{58}$ reaction, assuming σ_{eff} = 390 mb, E_{eff} = 2.9 Mev, and fission spectrum.

§ A 0.2% offset yield strength for all unirradiated samples and samples marked with a diamond. Upper yield point for all others.

¶ Maximum load was the yield-point load.

** Notched in weld metal.

†† Notched in heat-affected zone of indicated heat.

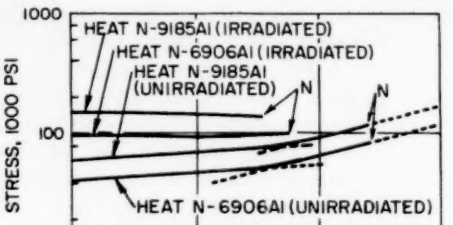

Fig. IV-5 Typical log-true-stress–log-true-plastic-strain curves of unirradiated and irradiated type 330 nickel (smooth base-plate samples).[7]

mens were tested at room temperature. Specimens were also prepared from weld metal and heat-affected-zone material adjacent to the weld metal. The results of these tests are shown in Table IV-3. The influence of neutron irradiation on the work-hardening coefficient is shown in Fig. IV-5. A yield point was noted for the irradiated but not for the unirradiated nickel. The notch sensitivity, however, was not enhanced by the irradiation. Property changes for the weld metal and in the heat-affected zone were similar after irradiation.

Russian[68] investigators have studied the change in the electrical resistivity of 80 wt.% nickel–20 wt.% chromium before and after irradiation of 5×10^{19} neutrons/cm^2. Battelle[97] personnel have studied the tensile properties of Hastelloy X cladding surrounding UO_2 after exposure for approximately 10,000 hr. The room-temperature properties after irradiation showed a slight decrease in yield and ultimate strength, accompanied by a 50% reduction in ductility. Further reduction in total elongation to 6.0 and 3.0% at 1200 and 1400°F test temperatures, respectively, was obtained.

The effect of irradiation was not completely removed after a 1-hr anneal at 1200°C. Cold-worked tungsten irradiated at room temperature to 3.2×10^{19} neutrons/cm^2 (>1 Mev) by General Electric[80] and tested subsequently in stress rupture at 1100°C showed about 1.6 times its preirradiation rupture life. Tungsten that had been annealed and recrystallized before irradiation had a slightly greater increase in rupture life, namely, by a factor of 2.6. A lower creep rate was obtained for the irradiated than for the unirradiated materials of each condition.

The effect of neutron irradiation on the creep properties of Zircaloy-2 and equipment used to study these properties are discussed by Canadian researchers.[98] Chalk River[7] workers have investigated the effect of neutron irradiation at 275°C on the impact properties of Zircaloy-2. The impact strength decreased as the hydrogen content increased from 20 to 250 ppm. In room-temperature tests the impact strength of the irradiated Zircaloy-2 was about half that of the unirradiated material, but by 400°C little difference remained. There was, however, no evidence of a transition temperature corresponding to the solution of hydrogen. A zirconium–2.5 wt.% niobium alloy, irradiated and subsequently impact tested over a range of temperatures, showed a decrease in impact strength. However, at temperatures above 350°C the irradiation damage was rapidly annealed out.

(F. R. Shober)

References

1. H. H. Klepfer, J. L. Jaech, R. E. Blood, and D. L. Douglass, Specific Zirconium Alloy Design Program, Quarterly Progress Report No. 5, April–June 1963, USAEC Report GEAP-4284, Vallecitos Atomic Laboratory, July 1, 1963.
2. H. H. Klepfer, Zirconium-Niobium Binary Alloys for Boiling Water Reactor Service. Part I — Corrosion Resistance, *J. Nucl. Mater.*, 9(1): 65-76 (June 1963).
3. H. H. Klepfer, Zirconium-Niobium Binary Alloys for Boiling Water Reactor Service. Part II — Corrosion Hydrogen Embrittlement, *J. Nucl. Mater.*, 9(1): 77-84 (June 1963).
4. S. Kass and J. D. Grozier, The Effect of Carbon upon the Corrosion and Tensile Properties of Zircaloy-2, USAEC Report WAPD-T-1508, Westinghouse Electric Corp., Bettis Atomic Power Laboratory, June 1962.
5. Hanford Atomic Products Operation, Metallurgy Research Operation Quarterly Progress Report, April–June 1963, USAEC Report HW-77954, July 15, 1963.
6. Hanford Atomic Products Operation, Ceramics Research and Development Operation Quarterly Report, April–June 1963, USAEC Report HW-76302, Nov. 4, 1963.
7. Atomic Energy of Canada, Ltd., 1963. (Unpublished)
8. B. Cox, Some Effects of Pressure on the Oxidation of Zircaloy-2 in Steam and Oxygen, *J. Less-Common Metals*, 5(4): 325-336 (August 1963).
9. B. Cox and B. R. Harder, The Effect of Dissolved Oxygen on the Oxidation of Zircaloy-2 by Steam,

J. Electrochem. Soc., 110(11): 1110-1113 (November 1963).

10. R. B. Richman, Radiation Effects on Aluminum Filming and Corrosion, USAEC Report HW-76642, Hanford Atomic Products Operation, Feb. 20, 1963.
11. F. W. Albaugh, Reactor and Fuels Laboratory Monthly Report, November 1963, USAEC Report HW-79726A, Hanford Atomic Products Operation, Dec. 15, 1963. (Classified; material cited is unclassified)
12. General Electric Company, Advanced Technology Services, High-Temperature Materials Program Progress Report No. 29, Part B, USAEC Report GEMP-29B, Dec. 6, 1963. (Classified; material cited is unclassified)
13. C. F. Cheng and H. L. Tymchyn, Chloride Stress Corrosion Cracking of Ni-Cr-Fe Alloys, USAEC Report KAPL-M-CC-3, Knolls Atomic Power Laboratory, Apr. 3, 1963.
14. A. P. Larrick, Corrosion Studies in Simulated N-Reactor Secondary System Water Environment, USAEC Report HW-76358, Hanford Atomic Products Operation, May 1963.
15. R. T. Pennington, Nuclear Superheat Project, Fourteenth Quarterly Report, October–December 1962, USAEC Report GEAP-4153, General Electric Company, Atomic Power Equipment Department, Jan. 15, 1962.
16. H. Graefen, A Laboratory Test for Determining Susceptibility of Nickel-Molybdenum and Nickel-Molybdenum-Chromium Alloy to Intercrystalline Corrosion and Its Use in the Development of Resistant Alloys, Report CONF-28-1, paper presented at the International Congress of Metallic Corrosion, New York, March 1963.
17. F. W. Albaugh, Reactor and Fuels Laboratory Monthly Report, September 1963, USAEC Report HW-79046A, Hanford Atomic Products Operation, Oct. 15, 1963. (Classified; material cited is unclassified)
18. W. L. Pearl, G. G. Gaul, and G. P. Wozaldo, General and Localized Corrosion Studies of Type 300 Series Austenitic Stainless Steels in Simulated Superheat Reactor Environment, USAEC Report GEAP-4310, General Electric Company, Atomic Power Equipment Department, July 1963.
19. Proceedings of the Nuclear Superheat Meeting, No. 8, March 20–22, 1963, Idaho Falls, Idaho, USAEC Report TID-7674, Apr. 15, 1963.
20. S. P. Rideout, Stress Corrosion Cracking of Type 304 Stainless Steel in High-Purity Heavy Water, USAEC Report DPSPU-62-30-26, Savannah River Plant, March 1963.
21. Société d'Études de Recherches et d'Applications pour l'Industrie, Studies of Steel Corrosion in High Temperature Water and Steam, Quarterly Report No. 3, January 1 to March 31, 1963, USAEC–Euratom Report EURAEC-704, Apr. 24, 1963.
22. E. A. Gulbransen, K. F. Andrew, and F. A. Brassart, Oxidation of Molybdenum from 550 to 1700°C, *J. Electrochem. Soc.*, 110(9): 952-957 (September 1963).
23. W. A. Gibeaut and J. J. English, Review of Recent Developments—Oxidation Resistant Coatings for Refractory Metals, DMIC Newsletter, Battelle Memorial Institute, Defense Metals Information Center, Jan. 24, 1964.
24. G. J. Dormer and E. G. Pike, Manufacturing Methods for High-Temperature Coating of Large Molybdenum Parts, Interim Engineering Report, August 1–October 31, 1963, The Pfaudler Co.
25. D. B. Warmuth and S. Baranow, Advancement of High-Temperature Protective Coatings for Columbium Alloys (II), Interim Progress Report, June 16–October 16, 1963, Thompson Ramo Wooldridge Inc.
26. L. Sama and G. Ladd, Development of Production Methods for High-Temperature Coating of Large Tantalum Parts, Interim Engineering Report, September 1–November 30, 1963, General Telephone and Electronics Laboratories, Inc.
27. W. J. Anderson, G. S. Sheffield, and A. J. Birkle, Development of Ferritic Steels for High Temperature Sodium Service, USAEC Report NAA-SR-7544, Atomics International, Nov. 30, 1963.
28. F. J. Leitz, Sodium Cooled Reactor Program, Fast Ceramic Reactor Development Program, Sixth Quarterly Report, January–March 1963, USAEC Report GEAP-4214, General Electric Company, Atomic Power Equipment Department, April 1963.
29. J. A. DeMastry, Fourth Quarterly Progress Report on Investigation of High Temperature Refractory Metals and Alloys for Thermionic Converters, Battelle Memorial Institute, on Contract AF 33(657)-10404, Oct. 10, 1964.
30. J. M. Lamberti and N. T. Saunders, Compatibility of Cesium Vapor with Selected Materials at Temperatures to 1200°F, Report NASA-TN-D-1739, National Aeronautics and Space Administration, Lewis Research Center, August 1963.
31. General Electric Company, Advanced Technology Services, High-Temperature Materials Program Progress Report No. 27, Part A, USAEC Report GEMP-27A, Sept. 30, 1963.
32. A. G. Imgram and H. R. Ogden, The Effect of Fabrication History and Microstructure on the Mechanical Properties of Refractory Metals and Alloys, Report DMIC-186, Battelle Memorial Institute, Defense Metals Information Center, July 10, 1963.
33. R. T. Begley, R. W. Buckman, J. L. Godshall, and R. Stickler, Development of Columbium-Base Alloys, Report WADC-TR-57-344(Pt. VII), Westinghouse Electric Corp., Astronuclear Laboratory, Apr. 1, 1963.
34. F. F. Schmidt and H. R. Ogden, The Engineering Properties of Columbium and Columbium Alloys,

Report DMIC-188, Battelle Memorial Institute, Defense Metals Information Center, Sept. 6, 1963.

35. F. F. Schmidt and H. R. Ogden, The Engineering Properties of Tantalum and Tantalum Alloys, Report DMIC-189, Battelle Memorial Institute, Defense Metals Information Center, Sept. 13, 1963.
36. F. F. Schmidt and H. R. Ogden, The Engineering Properties of Molybdenum and Molybdenum Alloys, Report DMIC-190, Battelle Memorial Institute, Defense Metals Information Center, Sept. 20, 1963.
37. F. F. Schmidt and H. R. Ogden, The Engineering Properties of Tungsten and Tungsten Alloys, Report DMIC-191, Battelle Memorial Institute, Defense Metals Information Center, Sept. 27, 1963.
38. E. S. Bartlett and J. A. Van Echo, Creep of Columbium Alloys, Report DMIC-Memo-170, Battelle Memorial Institute, Defense Metals Information Center, June 24, 1963.
39. B. S. Lement, D. A. Thomas, S. Weissmann, W. S. Owen, and P. B. Hirsch, Substructure and Mechanical Properties of Refractory Metals, Report ASD-TR-61-181(Pt. III), ManLabs, Inc., Apr. 5, 1963.
40. Metallurgy of Molybdenum, Niobium, and Molybdenum-Niobium Alloys, A Literature Search, USAEC Report TID-3572, April 1963.
41. H. J. Goldschmidt, E. A. Catherall, W. M. Ham, and D. A. Oliver, Investigation into the Tungsten-Rich Regions of the Binary Systems Tungsten-Carbon, Tungsten-Boron, and Tungsten-Beryllium, Report ASD-TDR-62-25 (Pt. II), Birmingham Small Arms, Ltd., June 1963.
42. J. L. Ratliff, W. A. Gibeaut, and H. R. Ogden, Tungsten Research and Development Review, 1960–1962, Report DMIC-193, Battelle Memorial Institute, Defense Metals Information Center, Oct. 23, 1963.
43. F. N. Rhines and R. W. Gould, The Zirconium-Iron System, *Advan. X-Ray Anal.*, 6: 62-73 (1963).
44. F. Macpherson (Comp.), Hydrogen and Helium Permeability of Steel and of Nickel, Copper, Aluminum, Gold, Platinum and Their Alloys, USAEC Report SCL-B-107, Sandia Corporation, May 1, 1963.
45. G. T. Murray, H. Kuzuu, and H. Klints, Permeability of Cladding Materials to Inert Gases, USAEC Report TID-15434, Materials Research Corporation, Nov. 14, 1961.
46. V. L. Gelezunas, P. K. Conn, and R. H. Price, The Diffusion Coefficients for Hydrogen in β-Zirconium, *J. Electrochem. Soc.*, 110: 799-805 (July 1963).
47. Argonne National Laboratory, Metallurgy Division Annual Report for 1962, USAEC Report ANL-6677.
48. Oak Ridge National Laboratory, Metals and Ceramics Division Annual Progress Report for Period Ending May 31, 1963, USAEC Report ORNL-3470, Nov. 11, 1963.
49. R. P. Elliott, Diffusion in Titanium and Titanium Alloys, Final Report, Report ARF-2208-16, Illinois Institute of Technology, Armour Research Foundation, March 1962.
50. Hanford Atomic Products Operation, Diffusion of Plutonium and Uranium in Magnesium, USAEC Translation HW-TR-61 [translated from D. Calais, et al., *Compt. Rend.*, 257: 1285-1287 (Aug. 5, 1963)].
51. E. L. Leler and A. B. Andreeva, Formation and Properties of Solid Solutions of ZrO_2 with Oxides of Rare-Earth Elements, *Ogneupory*, 5: 224-231 (1963).
52. R. B. Burdick and W. R. Hoskyns, Research on the Thermal Properties of Zirconia, Report ARL-63-170, Materiadyne, Div. of Pfaudler Permutit Inc., May 17, 1963.
53. L. A. McClaine (Ed.), Thermodynamic and Kinetic Studies for a Refractory Materials Program, Report ASD-TDR-62-204(Pt. II), Arthur D. Little, Inc., May 1963.
54. E. F. Batutis, A Study of Select Ceramic Oxide Compositions as High Temperature (1600–2100°K) Thermal Energy Storage Materials, Final Report, February 1962 to February 1963, Report NP-13158, General Electric Company, Missile and Space Division, May 7, 1963.
55. J. L. Pentecost and C. H. Wright, Preferred Orientation in Ceramic Materials Due to Forming Techniques, Report CONF-174-1, Melpar, Inc., August 1963.
56. C. T. Lynch and J. J. Krochmal, Importance of Purity in Development of Ceramics, *RTD Technol. Briefs*, 1: 1-6 (October 1963).
57. N. M. Parikh and W. Rostoker (Eds.), Studies of the Brittle Behavior of Ceramic Materials, Quarterly Report No. 2, April 15, 1963 to July 15, 1963, Report IITRI-B6012-2, Illinois Institute of Technology, Research Institute, Aug. 15, 1963.
58. J. B. Goldmann, Phase Relationships of Molybdenum, Niobium, and Tungsten Borides, Carbides and Silicides: An Annotated Bibliography, Report NP-12972, Lockheed Aircraft Corp., Missile and Space Division, December 1962.
59. J. R. Hague, J. F. Lynch, A. Rudnick, F. C. Holden, and W. H. Duckworth, Refractory Ceramics of Interest in Aerospace Structural Applications — A Materials Selection Handbook, Report RTD-TDR-63-4102, Battelle Memorial Institute, October 1963.
60. M. McCargo, J. A. Davies, and F. Brown, Range of Xe^{133} and Ar^{41} Ions of keV Energies in Tungsten, *Can. J. Phys.*, 41(8): 1231-1244 (August 1963).
61. R. S. Nelson, The Observations of Collision Sequences in UO_2, *J. Nucl. Mater.*, 10(2): 154-156 (1963).
62. M. W. Thompson, A Direct Measurement of the Focusing Energy for ⟨110⟩ Collision Sequences in Gold, *Phys. Letters*, 6(1): 24-26 (Aug. 15, 1963).

63. H. Lutz and R. Sizmann, Super Ranges of Fast Ions in Copper Single Crystals, *Phys. Letters*, 5(2): 113-114 (June 15, 1963).
64. P. R. B. Higgins and A. C. Roberts, The Nature and Annealing Behavior of Fission Fragment Damage in Molybdenum, British Report AERE-R-4390, September 1963.
65. S. Ceresara, T. Federighi, and D. Gelli, Recovery of Aluminum after Neutron-Irradiation at 78°K, *Nuovo Cimento*, 29(6): 1244-1261 (Sept. 16, 1963).
66. N. F. Pravdyuk and V. M. Golyanov, Electron Microscopic Investigation of Uranium Fission, USAEC Translation AEC-tr-6106, 1962.
67. J. Adam and M. D. Rogers, Radiation-Induced Phase Change and Recovery in ZrO_2, *J. Nucl. Mater.*, 9(2): 211-212 (1963).
68. S. M. Astrahantzev and Yu. I. Konnov, Structural Transformation in Nickel-Chromium Alloy (80 Ni/20 Cr) Under Irradiation, *J. Nucl. Mater.*, 10(1): 15-22 (1963).
69. S. Ceresara, Recovery of Diluted Binary Alloys Neutron Irradiated at 78°K, *Phys. Letters*, 6: 152 (Sept. 1, 1963).
70. C. Motoc and I. Teodorescu, Radiation Effects in Thin Films, *J. Nucl. Mater.*, 8(3): 320-328 (May 1963).
71. T. S. Elleman, R. B. Price, and D. N. Sunderman, Fission-Fragment-Induced Expansion in Single-Crystal Alpha Alumina, USAEC Report BMI-1646, Battelle Memorial Institute, Sept. 4, 1963.
72. G. W. Groves and A. Kelly, Neutron Damage in MgO, *Phil. Mag.*, 8: 1437-1454 (1963).
73. J. R. Parsons and R. W. Balluffi, Displacement Spike Crystallization of Amorphous Germanium During Irradiation, USAEC Report TID-19534, 1963.
74. R. L. Woolley, Thermal Resistivity of Irradiated Graphite, *Nature*, 199: 684-685 (Aug. 17, 1963).
75. J. E. Brocklehurst and J. W. Weeks, Dimensional Changes in Graphite: The Relationship Between Those Produced by Absorption of Bromine and Those Produced by Irradiation, *J. Nucl. Mater.*, 9: 197-210 (1963).
76. K. A. Muller, The Annealing of Neutron-irradiated Graphite Studied with Spin Resonance, Ampere Colloquium, Eindhoven, pp. 393-397, 1962.
77. R. L. Woolley, On the Theory of Irradiation Damage in Graphite at Power Reactor Temperatures, *Brit. J. Appl. Phys.*, 14: 778-783 (1963).
78. J. R. Beeler, Jr., and D. G. Besco, Energetic Atom Tunneling in a Wurtzite Structure, USAEC Report CONF-46-84, General Electric Company, Advanced Technology Services, May 8, 1963.
79. D. G. Besco and J. R. Beeler, Jr., Computer Programs Describing Collision Cascades in Binary Materials. III. Body-Centered Cubic and Face-Centered Cubic Structures, USAEC Report GEMP-243, General Electric Company, Advanced Technology Services, August 1963.
80. General Electric Company, Advanced Technology Services, High-Temperature Materials Program, Progress Report No. 29, Part A, USAEC Report GEMP-29A, Nov. 30, 1963.
81. J. R. Beeler, Jr., Effect of Sample Size on Radiation Damage in Neutron-Irradiated Iron, USAEC Report CONF-39-67, General Electric Company, Advanced Technology Services, June 1963.
82. Oak Ridge National Laboratory, Solid-State Division Annual Progress Report for Period Ending May 31, 1963, USAEC Report ORNL-3480, Aug. 23, 1963.
83. M. T. Robinson and O. S. Oen, Computer Studies of the Slowing Down of Energetic Atoms in Crystals, *Phys. Rev.*, 132(6): 2385-2398 (Dec. 15, 1963).
84. P. Sigmund, Effect of Channeling on Displacement Cascade Theory, *Phys. Letters*, 6(3): 251-253 (Sept. 15, 1963).
85. C. Erginsoy, Dynamics of Atomic Replacement Processes. II. The Influence of Crystal Lattice on Cascades, USAEC Report BNL-7156, Brookhaven National Laboratory, 1963.
86. R. Frere, Theory of Focusing Collision Chains, I, *Physica Status Solidi*, 3(7): 1252-1259 (1963); II, *ibid.*, 3(8): 1441-1452 (1963); III, *ibid.*, 3(8): 1453-1471 (1963).
87. O. Hauser, The Effects of Radiation on Solids, *Werkstoffe der Kerntechnik.*, Teil IV; pp. 93-141, VEB Deutscher Verlag der Wissenschaften, Berlin, 1963.
88. H. Dakin and R. Wallace, Range and Stopping-Power Data for Heavy-Ion Experimenters, USAEC Report UCRL-10565, University of California, Lawrence Radiation Laboratory, Oct. 29, 1963.
89. F. J. P. Clarke, D. H. Bowen, and R. S. Wilks, Irradiation Damage in Some Nonfissile Ceramics, *Trans. Brit. Ceram. Soc.*, 62(2): 83 (1963).
90. J. Spreadborough and C. Tribuno, Effects of Neutron Irradiation on the Thermal, Electrical, and Mechanical Properties of Graphite, *Termotecnica (Milan)*, 17: 397 (June 1963).
91. R. B. Nicholson, W. C. Nixon, and D. H. Warrington, Conference on Electron Microscopy, Cambridge, July 1963, *Brit. J. Appl. Phys.*, 14: 733-740 (1963).
92. I. L. Mogford and D. Hull, Effect of Temperature and Neutron Irradiation on Yield and Work Hardening in Iron, *J. Iron Steel Inst. (London)*, 201: 55-60 (January 1963).
93. D. R. Harries, A. F. Ardy, and A. F. Bartlett, Radiation Hardening in Mild and Low Alloy Steels, British Report AERE-R-4407, August 1963.
94. G. F. Carpenter, N. R. Knopf, and E. S. Byron, Anomalous Embrittling Effects Observed During Irradiation Studies on Pressure Vessel Steels, USAEC Report WAPD-T-1570, Westinghouse Electric Corp., Bettis Atomic Power Laboratory, 1962.
95. Sh. Sh. Ibragimov, I. M. Voronin, and A. S. Kurglov, The Effect of Neutron Irradiation on the

Structure and Mechanical Properties of Alloy Steels (in Russian), *At. Energ. (USSR)*, 15: 30-37 (July 1963).

96. A. N. Hughes and J. R. Caley, The Effects of Neutron Irradiation at Elevated Temperatures on the Tensile Properties of Some Austenitic Stainless Steel, *J. Nucl. Mater.*, 10: 60-62 (September 1963).
97. R. W. Dayton and R. F. Dickerson, Progress Relating to Civilian Applications During September 1963, USAEC Report BMI-1650, Battelle Memorial Institute, Oct. 1, 1963. (Classified)
98. J. Pefhany, Measurements of Metal Creep Under Fast Neutron Irradiation in a Reactor, Report CONF-82-1, paper presented at Canadian Nuclear Association Conference on Heavy Water Reactors, 1962.

Section

V

Reactor Materials

Special Fabrication Techniques

Melting, Casting, and Working

Techniques for the production of thin-walled tubing from refractory alloys are being investigated at numerous sites. Small quantities of niobium–10 wt.% tungsten–1 wt.% zirconium–0.1 wt.% carbon (D43), tantalum–8 wt.% tungsten–2 wt.% hafnium (T-111), and niobium–10 wt.% tungsten–10 wt.% tantalum tubing, 0.156 in. in inside diameter by 0.016 in. in wall thickness, have been made at Argonne.[1] The structural integrity of this material is being determined by X-ray and eddy-current techniques. Studies concerned with the production of duplex tubing are continuing.

Argonne[1] and Nuclear Metals[2] are employing arc-melted materials in their studies on refractory-metal alloys and systems. The former has prepared arc-melted buttons of niobium–15 wt.% titanium–6 wt.% vanadium, vanadium–5 wt.% molybdenum, vanadium–50 wt.% molybdenum, niobium–10 wt.% titanium, niobium–10 wt.% vanadium, and vanadium–40 wt.% titanium for future fabrication. Nuclear Metals[2] has employed arc melting to prepare 25-g buttons and 2-in.-diameter ingots for phase-diagram studies. Since the program has been in progress, sixteen binary systems and two ternary systems have been screen by hot hardness and oxidation tests. The 2-in.-diameter ingots were prepared from high-purity powder and an electode of the base material, since it had been noted that the use of an inert electrode of tungsten resulted in the pickup of 0.1 to 1.0 wt.% tungsten in the melt. The ingots were canned in TZM or tungsten and extruded at 140 in./min in a 1000-ton press to 0.5-in.-diameter rod utilizing a glass lubricant. Niobium- and tantalum-base alloys were extruded at 1850 to 1900°C; tungsten-base alloys were extruded at 2000°C. The correlation between the hot hardness and hot tensile strength of refractory alloys was established as yield strength, 0.2% offset (1000 psi) = 0.42 DPH – 3.4 and ultimate tensile strength (1000 psi) = 0.48 DPH + 6.7.

Although the emphasis in many research programs is placed on the refractory alloys, research is continuing on other materials and alloy systems. Investigations of the fabrication of yttrium and other rare earths are reported by Iowa State College.[3] Arc-melted ingots of yttrium were encapsulated in titanium and worked at 550°C into thin plates and wire. After the titanium was removed, 0.010 to 0.002-in.-thick sheets were produced from the plates by cold rolling with intermittent vacuum anneals at 750°C. The same procedure was employed to produce sheets of neodymium, erbium, praseodymium, and scandium. High-velocity forming studies indicate that yttrium loses its plasticity as the strain rate is increased. Studies of possible lubricants for the production of yttrium tubing have been unsuccessful to date. Among the lubricants investigated were glasses, MoS_2, fused salts, and colloidal graphite. The same laboratory has reported 90% reduction of high-purity arc-cast thorium ingots by direct rolling, swaging, and drawing at room temperature.

The National Lead Co. of Ohio[4,5] has recently issued the results of a study concerned with the coefficient of friction between uranium and mill rolls and also the results of a feasibility study concerned with the drilling of solid uranium billets to produce hollow extrusion blanks. During the latter study, holes up to 2 in. in diameter were bored in billets 20 in. long in less than 10 min. It is stated that the cost of drilling is more than offset in savings due to higher casting yield and lower mold cost. There is no accounting for the metal removed during

drilling or trepanning and the cost associated with reconstitution of this material.

Another fuel material, the uranium–14 wt.% molybdenum alloy, is being investigated at Argonne.[1] Bare extrusion of this alloy indicates that extrusion is feasible, but proper lubricants are essential. Attempts to roll the alloy from a Houghton-1550 salt bath at 950, 970, and 1030°C were unsuccessful, but the alloy can be rolled at 1000 and 1100°C if clad or jacketed.

Electron-beam purification studies on zirconium are being pursued by the Bureau of Mines.[6] Previous studies had shown that oxygen, carbon, and nitrogen cannot be lowered by electron-beam melting at low pressures. Present studies are utilizing BeF_2, boron, molybdenum, silicon, dysprosium, titanium, erbium, gadolinium, or samarium as doping agents to aid in the removal of the above interstitials. It was noted that zirconium containing 1600 ppm oxygen, when melted with samarium, gadolinium, erbium, and dysprosium, contained 600, 640, 670, and 870 ppm of oxygen, respectively, after 1-hr exposure. The addition of 0.5 wt.% titanium to the same-quality zirconium yielded zirconium with 780 and 430 ppm of oxygen after 1- and 2-hr exposure, respectively. None of the above additions tended to decrease the carbon or nitrogen in the zirconium. (N. E. Daniel)

Cladding

Rolling, Swaging, and Coextrusion

In swaging tests on UO_2 employing steel and zirconium tubes in a four-jaw machine, German investigators[7] reported densities of 75, 80, and 83.5% of theoretical. A reduction in cross section between 21 and 26% during cold swaging yielded the highest density (90 to 92% of theoretical). The UO_2 employed in this study was melted by the direct-current flow method in preparation for the swaging studies.

The Torrington Company is developing swaging methods for forming mockup pea-in-a-pod type fuel rods for Argonne,[1] employing type 406 stainless-steel cladding. The fuel rod consists of a tube swaged over a row of balls, and current work is centered around achieving desired finished dimensions (rod-diameter maxima and minima, tubing wall thicknesses, and ball spacing).

Extrusions of type 304 stainless steel with a plain vanadium core and with a nickel-plated vanadium core were evaluated metallographically at Argonne.[8] A very tight bond was observed at the vanadium–type 304 stainless-steel interface, with no evidence of separation. Certain areas showed a discontinuous string of very fine particles, possibly oxides, along the interface. A duplex billet, type 304 stainless steel with a vanadium core, was assembled in an inert atmosphere and extruded with a 4 to 1 reduction at 1200°C. Ultrasonic and X-ray examinations indicated a sound bond between the stainless steel and the core. The duplex extrusion will be processed into a small-diameter thin-walled tube of approximately 3.96 mm in inside diameter by 0.38 mm in total wall thickness. (R. J. Diersing)

Pressure Bonding

A detailed study[9] of gas-pressure bonding of several production-size Shippingport Pressurized-Water Reactor (PWR) core 2 plate type fuel elements was conducted by Westinghouse. This program, which involved the fabrication and evaluation of both direct-bonded and pack-bonded assemblies, was run concurrently with the initiation of PWR core 2 fabrication to better define process specifications. The effects of bonding temperature, assembly clearances, and postbond heat-treating were related to the bond quality, fuel-cladding reaction, surface characteristics, dimensions, corrosion resistance, and mechanical properties of the bonded units. The conclusions drawn from this work stressed the importance of fuel-width clearances, cleanliness of the starting fuel, carbon-coating thicknesses, and the beneficial effects of the postbonding beta heat-treatment.

The effects of gas-pressure bonding on types 304, 304L, and 347 stainless steels have been evaluated by Battelle.[10] In view of the slow-cooling representative of pressure bonding, this study concentrated on reducing the final grain size by cold working prior to bonding. Type 347 stainless steel developed a much finer grain size than types 304 or 304L; however, the final grain size was significantly reduced by initially cold working 35%. In the range of cold work investigated and the resulting variation in bonded grain size, no significant effects on the tensile properties of types 304L and 347 stainless steel were observed. It was concluded that control of the cladding microstructure in stainless-steel-clad fuel assemblies could be exerted through

the selection of the type of stainless steel and the use of cold work prior to pressure bonding.

The solid-phase joining of beryllium sheet stock into nuclear components and mechanical structures was briefly described in a recent article.[11] Pressure-bonding conditions of 4 hr at 1550 to 1850°F and 10,000 psi have yielded bonds of high integrity, with tensile strengths of 36,400 psi. Surface preparation has been established as an important factor in successful bonding. The preparation method outlined required grit blasting with iron grit, rinsing in dilute HNO_3, and etching in H_2SO_4, followed by a closely controlled wash cycle.

The application of gas-pressure bonding to the compaction of powder materials has been described in a recent Battelle paper.[12] It was noted that this approach represents an idealized hot-pressing system, generally requiring a compaction temperature lower than that for conventional hot pressing because of the higher pressures. Results obtained with refractory-metal powders, oxide ceramics, and mixtures of metal and ceramic powders were reviewed in terms of density, degree of particle bonding, and crystal size. With many of the oxide ceramics, it was noted that a wide range of crystal sizes was obtained over a bonding temperature range of 2100 to 2350°F, with densities on the order of 98% of theoretical. (S. W. Porembka)

Canning

Development and evaluation of sodium bonding of EBR-II fuel elements, in which the mode of imparting bonding energy to the fuel element was changed from vibratory action to a series of timed impacts, were reported[13] by Argonne. The element assembly consisted of a fuel pin in a thin-walled stainless-steel tube, with the annulus filled with sodium. The sodium provides a heat-transfer bond between the fuel pin and the fuel tube. Vibratory bonding of the assembly consisted of vibrating it at 60 cps while it was being heated to 500°C. The vibration cleared the annulus of gas bubbles and the gas pocket of trapped sodium. After the temperature of 500°C was reached to ensure wetting of internal surfaces by the sodium, the fuel element was progressively cooled from the bottom to the top to prevent shrinkage voids.

The necessity to recycle vibratory-bonded fuel elements to achieve acceptable bonds led to the impact-bonding technique, in which a sharp blow is delivered to the base of the fuel element. The fuel pin is then allowed to settle prior to the next impact. The impacting is done with the assembly at 500°C.

Initial impact bonding was employed to recover rejected production-line fuel elements. The overall recovery yield for 123 elements was 94%. Several tests were conducted in which optimum bonding conditions were determined as a function of flight amplitude, temperature, and number of impacts, with the optimum conditions being 1.25 to 1.5 in., 500°C, and 800 to 1000 impacts, respectively.

Further English[14] investigations have indicated that the sizes and quantities of UO_2 particles that can be vibro-compacted to 90% of theoretical density in a 0.5-in.-diameter stainless-steel can could be compacted to only 87 and 84% of theoretical density in 0.4- and 0.2-in.-diameter cans, respectively. This evidence, together with additional results of compacting trials to determine the effect of can length-to-diameter ratio on densification, suggests that the can diameter has a major influence on compacting efficiency.

Minutes of the Ceramic Fuels Meeting[15] include a comparison of pneumatic and electromagnetic vibration in the one-step preparation of completed fuel assemblies and a discussion of the development of arc-fused powder by General Electric. The high density attainable by vibratory compaction of fused UO_2, as compared with other types of UO_2 powders, is discussed.

Improved performance of the pneumatic impaction container assembly being developed by Hanford[16] for impaction of UO_2-PuO_2 fuel material for the Experimental Boiling-Water Reactor was accomplished by inserting a strip of mild-steel foil between the inner and outer cans. The steel reacts with oxygen within the assembly while it is being heated to 1200°C, thus preventing oxidation of the porous stainless-steel filter welded to the inside surface of the can lid.

Studies that relate bulk density of vibratory compacted (thorium-uranium) oxide, made by the Sol-Gel process, with particle-size distributions were reported by Oak Ridge.[17] A trilinear plot shows the relation between particle-size distribution of the ternary system, −6 +16, −50 +140, −200 mesh, and bulk density, with constant-density lines drawn for densities of 8.7, 8.8, and 8.9 g/cm^3. Ternary compositions of 60 wt.% −4 +16, 15 wt.% −50 +140, 25 wt.%

−200 and 60 wt.% −6 +10, 15 wt.% −35 +50, 25 wt.% −200 mesh distributions produced bulk densities of 9.0 and 9.1 g/cm^3, respectively, with the former not being entirely satisfactory for $\frac{1}{2}$-in.-diameter tubes because the large particles occasionally bridge in the tube. A plot of the relation between bulk density and the amount of coarse material is shown for binary systems of −6 +16, −200 and −4 +16, −200 mesh distributions. Maximum vibrated densities of thorium-uranium oxides are dependent on their chemical histories.

A device to impart a horizontal mode of vibration to specimens simultaneously with vertical vibration has been developed by Argonne.[18] The bridging condition previously reported was alleviated by the use of this device; however, during compacting, separations of the binary fractions took place, with the larger fractions being vertically displaced. The erratic results produced by separation of the fractions were corrected by loading the second-size fractions through a screen with apertures small enough to hold down the larger size components yet allow the second fraction to pass through into the larger fraction. This produced consistent experimental results.

A Yugoslavian paper[19] presented at the Prague Conference on New Nuclear Materials Technology discusses the investigation of the influence of frequency, acceleration, power, and binder, as well as vibrating time, on the vibratory compacting of UO_2 and several other oxides. Time was found to have a considerable influence on the density of the vibratory compacted specimens; the maximum densities were obtained after 15 min, but the gradient of density was negligible after about 5 min.

(V. D. Linse)

Nonelectrolytic Chemical-Plating Techniques

The work reviewed covers the use of chemical vapor deposition as a means of preparing refractory materials in massive form (including free-standing shapes), of joining refractory materials, and of forming protective coatings on refractory metallic and nonmetallic substrates.

In the case of high-temperature thermionic devices, chemical vapor deposition is being explored[20] as a means of regenerating molybdenum and tungsten surfaces. Hypothetical systems considered include tungsten-chlorine, molybdenum-chlorine, tungsten-molybdenum-chlorine, and tungsten-oxygen. Free-standing tungsten structures for thermionic-converter application also are under investigation.[21] Tungsten tubes $\frac{3}{4}$ in. in outside diameter by 0.20 in. in wall thickness by 14 in. in length were formed by hydrogen reduction[22] of WF_6. Halide conversion efficiencies as high as 90% were observed. Tungsten crystals were prepared by employing the water-cycle reaction in the treatment of powder-metallurgy bars at high temperature.[23]

A method was described[24] for producing a nonsooting carbon vapor by the addition of 0.1 to 5.0 vol.% nitric oxide to the carbon vapor. The carbon vapor is produced by decomposing carbonaceous material and causing the mixture to flow over a heated substrate on which a pyrolytic carbon deposit then forms.

Aluminum oxide whiskers can be formed either by aluminum halide oxidation[25] or by the use of hydrogen chloride gas as a transport medium.[26] The pyrolytic synthesis of TiB_2, B_4C, and SiC was described.[27,28] In the case of TiB_2, the resulting deposit was found to have a preferred atomic arrangement consisting of alternating layers of titanium and boron atoms perpendicular to the plane of deposition. Room-temperature physical properties of the compound were determined. Stoichiometric B_4C and SiC were deposited by hydrogen reduction of the appropriate chlorides in the presence of a hydrocarbon at elevated temperatures. The composition of boron carbide deposits could be controlled over the range 5 to 81 wt.% boron by variation of the deposition temperature and the reactant concentration. The formation of solid UC by reaction of UF_6 with CH_4 and H_2 in the gas phase was investigated.[29] The reaction is approximately 80% complete at 2000°K and 0.01 atm equilibrium pressure.

Experimental joining of refractory-metal components for thermionic converters with tungsten, applied by chemical vapor deposition, appears promising.[21]

A great deal of work is in progress in the field of coatings. These studies include the development of deposition systems and determination of coating-process variables for the following metals: molybdenum,[22] rhenium,[30] tantalum,[22] and tungsten.[21,22] New work on pyrolytic carbon as a coating material was described.[22] Also see Refs. 30 to 33. Oxide coatings are required on both metallic and non-

metallic substrates. Various combinations under investigation include HfO_2 and ZrO_2 on graphite.[34] Almost every refractory-metal silicide, both singly and in combination with other silicides, is being used in the effort to develop truly reliable coatings for the protection of refractory-metal substrates against high-temperature oxidation. Substrates receiving major attention at present are molybdenum,[35,36] tantalum-base alloys,[37] and tungsten.[38] (E. M. Sherwood)

Electroplating

Etching is essential for obtaining a good bond between uranium and nickel or silver electroplate. This was the conclusion of Los Alamos investigators,[39] who reported previously[40] on nickel-plating Oralloy for Godiva II. No procedure for obtaining good adhesion was revealed by studies of chemical and electrolytic treatments that avoided etching. A silver cyanide bath was preferred for avoiding bare spots and securing uniform coatings. For nickel plating, a solution with a *p*H of >3 should be adopted. Contacts had to moved frequently from one area to another to avoid porosity; 2 to 3 mils of nickel or another electroplate was necessary to provide good corrosion protection. Thinner electroplates were unsatisfactory.

Coumarin has been recommended[41] as an additive for Watts type nickel solutions that are used for leveling etched uranium and other rough substrate surfaces. Information developed at Wantage in England[42] showed that coumarin additions reduced the cathode efficiency for nickel plating in Watts type solution with a *p*H of 4. An efficiency of 98 to 100% was obtained with electrolyte containing no coumarin, whereas the plating efficiency was reduced to only 64 to 70% with the addition of 0.001 to 0.002 mole/liter of coumarin. Reduction of hydrogen ions accounted for 14 to 32% of the current, and reduction of coumarin to melilotic acid accounted for 7 to 13% of the current; 80 to 90% of the total consumed coumarin was reduced to melilotic acid. Part of the remainder was converted to an alcohol that boils at about 230°C.

Coumarin consumption increased with an increase in the rate of rotating the cathode and decreased as a function of the current density. With relatively low agitation, leveling increased with an increase in the coumarin concentration, up to 0.0025 mole. At higher speeds less leveling was obtained, and a maximum appeared with a concentration of 0.001 mole/liter.

A procedure for plating nickel on uranium and composites of uranium and aluminum was patented in England.[43] After being etched anodically in sulfuric or nitric acid solution, nickel is plated in a nickel sulfate–sodium citrate–ammonium chloride solution containing a wetting agent. The *p*H should be 4.5 and the temperature only 20°C.

A nonaqueous zinc acetate–formamide bath was devised for plating zinc on uranium, and a porosity test was developed at the Bureau of Standards.[44,45] Porosity was detected by the appearance of corrosion pits or blisters where exposed uranium was attacked by hydrogen gas at 200°C. The zinc coating adhered to uranium, but an oxide film was detected between the uranium and zinc during metallographic examination.

Hydrogen and deuterium embrittlement was studied during another investigation at the Bureau of Standards.[46,47] Although hydrogen permeated twice as fast as deuterium through SAE 4130 steel during cathodic charging, larger amounts of deuterium were detected in steel specimens electroplated with cadmium, copper, or chromium in D_2O solutions, by comparison with the amounts of hydrogen found after plating in H_2O solutions. Deuterium caused only very little embrittlement, however, during crushing tests on plated rings. The amount of gas introduced in the steel correlated with the degree of embrittlement but was not the only factor affecting embrittlement. The rate of escape of the gas paralleled the disappearance of embrittlement in the steel.

A decontamination factor of 6 was obtained at Hanford[48] for UO_2-PuO_2 codeposited from a LiCl-KCl fused mixture containing 20 and 0.4 wt.% uranium and plutonium, respectively. Selectively dissolving the UO_2 caused the decontamination factor to be increased to 300. A method also was developed for preparing UOS by electrodeposition from a fused-salt solution. The UOS decomposes above 1900°C.

High-purity liquid plutonium (99.98%) was produced by electrorefining with an alkali or alkaline-earth–metal-chloride fused-salt bath on cathodes with a large surface area.[49]

(W. H. Safranek)

Ceramic Coatings

Bendix[50] has fabricated alumina-molybdenum structures that can resist a 1500°C environment.

Los Alamos reported[51] the development of two types of ceramic-to-metal seals for use at 700 to 1200°C. Magnesia and nickel can be used in an oxidizing atmosphere near 700°C. For use in a nonoxidizing atmosphere near 1200°C, niobium and alumina can be joined with a braze of palladium. Under similar conditions, there appears to be some bonding between tungsten and the yttria in yttria-containing alumina.

The same laboratory[52] also reports that tungsten-metallized alumina, if brazed to niobium-zirconium alloy with palladium, can be used at 1500°C. For use at 1000°C or less, a palladium-cobalt braze alloy is satisfactory.

The procedures for fabricating metal-to-ceramic seals have been reviewed by Sperry.[53] The significance of some processing variables is evaluated. (B. W. King)

Explosive Forming

A program has been conducted by Explosiform, Inc., to determine the feasibility of metal forming by placing a high explosive in direct contact with the metal workpiece to be formed.[54] Experiments were conducted, using tetryl and nitroguanidine as the high explosive, in which the density of the explosive was varied in order to vary the detonation pressure. Bulge tests were conducted with low-carbon steel plate and tubes at various explosive densities and weights. The results of these tests revealed that, even at its minimum density, tetryl produced serious pitting and spalling of the workpiece surface, whereas no significant surface effects occurred with the various density nitroguanidine charges. Therefore it appears that direct-contact explosive metal forming using low-density nitroguanidine is feasible. The amount of forming achieved is controllable and directly related to the explosive density and weight.

An excellent paper on the energy considerations for explosive metalworking has been published by Pearson.[55] The differences in energy requirements and the means to determine these energy requirements for standoff and contact explosive-forming operations are described and discussed. The basic information pertaining to explosive forming which is presently available is reviewed, and the method for relating this information to a specific problem is discussed. (C. C. Simons)

Welding and Brazing

The development of nonfusion methods of joining metals and ceramic materials continues at a high rate. Brazing and diffusion-bonding processes are receiving a great amount of attention in both the reactor fabrication and aerospace equipment fields. Most of the work is for applications where very high temperatures are involved.

Two alloys showing much promise for brazing niobium–1 wt.% zirconium base metal are reported by Oak Ridge:[56] 48 wt.% titanium–48 wt.% zirconium–4 wt.% beryllium and 63 wt.% titanium–27 wt.% iron–10 wt.% molybdenum. They flow well in a vacuum and do not show fillet cracking or erode the base metal. Shear strengths in the range 25,000 to 30,000 psi at room temperature and 12,000 to 19,000 psi at 700°C can be expected.

The diffusion bonding of the Nb-752 niobium alloy skins to Haynes 25 cores is under study at North American Aviation.[57] Initial studies of titanium as an intermediate layer for bonding at 1100 to 1200°C for 3 hr and using 700-psi bonding pressure were not successful. A bond was obtained, but it was very weak. When titanium was not used, no bonding occurred. Solar is diffusion-bonding D-36, B-66, and D-43 niobium alloys at much higher pressures (10,000 psi) and shorter times (18 sec) without an intermediate layer.[58] Bonding temperatures are between 1200 and 1300°C. Higher temperature postbonding heat-treatments improve the joint properties and may indicate that the short bonding cycle only initiates diffusion.

The high-temperature honeycomb-sandwich-structure fabrication techniques are under development at Lockheed[59] and at Northrop.[60] The materials at Lockheed are molybdenum faces and Inconel 702 core. They have gone to silver-palladium brazing filler metals, because brittle joints formed when titanium or nickel was used, and low-melting eutectics formed when gold-palladium alloys were used. Successful René 41 sandwiches have been fabricated by Northrop, using a nickel-chromium-silicon-manganese alloy powder to which nickel powder was added. Inclusion of nickel powder allows the brazing alloy to react with the brazing powder rather than with the René 41 base material.

Thompson Ramo Wooldridge[61] is continuing its study of the weldability of niobium alloys, D-36, Nb-752, FS-85, and B-66. The tungsten-

inert-gas, electron-beam, and spot-welding processes are under study. Bend tests are being used to determine the ductile-to-brittle transition temperature associated with each of several sets of welding parameters. Room-temperature tensile strengths equivalent to those of the base metal were obtained for the D-36 and Nb-752, alloys, but not for the FS-85 or B-66 alloys.

Methods for the utilization of inert-gas-shielded arc welding when fabricating complex tungsten parts are being evaluated by Aerojet.[62] Elevated-temperature bend tests on base metal from three suppliers indicated that a preheat temperature of 700°F was needed for thicknesses around 0.060 in. In TIG welds made with preheats of 700°F and in thicknesses over 0.090 in., cracking was a serious problem. All welds were brittle at room temperature. Grain growth was a serious problem in 0.060-in.-thick material. Studies to reduce grain size included increased welding rate, roll planishing, shear spinning, and the addition of powders to the weld. Welding of 0.060-in.-thick material at 16 in./min gave the smallest grain size. Tensile tests of transverse specimens indicated that comparable properties between welded and nonwelded specimens are not obtained until the testing temperature reaches 3500°F. Below this temperature the weld strength is less than that of the parent metal. Two filler wires (50 wt.% rhenium–50 wt.% molybdenum and molybdenum–½ wt.% titanium) were evaluated to improve ductility. Weld cracking with the rhenium filler wire was worse than with pure tungsten, and no improvement was obtained from the use of molybdenum–½ wt.% titanium filler wire. Little success was attained with the MIG process. Porosity in the weld, the need for higher preheat temperatures, and pickup of interstitial contaminants contributed to this lack of success.

Postweld heat-treating schedules that appear to eliminate cracking in welded light-gauge Inconel have been reported by McDonnell.[63] They were unable to cause cracking in circular-patch welded restraint specimens when using this basic heat-treating schedule: 590°C thermal-stress relief, a 925°C stress relief, and a 2-hr 700°C age. Eighteen different cycles were used, based on combinations of three variables: (1) hold time at 590°C, (2) heating rate from 590°C to 925°C, and (3) hold time at 925°C. McDonnell[64] also reported that warpage in resistance-seam-welded Inconel X parts can be minimized if welding is done after heat-treatment and is followed by a re-aging treatment. This treatment produces welds with mechanical properties which approximate those obtained by welding annealed material and aging after welding.

North American,[65,66] after a study to find a replacement for eutectic bonding sintered-aluminum-powder-clad UO_2 fuel-element end closures, has recommended the use of the Kelsey-Hayes Koldweld process. This is a flash-welding technique. Butt welds tested both in tension and shear gave 100% efficient joints. Workers at General Electric's[67] Space Technology Laboratory can now vacuum braze aluminum-to-aluminum honeycomb structures at 65°C below the melting temperature of the base material. The use of a fluxless aluminum-silicon material is the key to the process.

Two reviews of refractory-metal-joining technology have been published recently. Scott and Knowlson[68] cover the present and future problems. The metallurgical characteristics are discussed, together with the influence of impurities on mechanical properties, alloy development, and weldability. Seaman and Seman[69] summarize the number and types of refractory-metal-welding facilities and the nature of their welding, and they project current methods and limitations in terms of the future.

(R. M. Evans)

Nondestructive Testing

Ultrasonic Techniques

Several factors must be considered in determining defect sizes in ultrasonic inspection. Two of these factors, diffraction and beam spread, were well demonstrated by experiments at Argonne.[1] During a resolution study, using a continuously pumped ultrasonic camera for image conversion, Argonne found that holes varying in diameter from λ to 10λ through thin plates (thicknesses less than the wavelength λ of the ultrasonic beam in water) produced good images when the plate was within about 3 cm of the detector. Beyond 3 cm the hole images were less sharp. Hole sizes 5λ or greater in diameter through plates 10λ thick produced good images within about 5 cm from the detector. However, diffraction effects made it

difficult to correlate image sizes with hole sizes less than 5λ in these thicker plates, although they could be easily detected at distances to 7.5 cm. (D. Ensminger)

NDT Techniques Other Than Ultrasonic

A thermal-diffusivity method (*J. Appl. Phys.*, 32: 1697) is being investigated at Argonne[8,18] for possible value in the determination of bond quality. A flash tube, energized for very short periods (~500 μsec), serves as the heat source, and thermocouples serve as detectors. Good agreement was obtained with published data on thermal diffusivity of a number of metals. Experiments on soft-soldered copper specimens indicated that the method is sensitive to bond variations over small regions (1 to 2 mm).

In working with fueled-graphite spheres, Oak Ridge[28] has developed an eddy-current method for automatic measurement of sphere diameter and inspection of surface symmetry. Diameter changes of 1 mil were detected, but the sphere diameter was not stated. An eddy-current probe with a Teflon tip is held in contact with the surface of the sphere 180° from a fixed reference surface so that the position of the probe varies with the sphere diameter as the sphere is rotated. The sphere is indexed to a new scanning circumference with each rotation, and data are collected on a strip-chart recorder. (A. F. Leatherman)

References

1. Argonne National Laboratory, Reactor Development Program Progress Report, September 1963, USAEC Report ANL-6784, Oct. 15, 1963.
2. A. L. Geary, Fundamental and Applied Research and Development in Metallurgy. High Temperature Properties of Refractory Alloys, USAEC Report NMI-1258, Nuclear Metals, Inc., Sept. 17, 1963.
3. Ames Laboratory, Annual Summary Research Report of Chemistry, Engineering, Metallurgy, Physics, and Reactor Divisions, July 1, 1962–June 30, 1963, USAEC Report IS-700, September 1963.
4. National Lead Co. of Ohio, Summary Technical Report for the Period July 1, 1963–September 30, 1963, USAEC Report NLCO-890, Oct. 28, 1963.
5. R. J. Jansen, Drilling Uranium Billets on a Leblond-Carlstedt Rapid Borer, USAEC Report NLCO-886, National Lead Co. of Ohio, Sept. 13, 1963.
6. Bureau of Mines, Quarterly Metallurgical Progress Report No. 20, July 1–September 30, 1963, USAEC Report USBM-U-1082.
7. P. Himmelstein, W. Hoppe, H. Kroll, B. Liebmann, and O. Neumann, Production of Swaged Fuel Elements, Quarterly Report No. 11, January 1 to March 31, 1963, USAEC-Euratom Report EURAEC-648, Nuklear-Chemie und -Metallurgie G.M.B.H., Nov. 15, 1963.
8. Argonne National Laboratory, Reactor Development Program Progress Report, August 1963, USAEC Report ANL-6780, Sept. 15, 1963.
9. F. O. Bingman and C. R. Woods, Gas Pressure Bonding of Production Size PWR Core 2 Plate Type Fuel Elements Containing Ceramic Fuel, USAEC Report WAPD-245, Westinghouse Electric Corp., Bettis Atomic Power Laboratory, May 1963.
10. E. S. Hodge, S. W. Porembka, C. B. Boyer, R. J. Diersing, Use of Agglomerated UO_2 in Pressure-Bonded Stainless Steel-Clad Fuel Rods, USAEC Report BMI-1640, Battelle Memorial Institute, July 23, 1963.
11. Pressure Bonding Beryllium, *Nucleonics*, 21(10): 72 (October 1963).
12. S. W. Porembka, Gas Pressure Bonding, *Ceram. Age*, 79(11): 68-71 (November 1963).
13. T. C. Cameron and H. M. McCall, Jr., Development and Evaluation of Prototype Remote-Controlled Sodium-Bonding and Bond-Inspection Processes for EBR-II Fuel Cycle Facility, USAEC Report ANL-6724, Argonne National Laboratory, May 1963.
14. United Kingdom Atomic Energy Authority, September 1963. (Unpublished)
15. Minutes of Ceramic Fuels Meeting Held in Brussels, October 3–5, 1962, USAEC Report TID-7666.
16. Hanford Atomic Products Operation, Ceramics Research and Development Operation Quarterly Report, April–June 1963, USAEC Report HW-76302.
17. D. E. Ferguson (Comp.), Status and Progress Report for Thorium Fuel Cycle Development for Period Ending December 31, 1962, USAEC Report ORNL-3385, Oak Ridge National Laboratory, Oct. 28, 1963.
18. Argonne National Laboratory, Reactor Development Program Progress Report, October 1963, USAEC Report ANL-6801, Nov. 15, 1963.
19. B. Zivanović, D. Jovanović, and M. M. Ristik, The Influence of Time upon Vibratory Compaction of the UO_2 Powder, Paper CN-16/55, presented at Conference on New Nuclear Materials Technology, Prague, July 1963, Report CONF-120-16.
20. L. K. Tower, Analyses of the Chemical Regeneration of Sublimating Thermionic Components, *Advanced Energy Conversion*, 3(1): 185-198 (January–March 1963).

21. D. L. Dresser, J. D. Dunlop, H. Huber, R. LeBihan, V. L. Hill, N. D. McMurray, and K. E. Muszer, Investigation of Capillary Emitter Thermionic Converters, Report ASD-TDR-63-865, General Motors Corp., Allison Division, August 1963.
22. Oak Ridge National Laboratory, Metals and Ceramics Division Annual Progress Report for the Period Ending May 31, 1963, USAEC Report ORNL-3470, Nov. 11, 1963.
23. O. Mitrofanov, Growing Tungsten Crystals from Vapors, *Kristallografiya*, 7(5): 780-783 (1962).
24. R. Diefendorf, Process for Deposition of Pyrolytic Graphite, U. S. Patent 3,107,180, Oct. 15, 1963.
25. W. B. Campbell, Feasibility of Forming Refractory Fibers by a Continuous Process, First Quarterly Progress Report, February 25–May 25, 1963, on Contract DA-19-020-AMC-0068(X), Lexington Laboratories, Inc.
26. J. Kerrigan, Studies on the Transport and Deposition of Alpha-Aluminum Oxide, *J. Appl. Phys.*, 34(11): 3408-3410 (November 1963).
27. R. E. Gannon, R. C. Folweiler, and T. Vasilos, Pyrolytic Synthesis of Titanium Diboride, *J. Am. Ceram. Soc.*, 46(10): 496-499 (Oct. 21, 1963).
28. Oak Ridge National Laboratory, Oct. 9, 1963. (Unpublished)
29. R. G. Wymer and O. C. Dean, The Feasibility of Direct Gas-Phase Conversion of UF_6 to UC, USAEC Report ORNL-TM-669, Oak Ridge National Laboratory, Sept. 6, 1963.
30. A. Zelikman, N. Bary'shnikov, and M. Teslitskaya, Producing Rhenium Coatings by the Method of Thermal Dissociation of Oxychloride, *Izv. Akad. Nauk SSSR, Met. i Gornoe Delo*, (4): 161-168 (1963).
31. A. O. Jensen, Research Program Related to Vapor Thermionic Converters for Nuclear Application, Quarterly Progress Report, March 27–June 27, 1963, USAEC Report NP-13070, Electro-Optical Systems, Inc., July 30, 1963.
32. I. Weissman and M. Kinter, Improved Thermionic Converter Using Uniaxially Oriented Tungsten, *J. Appl. Phys.*, 34(11): 3187-3194 (November 1963).
33. Zirconium Coatings, *Galvano*, 32(316): 379-382 (May 1963).
34. K. S. Mazdiyasni and C. T. Lynch, Synthesis and Pyrolysis of Metal Alkoxides as Potential Refractory Oxide Coatings for Graphite, Report ASD-TDR-63-322, Aeronautical Systems Division, Wright-Patterson AFB, April 1963.
35. J. Zupan, E. G. Pike, and J. B. Whitney, Investigation of Practical Techniques for Coating Refractory Metals, Quarterly Progress Report No. 1, May 1–July 31, 1963, on Contract AF33(657)-8920.
36. G. Dormer and E. Pike, Manufacturing Methods for High-Temperature Coating of Large Molybdenum Parts, Interim Engineering Progress Report, May 1–July 31, 1963, Report IR-7-977(IV), The Pfaudler Co., Aug. 15, 1963.
37. J. B. Hallowell, D. J. Maykuth, and H. R. Ogden, Coatings for Tantalum-Base Alloys, Report ASD-TDR-63-232, Battelle Memorial Institute, Feb. 28, 1963.
38. H. J. Nolting and R. A. Jefferys, Oxidation-Resistant High-Temperature Protective Coatings for Tungsten, Report ASD-TDR-63-459, Thompson Ramo Wooldridge Inc., May 1963.
39. J. K. Gore and R. Seegmiller, Surface Treatments and Electroplated Coatings on Uranium, *Plating*, 50: 215-220 (March 1963)
40. L. J. Quintana, J. K. Gore, and J. M. Taub, Nickel Plating of Oralloy for Godiva II, USAEC Report LAMS-2266, Los Alamos Scientific Laboratory, March 1958.
41. J. G. Beach and C. L. Faust, Electroplates on Thorium and Uranium for Corrosion Protection and to Aid Joining, USAEC Report BMI-1537, Battelle Memorial Institute, Aug. 14, 1961.
42. G. T. Rogers and K. J. Taylor, The Effects of Coumarin on the Electrodeposition of Nickel, British Report AERE-R-4371, May 1963.
43. Improvements in or Relating to the Electroplating of Uranium, British Patent 928,507, June 12, 1963.
44. Depositing Metals on Uranium, *Prod. Finishing (Cincinnati)*, 27(8): 158, 160 (May 1963).
45. Metal Deposition on Uranium to Inhibit Corrosion, *Corrosion Technol.*, 10(2): 43 (February 1963).
46. G. B. Wood, A Study of Embrittlement of High Strength Steels by Hydrogen Isotopes: I. Testing of Steel Rings or Specimens, a Comparison of Hydrogen and Deuterium Embrittlement, and Permeation Studies, *J. Electrochem. Soc.*, 110: 867-877 (August 1963).
47. G. B. Wood, A Study of Embrittlement of High Strength Steels by Hydrogen Isotopes: II. A Comparison of Gas Contents and Hydrogen or Deuterium Embrittlement Resulting from Electroplating Processes, *J. Electrochem. Soc.*, 110: 877-885 (August 1963).
48. M. M. Hendrickson and J. K. Green (Eds.), Research and Development Programs Executed for the Division of Reactor Development, Quarterly Progress Report, January–March 1963, USAEC Report HW-78118, Hanford Atomic Products Operation, April 1963.
49. L. J. Mullins, Jr., J. A. Leary, C. W. Bjorklund, and W. J. Maraman, Plutonium Electrorefining Cells, U. S. Patent 3,098,028 (to USAEC), July 16, 1963.
50. Bendix Corp., Ceramic-to-Metal Seals for High-Temperature Thermionic Converters, Quarterly Technical Report No. 3, Report RBESO-3404-3 (AD-410101), July 15, 1963.
51. R. E. Cowan and S. D. Stoddard, Ceramic Materials for Nuclear Thermionic Converters, USAEC

Report LADC-5598 (CONF-50-1), Los Alamos Scientific Laboratory, 1963.

52. E. L. Brundige and G. S. Hanks, Ceramic-to-Metal Seals for High Temperature Operation, USAEC Report LAMS-2917, Los Alamos Scientific Laboratory, Apr. 1, 1963.
53. C. W. Johnson and E. W. Cheatham, Manual of Metal-to-Ceramic Sealing Techniques, Report NP-13027, Sperry Gyroscope Co., May 1963.
54. J. Savitt, Direct Contact Explosives Metal Forming, Report ASD-TDR-62-1035, Explosiform, Inc., October 1962.
55. J. Pearson, Energy Considerations in Explosive Metal Working, Paper SP63-26, presented at Creative Metal Forming Seminar, 1962–63, ASTME, Detroit 38, Michigan.
56. G. M. Slaughter, Joining of Exotic Materials, USAEC Report CONF-94-5, Oak Ridge National Laboratory, Sept. 24, 1963.
57. J. P. King, Jr., and R. R. Janssen, Diffusion Bonded Honeycomb Sandwich Panels, Interim Engineering Progress Report, January 27–April 27, 1963, Report IR-7-980(III), North American Aviation, Inc., Los Angeles Division.
58. A. G. Metcalfe, T. B. Lindemer, and F. K. Rose, Diffusion Bonding of Refractory Metals, Interim Technical Documentary Progress Report 4, March 29–June 28, 1963, Solar Aircraft Co., July 1, 1963.
59. R. K. Titus, M. Amico, and J. H. Long, Development of Lightweight, High-Temperature Structures, Phase II–Manufacturing Development, Report ASD-TDR-7-938(III), Lockheed Aircraft Corp., Missiles and Space Division, May 1963.
60. L. H. Stone and A. H. Freedman, Brazing Thin Gage René 41 Honeycomb, Report NOR 63-70, Norair Corp., May 1963.
61. T. L. Fullerton and J. M. Gerken, Investigation of Weldability of Additional Columbium Alloys, Report ER-5294, Thompson Ramo Wooldridge, Inc., Apr. 15, 1963.
62. R. E. Handley, Tungsten Inert Gas and Metal Arc Inert Gas Welding of Tungsten Sheet, Report NOrd-17017, Aerojet-General Corporation, June 28, 1963.
63. J. Heubner, Inconel X Weldments–Special Heat Treating, Report A066, McDonnell Aircraft Corp., Sept. 10, 1963.
64. J. Heubner, Reaging of Inconel X Sheet Material After Seam Welding, Report A065, McDonnell Aircraft Corp., Sept. 10, 1963.
65. E. C. Supan, Evaluation of the Koldweld Process for Joining APM Alloys, USAEC Report NAA-SR-Memo-7748, Atomics International, Sept. 24, 1962.
66. E. C. Supan, W. F. Friske, and G. V. Alm, Joining of APM Aluminum Alloys for Reactor Fuel Applications, USAEC Report NAA-SR-8578, Atomics International, June 1, 1963.
67. Metalworking Week and Technical Outlook, *Steel (USSR) (English Transl.)*, 153(16): 34 (Oct. 14, 1963).
68. M. H. Scott and P. M. Knowlson, The Welding and Brazing of Refractory Metals Niobium, Tantalum, Molybdenum, and Tungsten, A Review, *J. Less-Common Metals*, 5: 205-244 (1963).
69. F. D. Seaman and D. J. Seman, The State-of-the-Art of Welding of Refractory Metals, report prepared under Navy Contract NOw-63-0043-c, Universal-Cyclops Steel Corporation, June 1963.

LEGAL NOTICE

This document was prepared under the sponsorship of the U. S. Atomic Energy Commission. Neither the United States, nor the Commission, nor any person acting on behalf of the Commission:

A. Makes any warranty or representation, expressed or implied, with respect to the accuracy, completeness, or usefulness of the information contained in this report, or that the use of any information, apparatus, method, or process disclosed in this report may not infringe privately owned rights; or

B. Assumes any liabilities with respect to the use of, or for damages resulting from the use of any information, apparatus, method, or process disclosed in this report.

As used in the above, "person acting on behalf of the Commission" includes any employee or contractor of the Commission, or employee of such contractor, to the extent that such employee or contractor of the Commission, or employee of such contractor prepares, disseminates, or provides access to, any information pursuant to his employment or contract with the Commission, or his employment with such contractor.

NUCLEAR SCIENCE ABSTRACTS

The U. S. Atomic Energy Commission, Division of Technical Information, publishes *Nuclear Science Abstracts (NSA)*, a semimonthly journal containing abstracts of the literature of nuclear science and engineering.

NSA covers (1) research reports of the U. S. Atomic Energy Commission and its contractors; (2) research reports of government agencies, universities, and industrial research organizations on a world-wide basis; and (3) translations, patents, books, and articles appearing in technical and scientific journals.

Complete indexes covering subject, author, source, and report number are included in each issue. These are cumulated quarterly, semiannually, and annually providing a detailed and convenient key to the literature.

Availability of *NSA*

SALE *NSA* is available on subscription from the Superintendent of Documents, U. S. Government Printing Office, Washington, D. C., 20402, at $30.00 per year for the semimonthly abstract issues and $22.00 per year for the four cumulated-index issues. Subscriptions are postpaid within the United States, Canada, Mexico, and all Central and South American countries, except Argentina, Brazil, British and French Guiana, Surinam, and British Honduras. Subscribers in these Central and South American countries, and in all other countries throughout the world, should remit $37.00 per year for subscriptions to semimonthly abstract issues and $25.00 per year for the four cumulated-index issues.

EXCHANGE *NSA* is also available on an exchange basis to universities, research institutions, industrial firms, and publishers of scientific information. Inquiries should be directed to the Division of Technical Information Extension, U. S. Atomic Energy Commission, P. O. Box 62, Oak Ridge, Tennessee, 37831.